Supporting Information

Graphdiyne Anchored Ultrafine Ag Nanoparticles for High Efficient and Solvent-Free Catalysis of CO_2 Cycloaddition

Chang Liu, Chao Zhang and Tong-Bu Lu*

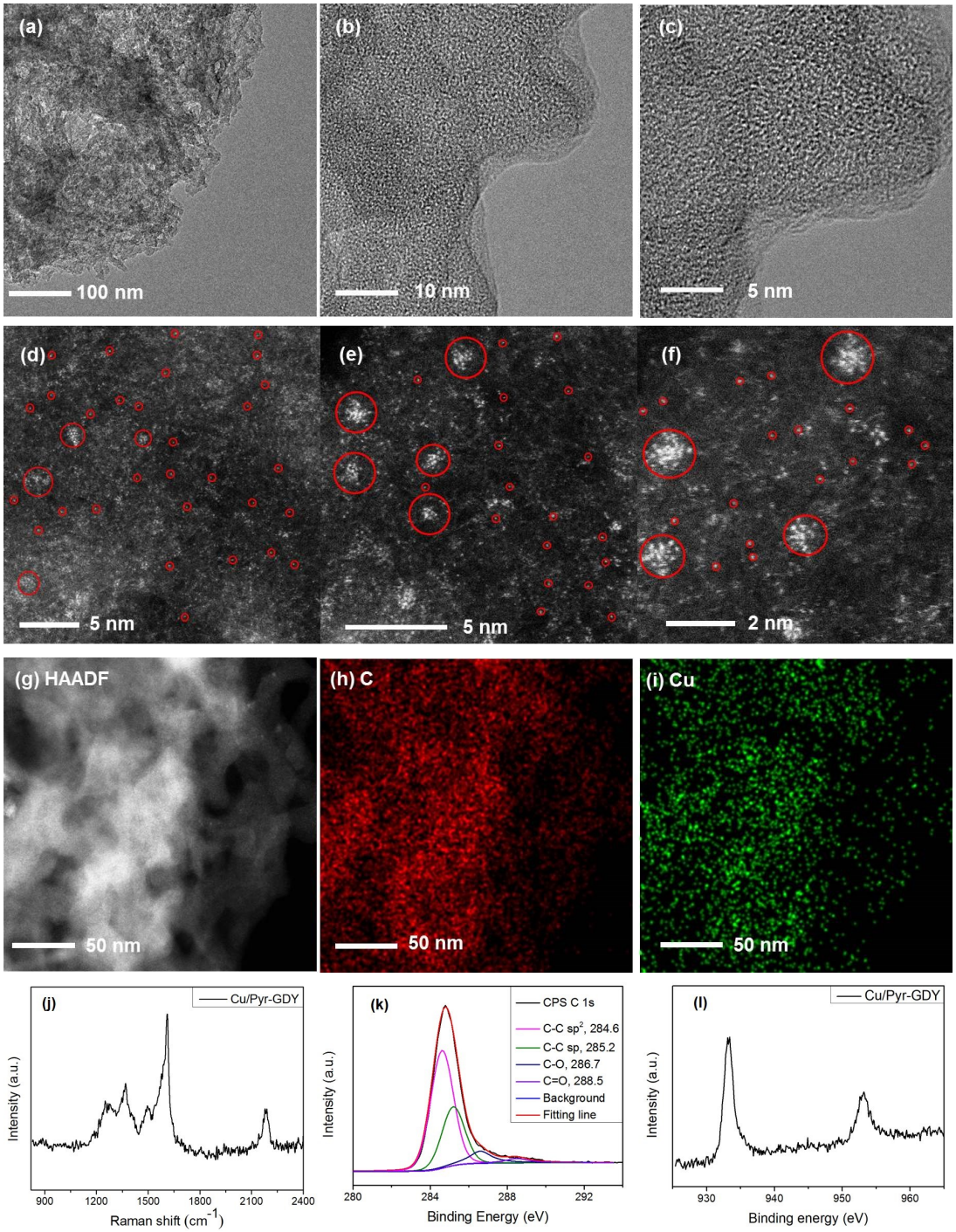

Figure S1. (a–c) HRTEM images of Cu/Pyr-GDY at different scales; (d-f) Aberration-corrected high-magnification high-angle annular dark-field scanning transmission electron microscopy (HAADF-STEM) images of the as-prepared Cu/Pyr-GDY ((f) Zoomed-in image from (e)); (g-i) HAADF-STEM elemental mapping images of Cu/Pyr-GDY; (j) Raman spectrum of Cu/Pyr-GDY; (k) XPS spectrum for C 1s of Cu/Pyr-GDY; (l) XPS spectrum for Cu 2p of Cu/Pyr-GDY.

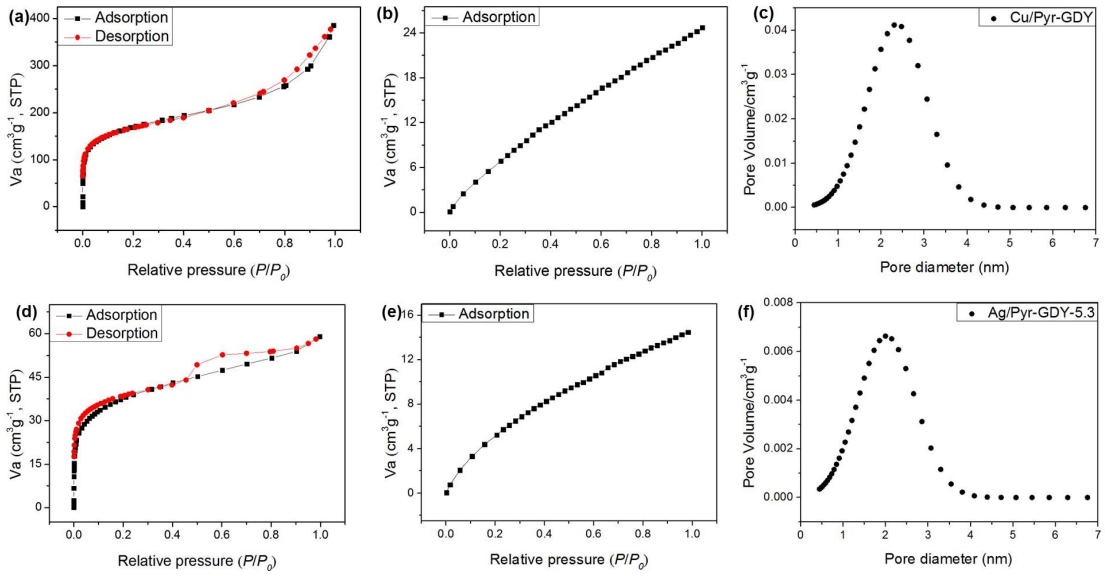

Figure S2. (a) N_2 adsorption–desorption isotherm of Cu/Pyr-GDY; (b) CO_2 adsorption isotherm of Cu/Pyr-GDY; (c) Pore diameter of Cu/Pyr-GDY; (d) N_2 adsorption–desorption isotherm of Ag/Pyr-GDY-5.3; (e) CO_2 adsorption isotherm of Ag/Pyr-GDY-5.3. (f) Pore diameter of Ag/Pyr-GDY-5.3. (Before the experiment, the powders of Cu/Pyr-GDY and Ag/Pyr-GDY-5.3 were heated at 120°C for 10 h.).

The difference of desorption curves for Cu/Pyr-GDY and Ag/Pyr-GDY-5.3 samples could be attributed to the existence of larger Ag nanoparticles in Ag/Pyr-GDY-5.3, which makes the desorption of N_2 more difficult compared with that of Cu/Pyr-GDY, thus Ag/Pyr-GDY-5.3 displays a desorption hysteresis. The pore size distribution was determined by the density functional theory (DFT) calculation.

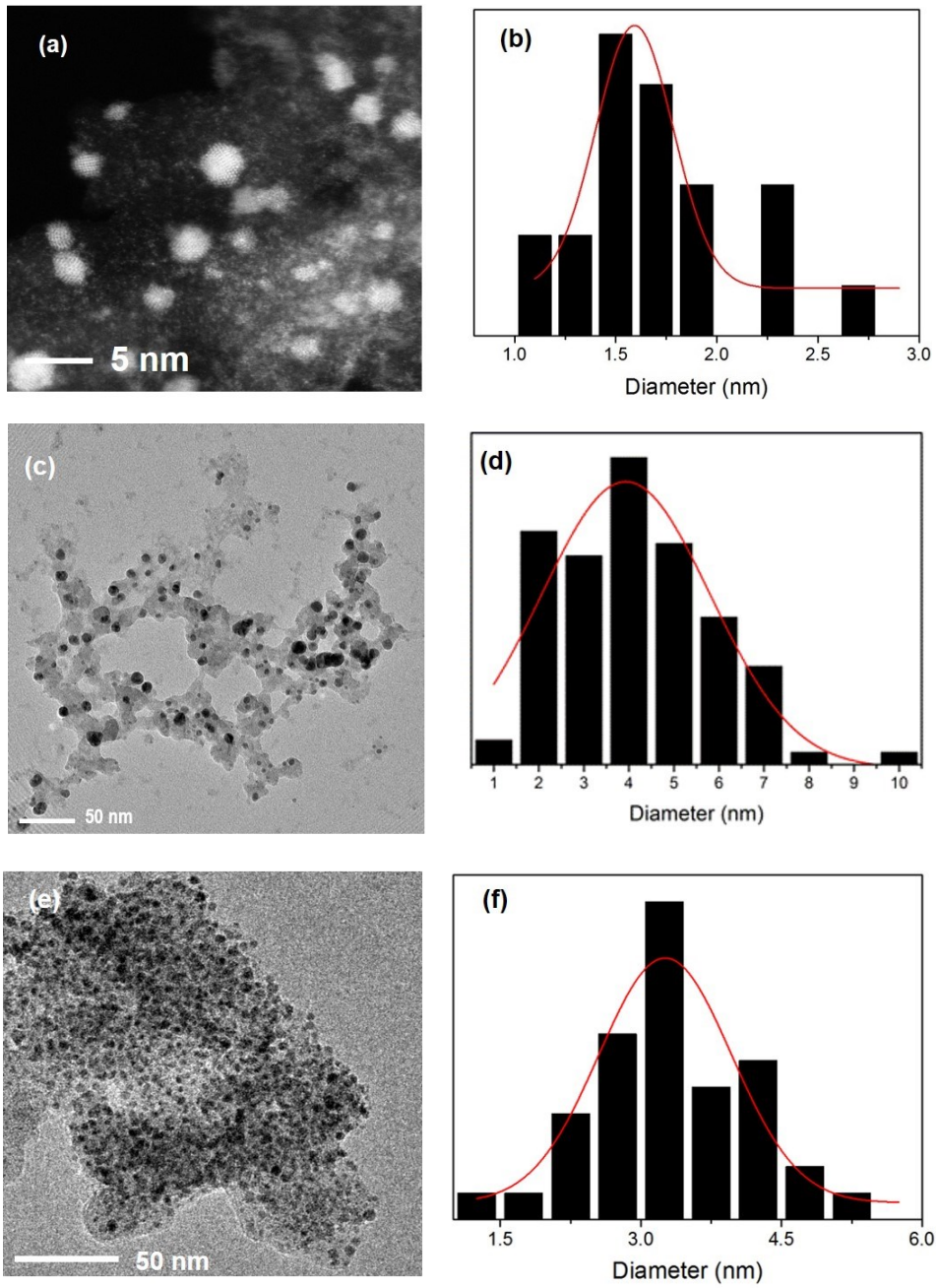

Figure S3. (a) Aberration-corrected high-magnification high-angle annular dark-field scanning transmission electron microscopy (HAADF-STEM) images of Ag/Pyr-GDY-5.3; (b) histogram for the size distribution of Ag particles in Ag/Pyr-GDY-5.3; (c) scanning transmission electron microscopy(STEM) images of Ag/Pyr-GDY-12.0 at various scales; (d) histogram for the size distribution of Ag particles in Ag/Pyr-GDY-12.0; (e) scanning transmission electron microscopy(STEM) images of Ag/Pyr-GDY-19.5 at various scales; (f) histogram for the size distribution of Ag particles in Ag/Pyr-GDY-19.5.

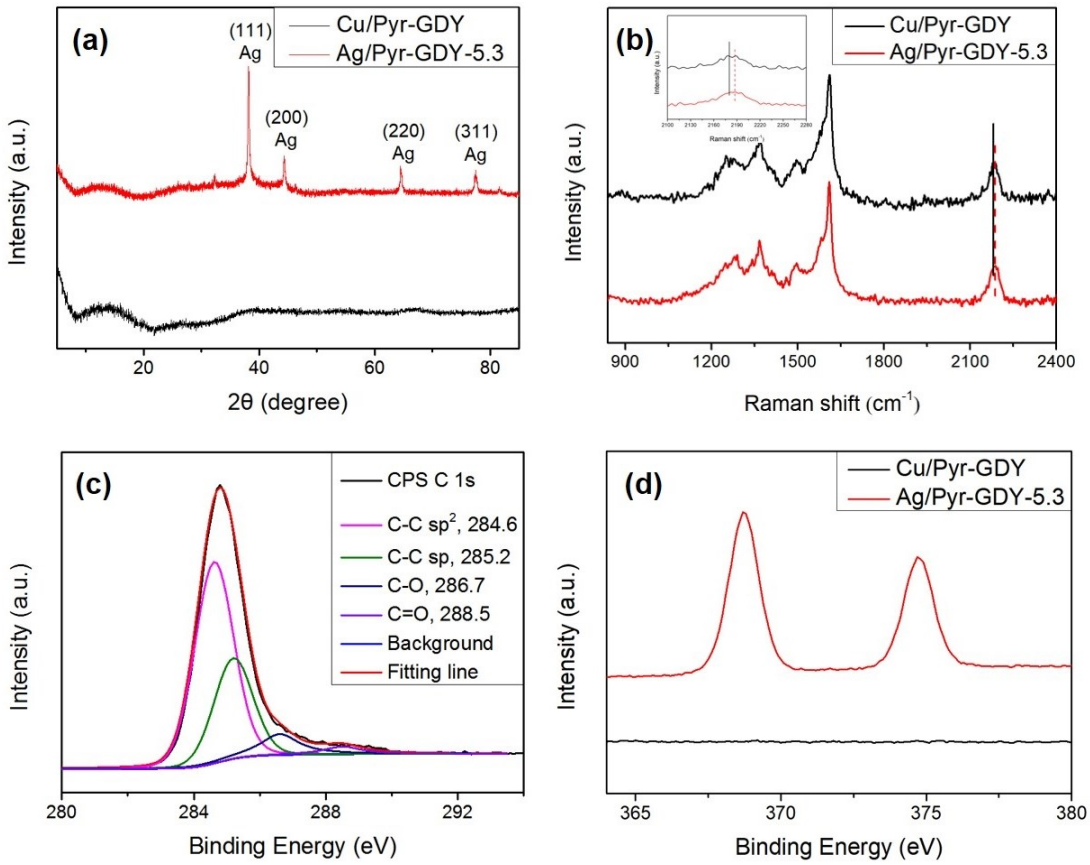

Figure S4. (a) XRD patterns of Cu/Pyr-GDY and Ag/Pyr-GDY-5.3; (b) Raman spectra of Cu/Pyr-GDY and Ag/Pyr-GDY-5.3; (c) XPS pattern for C 1s of Ag/Pyr-GDY-5.3; (d) XPS patterns for Ag 3d of Cu/Pyr-GDY and Ag/Pyr-GDY-5.3.

Catalyst Stability Test

Catalyst stability test was performed to exclude the possibility of homogeneous Ag species contributing to the catalytic performance. As shown in **Figure S4**, after the reaction for 1 h, the catalyst Ag/Pyr-GDY-5.3 was filtered, and the clear filtrate was stirred for another 1 h. It was found that the cycloaddition reaction completely stopped after the removal of the catalyst. The control experiment showed the conversion of benzylprop-2-ynylamine completed after 2 h in the presence of the catalyst. This catalyst was separated by centrifugation, and analyzed by ICP-MS. The Ag loading was determined to be 5.33%. The experiments described above confirmed that the reaction was catalyzed in a heterogeneous manner by Ag/Pyr-GDY-5.3.

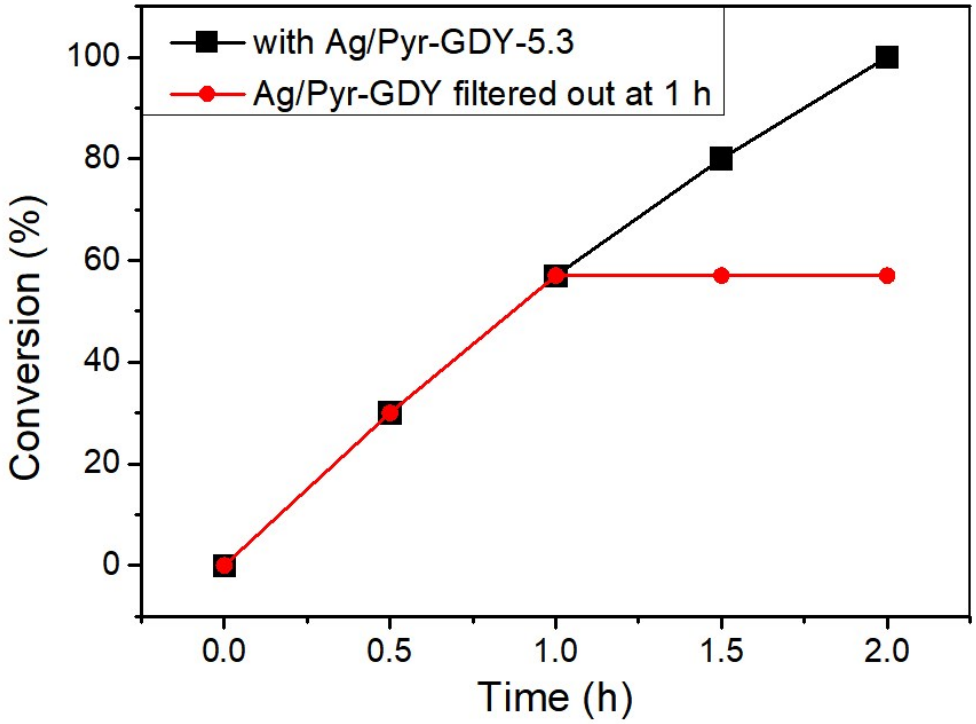

Figure S5. Comparison of the conversions over time for a normally conducted reaction (black line), and a reaction in which the catalyst was filtered out after 1 h reaction (red line).

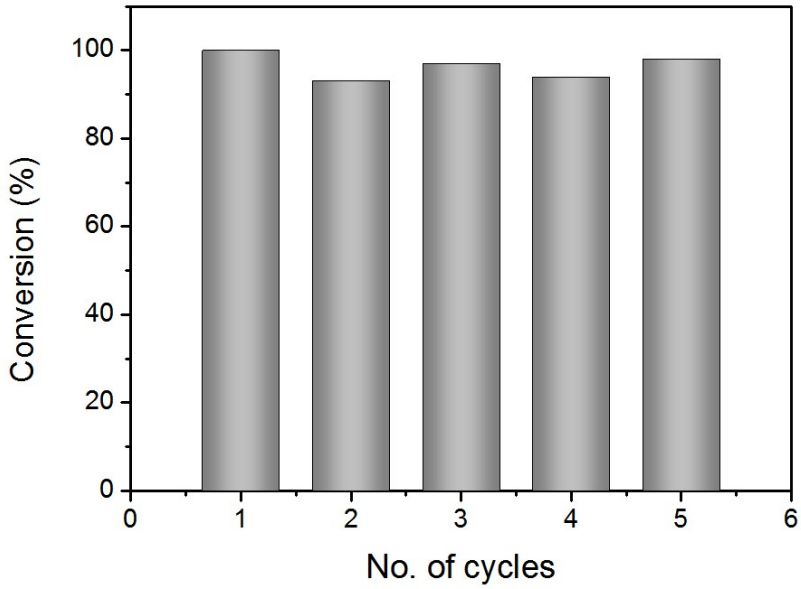

Figure S6. The recycling experiments for Ag/Pyr-GDY-5.3.

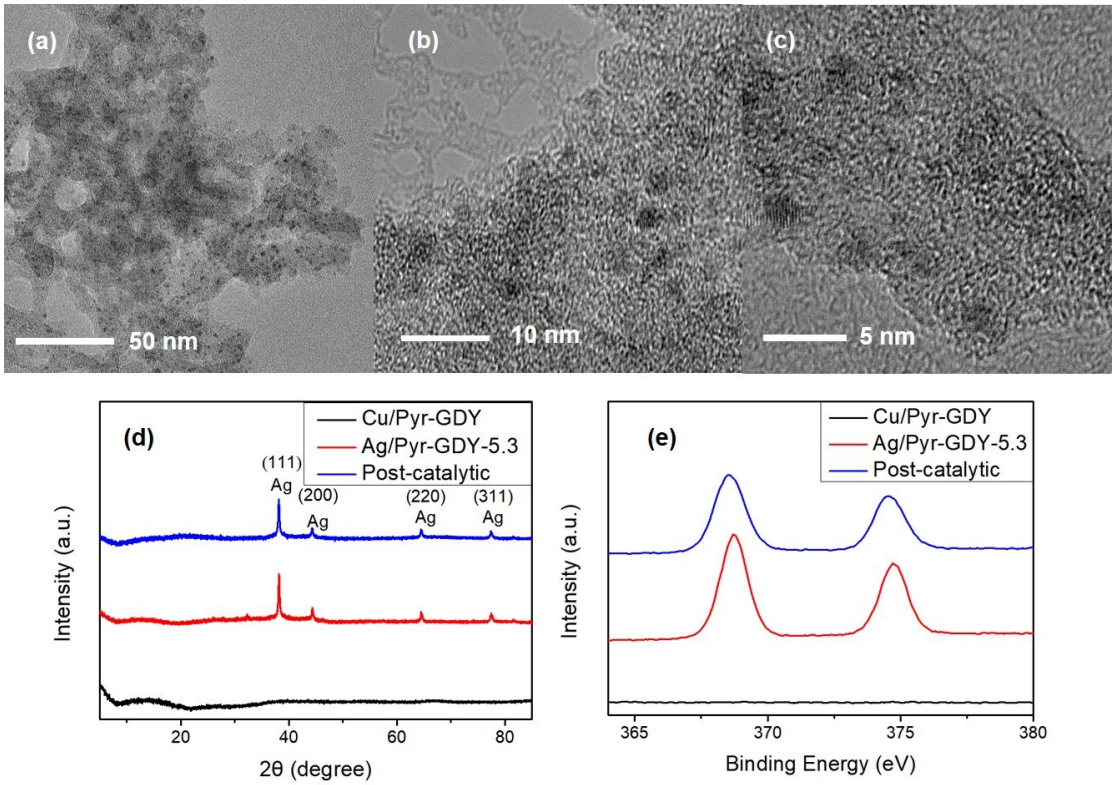

Figure S7. (a–c) HRTEM images of the recycled Ag/Pyr-GDY-5.3 at different magnifications; (d) XRD patterns of Cu/Pyr-GDY, as-prepared and post-catalytic Ag/Pyr-GDY-5.3; (e) XPS profiles for Ag 3d of Cu/Pyr-GDY, as-prepared and post-catalytic Ag/Pyr-GDY-5.3.

Preparation of 1

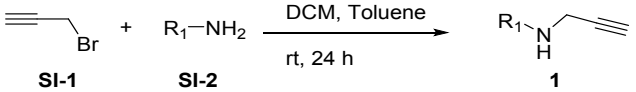

To a solution of the primary amine **SI-2** (25 mmol) in DCM (10 mL) was added dropwise a solution of 3-bromo-1-propyne **SI-1** (5 mmol)in toluene (10 mL). The mixture was stirred for 24 h, and then washed 3 times with distilled water (20 mL). The resulting organic phase was dried with anhydrous Na_2SO_4, and then filtered, and the solvent was evaporated under reduced pressure. Purification of the desired product was performed by column chromatography (petroleum ether/ethyl acetate, 5:1, v/v).

<u>Synthesis of 2</u>

General Procedure:

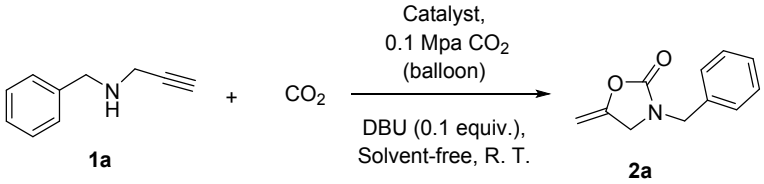

A sealed reaction tube containing the catalyst,1,8-diazabicyclo[5.4.0]undec-7-ene (DBU, 0.02 mmol, 0.1 equiv.), **1a** (0.2 mmol, 1.0 equiv.) were evacuated and purged with CO_2 gas three times. The tube was then connected to a balloon filled with CO_2, and the mixture therein was stirred at room temperature for 2 h. The mixture was purified by column chromatography onsilica gel (petroleum ether/ethyl acetate, 2:1, v/v) to afford the desired pure products **2** (yellow oil, 37 mg, 98% yield).

To evaluate the efficiency of Ag/Pyr-GDY, the reaction of **1a** and CO_2 was scaled up to a gram scale. Ag/Pyr-GDY-5.3 (1.5 mg), propargylamines **1a** (1.1607 g, 8 mmol), DBU (0.08 mmol) were evacuated and purged with CO_2 gas three times. The tube was then connected to a balloon filled with CO_2 and stirred at room temperature. After 60 h, the yield of **2a** was >99%, as determined by ^{1}H NMR spectroscopy using 1,3,5-trimethoxybenzene as the internal standard. The TON was calculated according to the equation (TON = mole of products/mol of catalytic sites) and the values of TON and TOF were 10971 and 183 h^{-1}, respectively.

To evaluate the efficiency of Ag/Pyr-GDY, the reaction of **1a** and CO_2 was scaled up to a gram scale. Ag/Pyr-GDY-5.3 (1.5 mg), propargylamines **1a** (2.6116 g, 18

mmol), DBU (0.18 mmol) were evacuated and purged with CO_2 gas three times. The tube was then connected to a balloon filled with CO_2 and stirred at room temperature. After 220 h, the yield of **2a** was 83%, as determined by ^{1}H NMR spectroscopy using 1,3,5-trimethoxybenzene as the internal standard. The TON was calculated according to the equation (TON = mole of products/mol of catalytic sites) and the values of TON and TOF were 20488 and 93 h^{-1}, respectively.

The Reaction Process Monitored by ^{1}H NMR ($CDCl_3$).

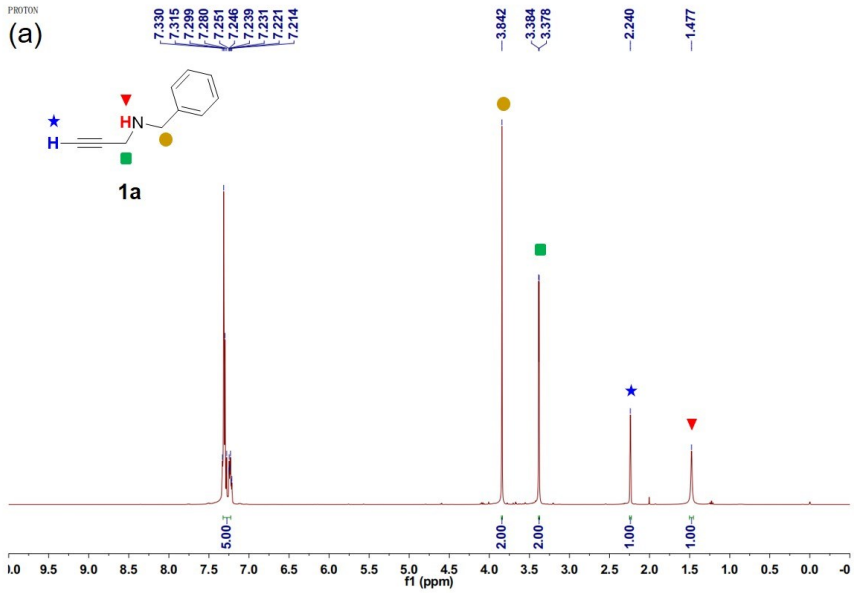

Figure S8a. ^{1}H NMR of **1a** (400 MHz, $CDCl_3$), δ 7.32 – 7.23 (m, 5.0H, Ph-*H*), 3.84 (s, 2.0H, NCH_2Ph), 3.38 (d, J = 2.4 Hz, 2.0H, NHCH_2C≡CH), 2.24 (s, 1.0H, C≡C*H*), 1.48 (s, 1.0H, NH).

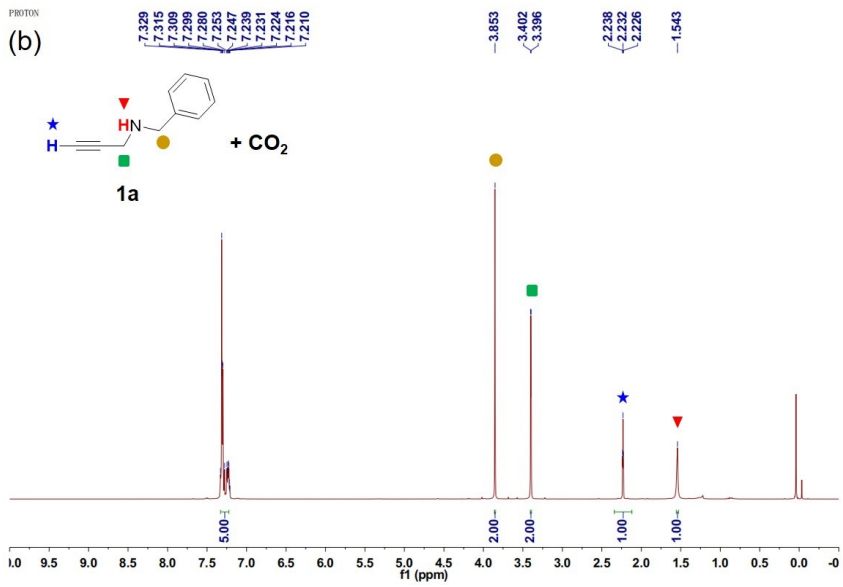

Figure S8b. ^{1}H NMR of **1a** with CO_2 (400 MHz, $CDCl_3$), δ 7.33 – 7.22 (m, 5.0H, Ph-*H*), 3.85 (s, 2.0H, NC*H*$_2$Ph), 3.40 (d, *J* = 2.4 Hz, 2.0H, NHC*H*$_2$C≡CH), 2.23 (t, *J* = 2.3 Hz, 1.0H, C≡C*H*), 1.54 (s, 1.0H, NH).

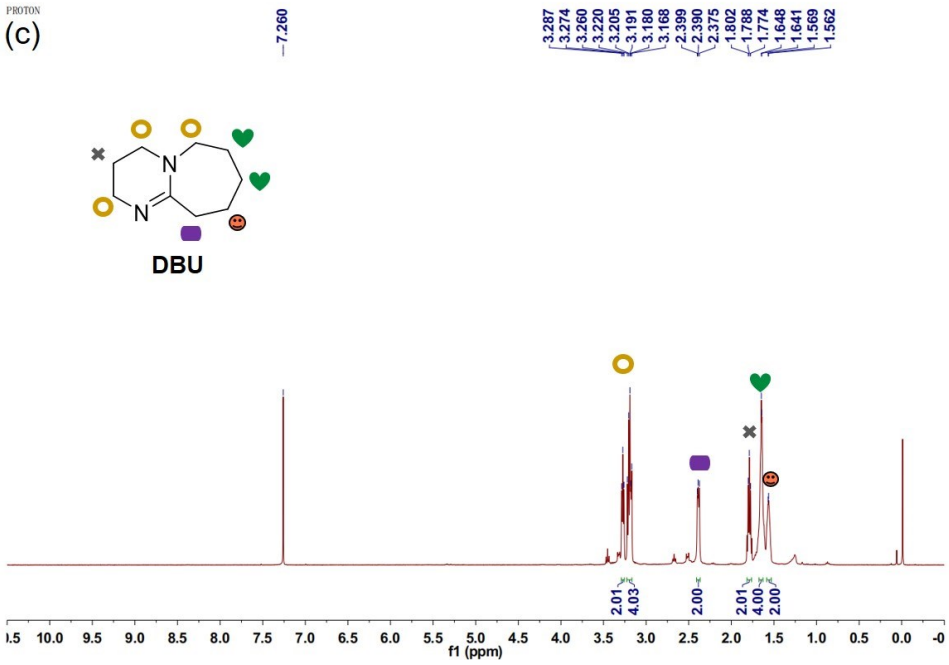

Figure S8c. ^{1}H NMR of DBU (400 MHz, $CDCl_3$), δ 3.29 – 3.25 (m, 2.0H), 3.23 – 3.17 (m, 4.0H), 2.41 – 2.37 (m, 2.0H), 1.82 – 1.76 (m, 2.0H), 1.64 (d, *J* = 2.7 Hz, 4.0H), 1.57 (d, *J* = 2.7 Hz, 2.0H).

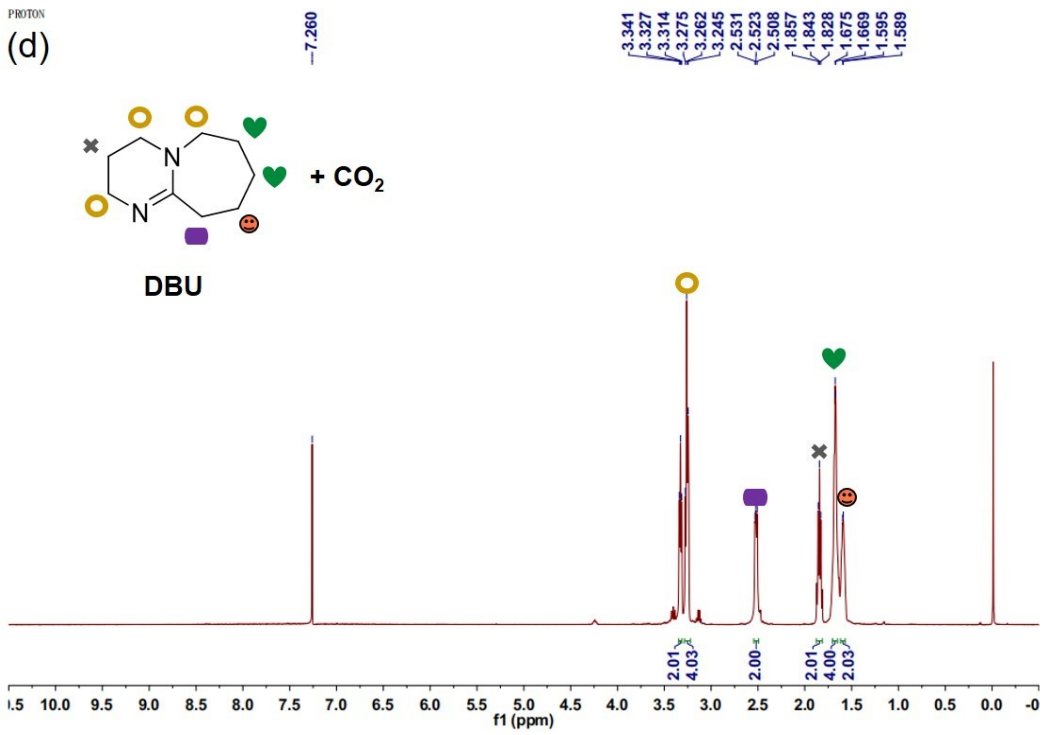

Figure S8d. ^{1}H NMR of DBU + CO_2 (400 MHz, $CDCl_3$), δ 3.35 – 3.31 (m, 2.0H), 3.26 (t, J = 6.1 Hz, 4.0H), 2.54 – 2.49 (m, 2.0H), 1.87 – 1.81 (m, 2.0H), 1.67 (d, J = 2.4 Hz, 4.0H), 1.59 (d, J = 2.7 Hz, 2.0H).

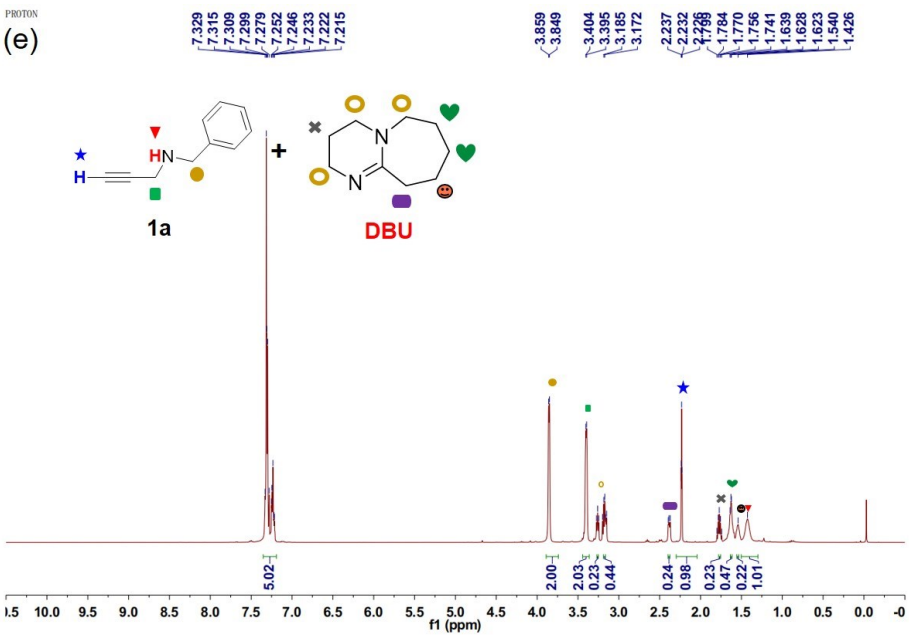

Figure S8e. ^{1}H NMR of **1a** + DBU (400 MHz, $CDCl_3$), δ 7.35 – 7.19 (m, 5.0H, **1a**), 3.85 (d, J = 4.2 Hz, 2.0H, **1a**), 3.40 (d, J = 3.6 Hz, 2.0H, **1a**), 3.26 (s, 0.2H, **DBU**), 3.18 (d, J = 5.3 Hz, 0.4H, **DBU**), 2.39 (d, J = 3.4 Hz, 0.2H, **DBU**), 2.23 (t, J = 2.3 Hz, 1.0H, **1a**), 1.76 (d, J = 5.8 Hz, 0.2H, **DBU**), 1.63 (d, J = 2.2 Hz, 0.4H, **DBU**), 1.54 (s, 0.2H, **DBU**), 1.36 (d, J = 49.8 Hz, 1.0H, **1a**).

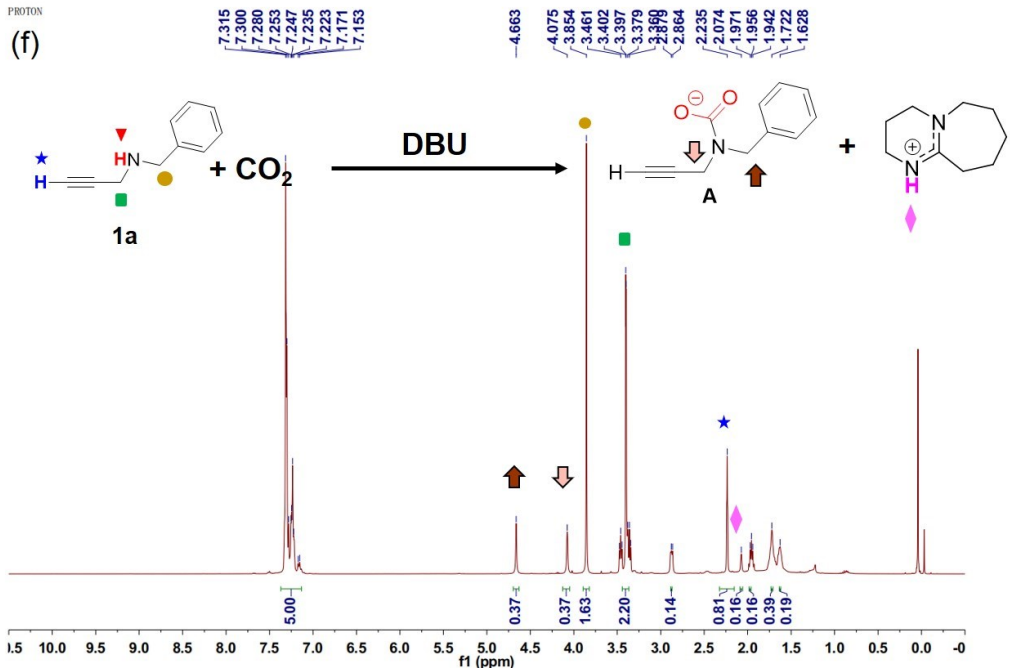

Figure S8f. ^{1}H NMR of **1a** + DBU + CO_2 (400 MHz, $CDCl_3$), δ 7.37 – 7.13 (m, 5.0H, **1a** + **A**), 4.66 (s, 0.4H, **A**), 4.08 (s, 0.4H, **A**), 3.85 (s, 1.6H, **1a**), 3.39 (t, J = 4.7 Hz, 2.2H, **1a** + **DBU**), 2.88 (s, 0.1H, **DBU**), 2.23 (s, 0.8H, **1a**), 2.07 (s, 0.2H, **DBU**), 1.98 – 1.93 (m, 0.2H, **DBU**), 1.72 (s, 0.4H, **DBU**), 1.63 (s, 0.2H, **DBU**).

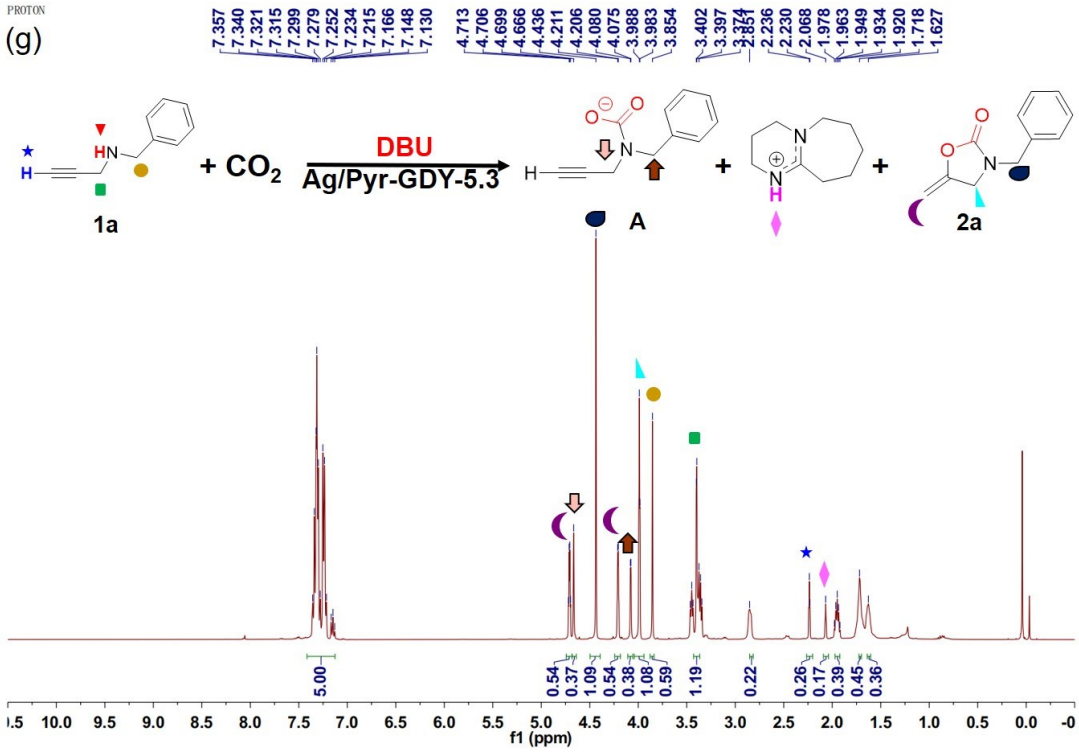

Figure S8g. ^{1}H NMR of **1a** + DBU + CO_2 + Ag/Pyr-GDY-5.3 (400 MHz, $CDCl_3$), δ 7.42 – 7.13 (m, 5H, **1a** + **2a** + **A**), 4.71 (q, J = 2.7 Hz, 0.5H, **2a**), 4.67 (s, 0.4H, **A**),

4.44 (s, 1.1H, **2a**), 4.21 (d, *J* = 2.3 Hz, 0.5H, **2a**), 4.08 (d, *J* = 1.8 Hz, 0.4H, **A**), 3.99 (d, *J* = 2.1 Hz, 1.1H, **2a**), 3.85 (s, 0.6H,**1a**), 3.39 (t, *J* = 5.6 Hz, 1.2H, **1a** + **DBU**), 2.85 – 2.81 (m, 0.2H, **DBU**), 2.23 (d, *J* = 2.2 Hz, 0.3H, **1a**), 2.07 (s, 0.2H, **DBU**), 1.97 – 1.92 (m, 0.4H , **DBU**), 1.72 (s, 0.5H , **DBU**), 1.63 (s, 0.4H , **DBU**).

Characterization of 1

N-benzylprop-2-yn-1-amine (**1a**)

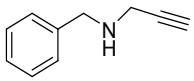

Yellow oil. (0.62 g, 86%); ^{1}H NMR (400 MHz, $CDCl_3$) δ 7.32 – 7.23 (m, 5H, Ph-*H*), 3.84 (s, 2H, NCH_2Ph), 3.38 (d, *J* = 2.4 Hz, 2H, NHCH_2C≡CH), 2.24 (s, 1H, C≡C*H*), 1.48 (s, 1H, NH); ^{13}C NMR (100 MHz, $CDCl_3$) δ 139.3, 128.3, 128.3, 127.1, 82.0, 71.5, 52.2, 37.2.

3-(4-fluorobenzyl)-5-methyleneoxazolidin-2-one (**1b**)

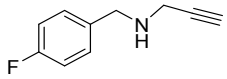

Yellow oil. (0.41 g, 50%);^{1}H NMR (400 MHz, $CDCl_3$) δ 7.29 (dd, *J* = 8.4, 5.6 Hz, 2H), 6.99 (t, *J* = 8.7 Hz, 2H), 3.81 (s, 2H), 3.37 (d, *J* = 2.4 Hz, 2H), 2.27 (t, *J* = 2.4 Hz, 1H), 1.52 (s, 1H); ^{13}C NMR (100 MHz, $CDCl_3$) δ 161.8 (d, *J* = 250.6 Hz), 134.9(d, *J* = 3.1 Hz), 129.8 (d, *J* = 7.9 Hz), 114.9 (d, *J* = 27.1 Hz), 81.8, 71.5, 51.2, 36.9; ^{19}F NMR (376 MHz, $CDCl_3$) δ -115.63.

N-(4-chlorobenzyl)prop-2-yn-1-amine (**1c**)

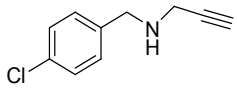

Yellow oil. (0.48 g, 54%); ^{1}H NMR (400 MHz, $CDCl_3$) δ 7.25 (s, 4H), 3.82 – 3.78 (m, 2H), 3.38 –3.34 (m, 2H), 2.27 (t, *J* = 2.4 Hz, 1H), 1.51 (s, 1H); ^{13}C NMR (100 MHz, $CDCl_3$) δ 137.7, 132.5, 129.4, 128.2, 81.7, 71.6, 51.1, 36.9.

N-(4-bromobenzyl)prop-2-yn-1-amine (**1d**)

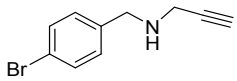

Yellow oil. (0.50 g, 45%); ^{1}H NMR (400 MHz, $CDCl_3$) δ 7.41 (d, *J* = 8.4 Hz, 2H), 7.19 (d, *J* = 8.4 Hz, 2H), 3.78 (s, 2H), 3.36 (d, *J* = 2.4 Hz, 2H), 2.27 (t, *J* = 2.4 Hz, 1H), 1.51 (s, 1H); ^{13}C NMR (100 MHz, $CDCl_3$) δ 138.1, 131.2, 129.8, 120.6, 81.7, 71.6, 51.1, 36.9.

N-(4-methoxybenzyl)prop-2-yn-1-amine (**1e**)

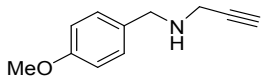

Yellow oil. (0.61 g, 70%); ^{1}H NMR (400 MHz, $CDCl_3$) δ 7.27 – 7.22 (m, 2H), 6.88 –

6.82 (m, 2H), 3.79 (s, 2H), 3.77 (s, 3H), 3.38 (d, J = 2.4 Hz, 2H), 2.26 (t, J = 2.4 Hz, 1H), 1.50 (s, 1H); ^{13}C NMR (100 MHz, $CDCl_3$) δ 158.6, 131.3, 129.4, 113.6, 82.0, 71.4, 55.0, 51.4, 37.0.

N-(4-methylbenzyl)prop-2-yn-1-amine (**1f**)

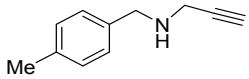

Yellow oil. (0.46 g, 58%); ^{1}H NMR (400 MHz, $CDCl_3$) δ 7.20 (d, J = 7.9 Hz, 2H), 7.10 (d, J = 7.9 Hz, 2H), 3.78 (s, 2H), 3.35 (d, J = 2.4 Hz, 2H), 2.30 (s, 3H), 2.22 (t, J = 2.4 Hz, 1H), 1.48 (s, 1H); ^{13}C NMR (100 MHz, $CDCl_3$) δ 136.3, 136.1, 128.8, 128.1, 81.9, 71.3, 51.6, 36.9, 20.8.

N-(4-(tert-butyl)benzyl)prop-2-yn-1-amine (**1g**)

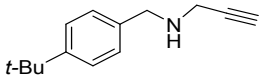

Yellow oil. (0.56 g, 56%);. ^{1}H NMR (400 MHz, $CDCl_3$) δ 7.39 – 7.33 (m, 2H), 7.30 – 7.27 (m, 2H), 3.86 (s, 2H), 3.43 (d, J = 2.4 Hz, 2H), 2.26 (t, J = 2.4 Hz, 1H), 1.58 (s, 1H), 1.31 (s, 9H); ^{13}C NMR (100 MHz, $CDCl_3$) δ 150.1, 136.3, 128.1, 125.4, 82.1, 71.5, 51.9, 37.3, 34.5, 31.4.

N-(3-methylbenzyl)prop-2-yn-1-amine (**1h**)

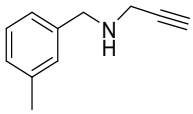

Yellow oil. (0.43 g, 54%); ^{1}H NMR (400 MHz, $CDCl_3$) δ 7.20 – 7.02 (m, 4H), 3.79 (s, 2H), 3.37 (d, J = 2.4 Hz, 2H), 2.31 (s, 3H), 2.23 (t, J = 2.4 Hz, 1H), 1.46 (s, 1H); ^{13}C NMR (100 MHz, $CDCl_3$) δ 139.1, 137.7, 128.9, 128.0, 127.6, 125.2, 81.9, 71.3, 51.9, 37.0, 21.1.

N-(2-chlorobenzyl)prop-2-yn-1-amine (**1i**)

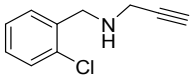

Yellow oil. (0.55 g, 61%); ^{1}H NMR (400 MHz, $CDCl_3$) δ 7.42 – 7.20 (m, 4H), 3.97 (s, 2H), 3.46 – 3.43 (m, 2H), 2.27 (t, J = 2.4 Hz, 1H), 1.66 (s, 1H); ^{13}C NMR (100 MHz, $CDCl_3$) δ 136.8, 133.8, 130.2, 129.5, 128.5, 126.8, 81.8, 71.7, 49.8, 37.5.

N-(2-methylbenzyl)prop-2-yn-1-amine (**1j**)

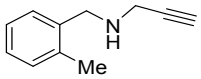

Yellow oil. (0.48 g, 60%); ^{1}H NMR (400 MHz, $CDCl_3$) δ 7.32 – 7.27 (m, 1H), 7.19 – 7.12 (m, 3H), 3.85 (s, 2H), 3.44 (d, *J* = 2.4 Hz, 2H), 2.36 (s, 3H), 2.26 (t, *J* = 2.4 Hz, 1H), 1.39 (s, 1H); ^{13}C NMR (100 MHz, $CDCl_3$) δ 137.3, 136.5, 130.2, 128.6, 127.1, 125.8, 82.2, 71.4, 49.9, 37.6, 18.8.

N-benzylbut-2-yn-1-amine (**1k**)

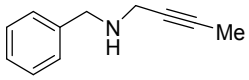

Yellow oil. (0.68 g, 85%); ^{1}H NMR (400 MHz, $CDCl_3$) δ 7.38 – 7.20 (m, 5H), 3.84 (s, 2H), 3.36 (q, *J* = 2.3 Hz, 2H), 1.83 (t, *J* = 2.4 Hz, 3H), 1.51 (s, 1H); ^{13}C NMR (100 MHz, $CDCl_3$) δ139.5, 128.2, 128.2, 126.8, 79.0, 53.0, 52.3, 37.7, 3.3.

N-(1-phenylethyl)prop-2-yn-1-amine (**1l**)

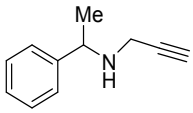

Yellow oil. (0.68 g, 85%); ^{1}H NMR (400 MHz, $CDCl_3$) δ 7.35 – 7.22 (m, 5H), 4.00 (q, *J* = 6.6 Hz, 1H), 3.24 (ddd, *J* = 77.9, 17.1, 2.4 Hz, 2H), 2.20 (t, *J* = 2.4 Hz, 1H), 1.61 (s, 1H), 1.35 (d, *J* = 6.6 Hz, 3H); ^{13}C NMR (100 MHz, $CDCl_3$) δ 144.3, 128.4, 127.1, 126.8, 82.2, 71.2, 56.2, 35.8, 23.8.

N-(prop-2-yn-1-yl)aniline (**1m**)

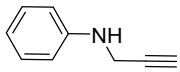

Red oil. (0.36 g, 55%); ^{1}H NMR (400 MHz, $CDCl_3$) δ 7.22 – 7.17 (m, 2H), 6.81 – 6.74 (m, 1H), 6.67 – 6.63 (m, 2H), 3.87 (d, *J* = 2.5 Hz, 2H), 3.81 (s, 1H), 2.19 (t, *J* = 2.4 Hz, 1H); ^{13}C NMR (100 MHz, $CDCl_3$) δ 146.72, 129.12, 118.47, 113.39, 80.97, 71.20, 33.44.

Characterization of 2

3-benzyl-5-methyleneoxazolidin-2-one (**2a**)

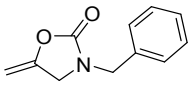

Yellow oil. (37 mg, 98%); ^{1}H NMR (400 MHz, $CDCl_3$) δ 7.37 – 7.22 (m, 5H, Ph-*H*), 4.71 (dd, *J* = 5.6, 2.7 Hz, 1H, C=C*H*aHb), 4.44 (s, 2H, NCH_2Ph), 4.21 (dd, *J* = 5.3, 2.2 Hz, 1H, *C*=*C*H*aHb*), 3.99 (t, *J* = 2.4 Hz, 2H, H_2C=CCH_2); ^{13}C NMR (100 MHz, $CDCl_3$) δ 155.6 (*C*=O), 148.9 (H_2C=*C*), 134.9 (Ar*C*), 128.9 (Ar*C*), 128.2 (Ar*C*), 128.1 (Ar*C*), 86.7(H_2*C*=C),, 47.8 (N*C*H_2Ph), 47.2 (C*C*H_2N).

3-(4-fluorobenzyl)-5-methyleneoxazolidin-2-one (**2b**)

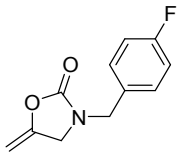

Yellow oil. (37 mg, 89%); ^{1}H NMR (400 MHz, $CDCl_3$) δ 7.35 – 7.20 (m, 2H), 7.05 (t, *J* = 8.5 Hz, 2H), 4.74 (d, *J* = 2.5 Hz, 1H), 4.44 (s, 2H), 4.26 (d, *J* = 1.7 Hz, 1H), 4.03 (s, 2H); ^{13}C NMR (100 MHz, $CDCl_3$) δ 162.5 (d, *J* = 245.5 Hz), 155.5, 148.7, 130.8 (d, *J* = 3.2 Hz), 129.9 (d, *J* = 7.2 Hz), 115.8 (d, *J* = 21.5 Hz), 86.8, 47.1, 47.0; ^{19}F NMR (376 MHz, $CDCl_3$) δ -113.69.

3-(4-chlorobenzyl)-5-methyleneoxazolidin-2-one (**2c**)

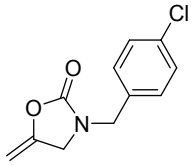

White soild. (42 mg, 95%);^{1}H NMR (400 MHz, $CDCl_3$) δ 7.36 – 7.31 (m, 2H), 7.25 – 7.20 (m, 2H), 4.75 (dd, *J* = 5.7, 2.7 Hz, 1H), 4.44 (s, 2H), 4.27 (dd, *J* = 5.3, 2.2 Hz, 1H), 4.03 (t, *J* = 2.3 Hz, 2H); ^{13}C NMR (100 MHz, $CDCl_3$) δ 155.5, 148.6, 134.1, 133.5, 129.4, 129.1, 87.0, 47.1, 47.1.

3-(4-bromobenzyl)-5-methyleneoxazolidin-2-one (**2d**)

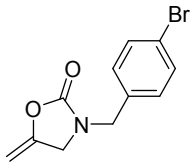

White soild. (49 mg, 92%);^{1}H NMR (400 MHz, $CDCl_3$) δ 7.45 (d, *J* = 8.4 Hz, 2H), 7.13 (d, *J* = 8.3 Hz, 2H), 4.71 (dd, *J* = 5.6, 2.7 Hz, 1H), 4.38 (s, 2H), 4.23 (dd, *J* = 5.3, 2.2 Hz, 1H), 4.00 (t, *J* = 2.3 Hz, 2H); ^{13}C NMR (100 MHz, $CDCl_3$) δ 155.4, 148.6, 133.9, 131.9, 129.7, 122.1, 86.9, 47.1, 47.0.

3-(4-methoxybenzyl)-5-methyleneoxazolidin-2-one (**2e**)

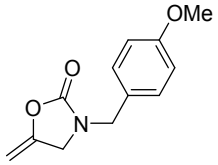

Yellow oil. (43 mg, 98%); ^{1}H NMR (400 MHz, $CDCl_3$) δ 7.20 (d, *J* = 8.6 Hz, 2H), 6.88 (d, *J* = 8.6 Hz, 2H), 4.70 (dd, *J* = 5.5, 2.7 Hz, 1H), 4.39 (s, 2H), 4.23 (dd, *J* = 5.0, 2.2 Hz, 1H), 4.01 (t, *J* = 2.3 Hz, 2H), 3.80 (s, 3H); ^{13}C NMR (100 MHz, $CDCl_3$) δ 159.3, 155.3, 148.9, 129.4, 126.8, 114.1, 86.4, 55.1, 47.0, 46.8.

3-(4-methylbenzyl)-5-methyleneoxazolidin-2-one (**2f**)

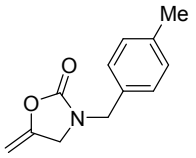

White soild. (39 mg, 96%); ^{1}H NMR (400 MHz, $CDCl_3$) δ 7.09 (s, 4H), 4.65 (dd, *J* = 5.6, 2.7 Hz, 1H), 4.35 (s, 2H), 4.15 (dd, *J* = 5.2, 2.2 Hz, 1H), 3.93 (t, *J* = 2.4 Hz, 2H), 2.28 (s, 3H); ^{13}C NMR (100 MHz, $CDCl_3$) δ 155.6, 149.0, 138.0, 131.8, 129.6, 128.2, 86.6, 47.5, 47.1, 21.1.

3-(4-(tert-butyl)benzyl)-5-methyleneoxazolidin-2-one (**2g**)

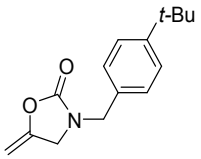

White soild. (48 mg, 97%);^{1}H NMR (400 MHz, $CDCl_3$) δ 7.38 (d, *J* = 8.3 Hz, 2H), 7.20 (d, *J* = 8.2 Hz, 2H), 4.73 (dd, *J* = 5.5, 2.7 Hz, 1H), 4.43 (s, 2H), 4.23 (dd, *J* = 5.1, 2.2 Hz, 1H), 4.02 (t, *J* = 2.3 Hz, 2H), 1.31 (s, 9H); ^{13}C NMR (100 MHz, $CDCl_3$) δ

155.6, 151.3, 149.0, 131.9, 128.0, 125.8, 86.6, 47.4, 47.2, 34.6, 31.3.

3-(3-methylbenzyl)-5-methyleneoxazolidin-2-one (**2h**)

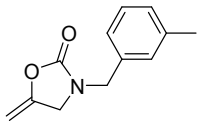

Yellow oil. (39 mg, 95%); ^{1}H NMR (400 MHz, $CDCl_3$) δ 7.30 – 7.03 (m, 4H), 4.73 (d, *J* = 2.5 Hz, 1H), 4.42 (s, 2H), 4.24 (d, *J* = 2.0 Hz, 1H), 4.02 (s, 2H), 2.35 (s, 3H); ^{13}C NMR (100 MHz, $CDCl_3$) δ 155.6, 148.9, 138.7, 134.8, 128.9, 128.8, 128.7, 125.2, 86.6, 47.7, 47.1, 21.3.

3-(2-chlorobenzyl)-5-methyleneoxazolidin-2-one (**2i**)

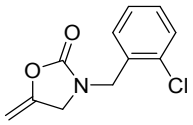

White soild. (44 mg, 98%);^{1}H NMR (400 MHz, $CDCl_3$) δ 7.34 – 7.18 (m, 4H), 4.67 (dd, *J* = 5.7, 2.7 Hz, 1H), 4.54 (s, 2H), 4.19 (dd, *J* = 5.3, 2.2 Hz, 1H), 4.02 (t, *J* = 2.4 Hz, 2H); ^{13}C NMR (100 MHz, $CDCl_3$) δ 155.5, 148.8, 133.7, 132.6, 130.3, 129.8, 129.6, 127.4, 86.8, 47.6, 45.1.

3-(2-methylbenzyl)-5-methyleneoxazolidin-2-one (**2j**)

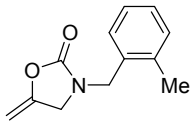

White soild. (39 mg, 97%); ^{1}H NMR (400 MHz, $CDCl_3$) δ 7.28 – 7.16 (m, 4H), 4.74 (dd, *J* = 5.6, 2.7 Hz, 1H), 4.50 (s, 2H), 4.23 (dd, *J* = 5.2, 2.2 Hz, 1H), 3.96 (t, *J* = 2.3 Hz, 2H), 2.34 (s, 3H); ^{13}C NMR (100 MHz, $CDCl_3$) δ 155.3, 148.9, 136.9, 132.7, 130.9, 129.1, 128.5, 126.3, 86.8, 47.2, 46.0, 19.0.

(Z)-3-benzyl-5-ethylideneoxazolidin-2-one (**2k**)

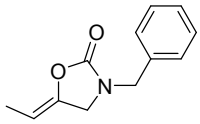

Yellow oil. (39 mg, 96%); ^{1}H NMR (400 MHz, $CDCl_3$) δ 7.40 – 7.25 (m, 5H), 4.60 – 4.51 (m, 1H), 4.46 (s, 2H), 3.99 – 3.90 (m, 2H), 1.67 (dt, *J* = 6.9, 2.2 Hz, 3H); ^{13}C NMR (100 MHz, $CDCl_3$) δ 156.0, 141.6, 135.1, 128.9, 128.1, 128.1, 97.5, 47.8, 47.0, 9.9.

5-methylene-3-(1-phenylethyl)oxazolidin-2-one (**2l**).

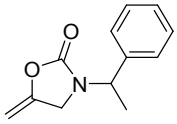

Yellow oil. (39 mg, 97%); ^{1}H NMR (400 MHz, $CDCl_3$) δ 7.33 – 7.20 (m, 5H), 5.19 (q, *J* = 7.1 Hz, 1H), 4.63 (dd, *J* = 5.5, 2.7 Hz, 1H), 4.14 (dd, *J* = 5.1, 2.2 Hz, 1H), 4.03 (dt, *J* = 14.2, 2.3 Hz, 1H), 3.69 (dt, *J* = 14.2, 2.4 Hz, 1H), 1.52 (d, *J* = 7.1 Hz, 3H); ^{13}C NMR (100 MHz, $CDCl_3$) δ 155.0, 149.2, 138.7, 128.8, 128.1, 126.9, 86.5, 51.3, 43.6, 16.3.

^{1}H and ^{13}C NMR Spectra

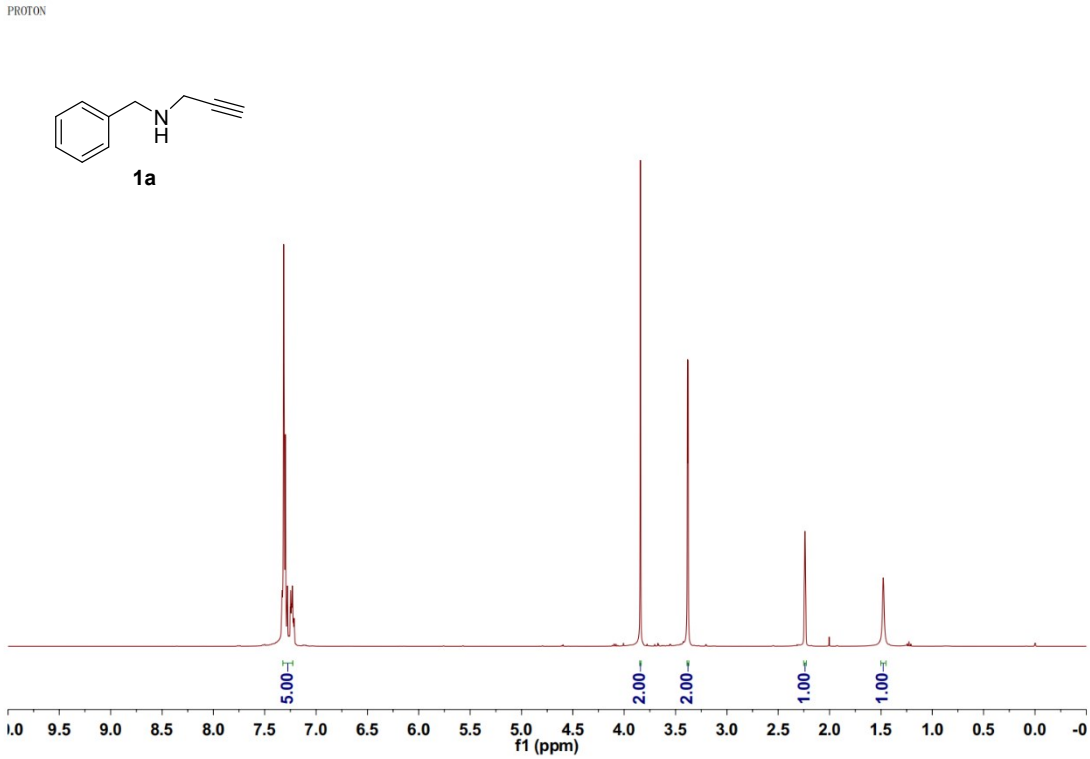

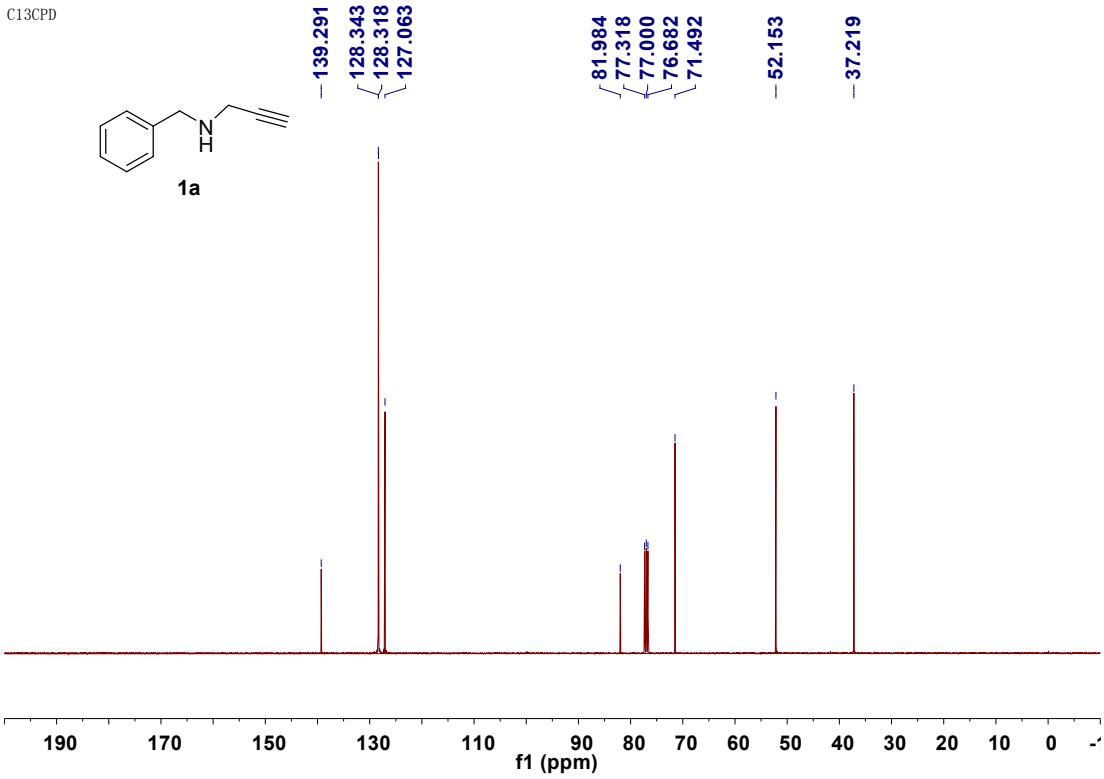

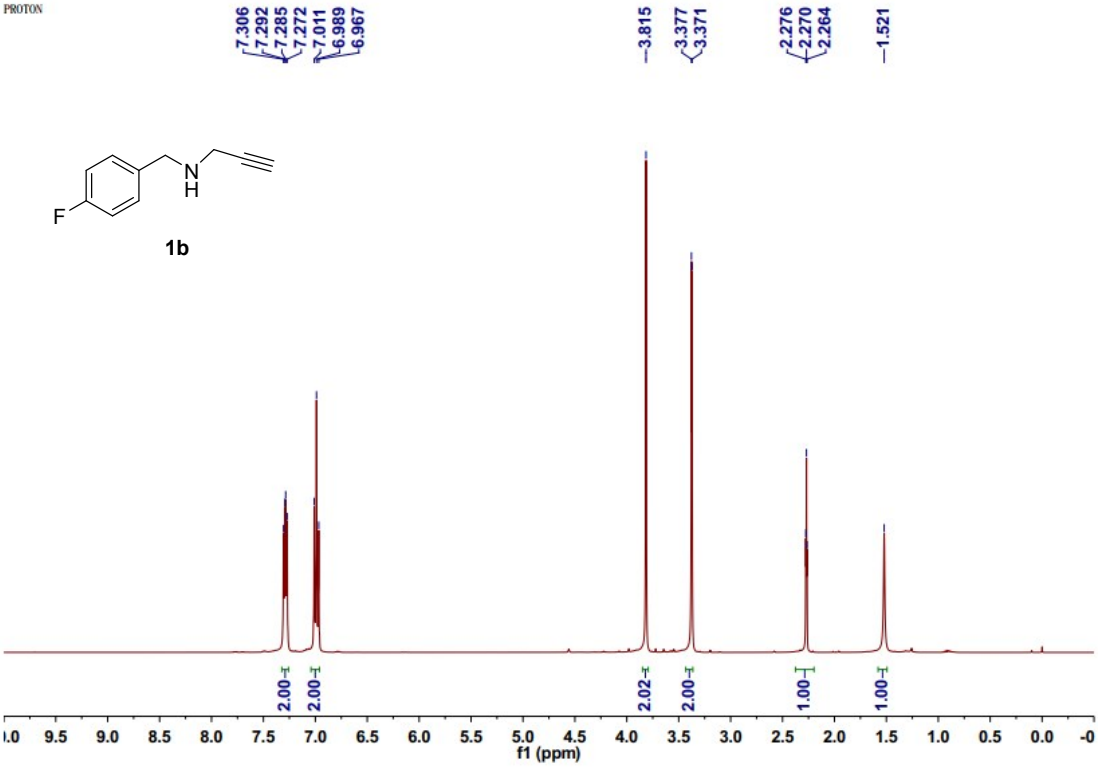
PROTON
7.306
7.292
7.285
7.272
7.011
6.989
6.967
3.815
3.377
3.371
2.276
2.270
2.264
1.521
F
N
H
1b
2.00
2.00
2.02
2.00
1.00
1.00
f1 (ppm)

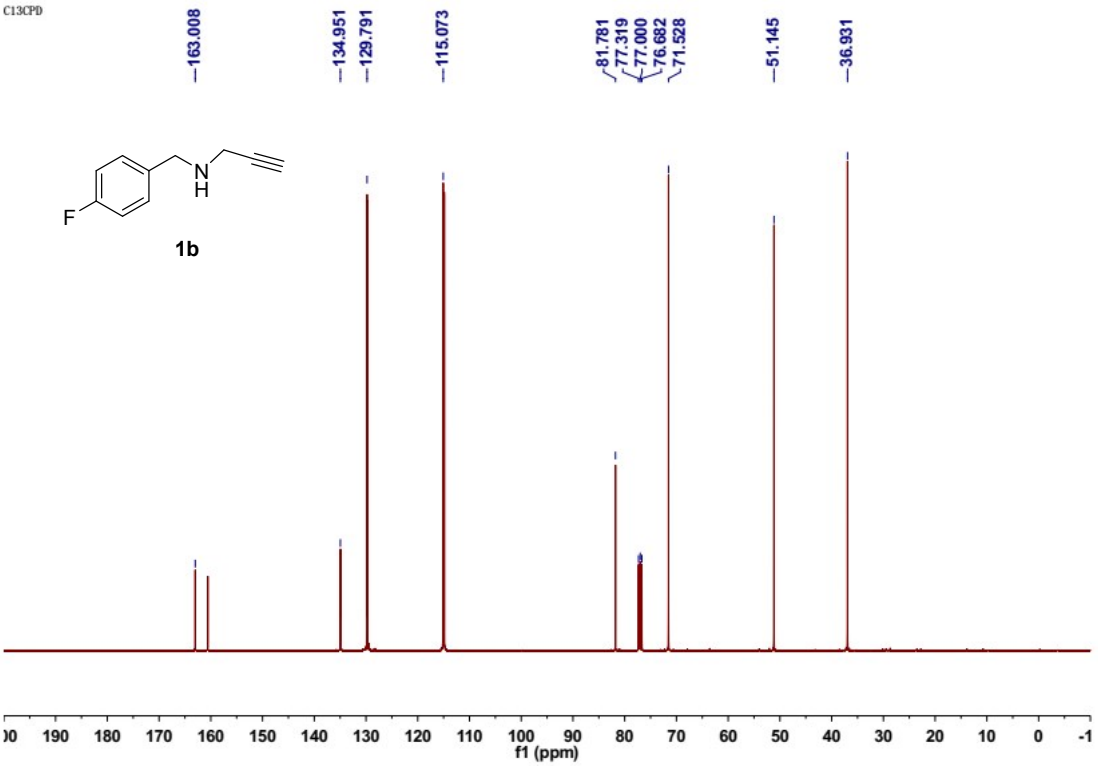
C13CPD
163.008
134.951
129.791
115.073
81.781
77.319
77.000
76.682
71.528
51.145
36.931
F
N
H
1b
f1 (ppm)

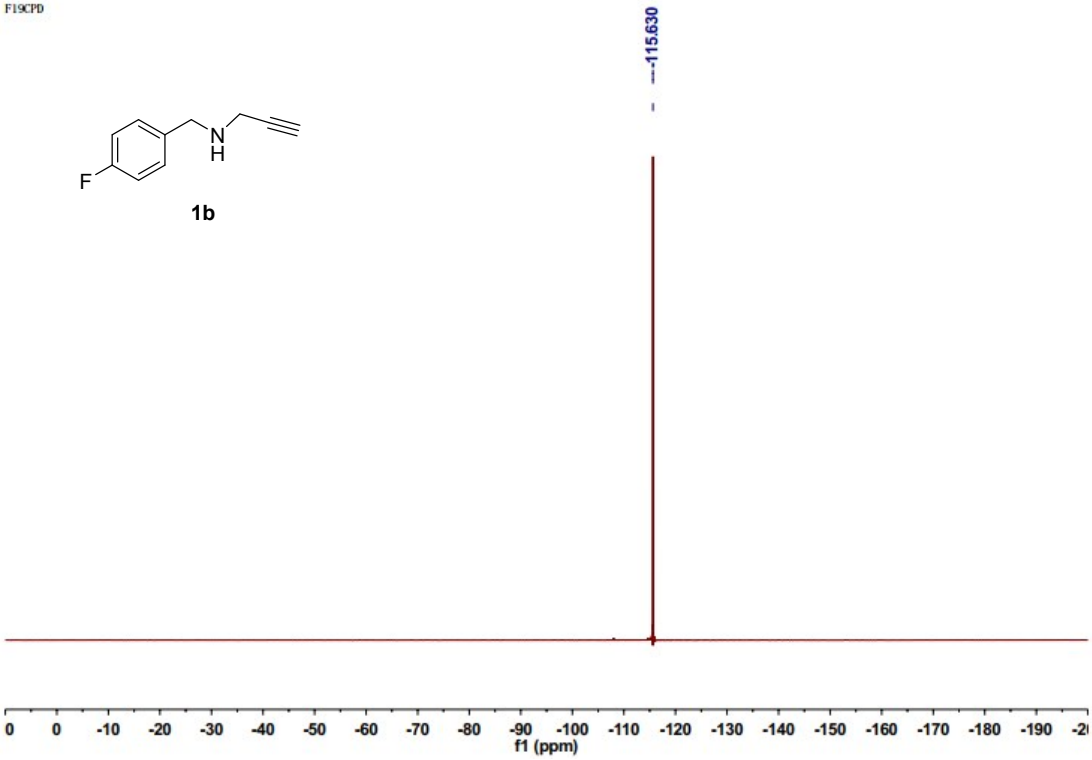
F19CPD
-115.630
N
H
F
1b
0
0
-10
-20
-30
-40
-50
-60
-70
-80
-90
-100
-110
-120
-130
-140
-150
-160
-170
-180
-190
f1 (ppm)

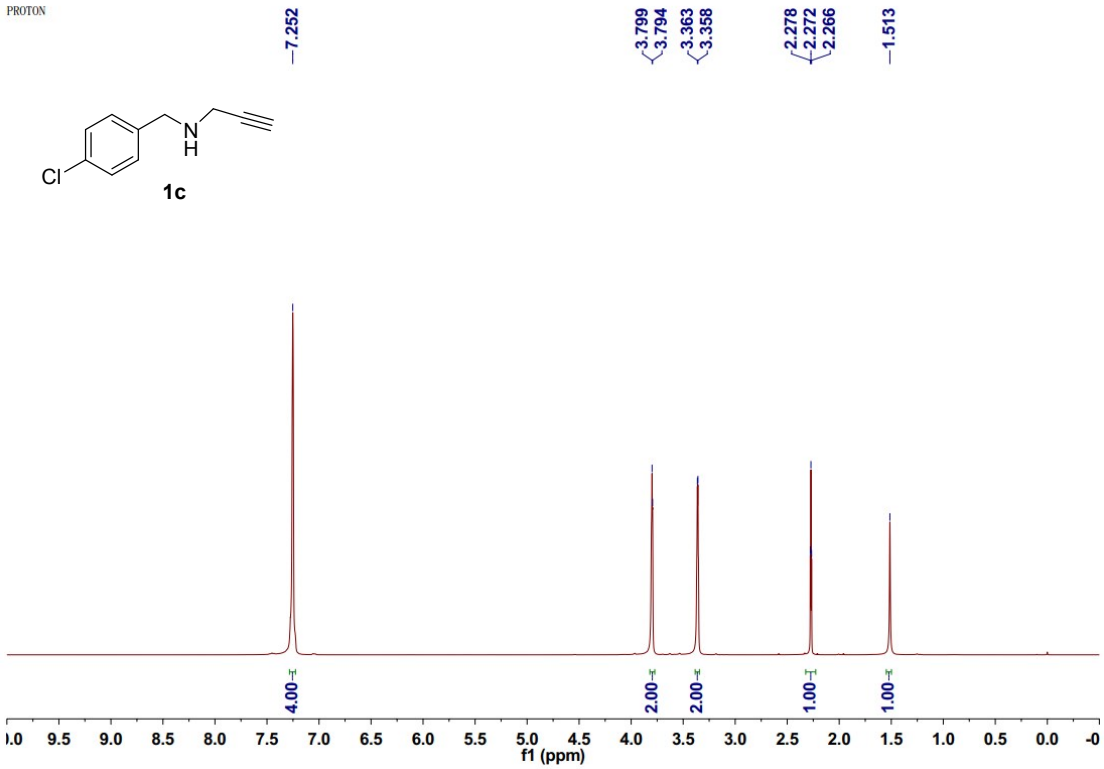
PROTON
7.252
3.799
3.794
3.363
3.358
2.278
2.272
2.266
1.513
Cl
N
H
1c
4.00
2.00
2.00
1.00
1.00
f1 (ppm)

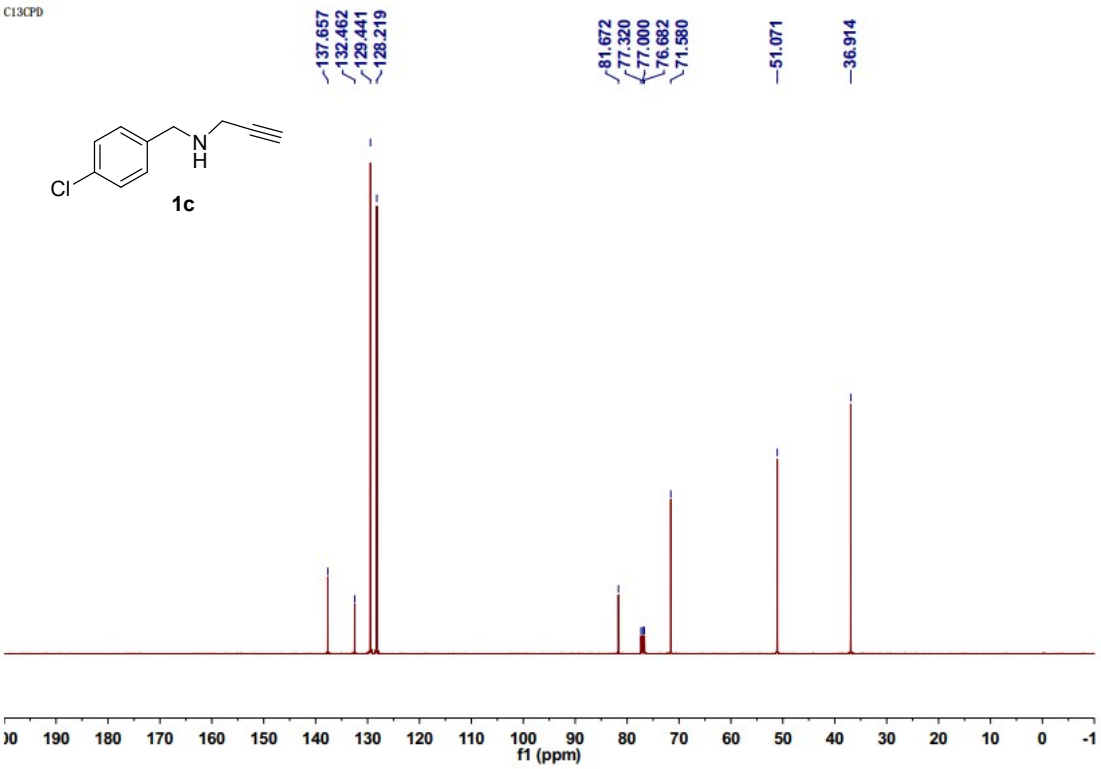
C13CPD
137.657
132.462
129.441
128.219
81.672
77.320
77.000
76.682
71.580
51.071
36.914
Cl
N
H
1c
f1 (ppm)

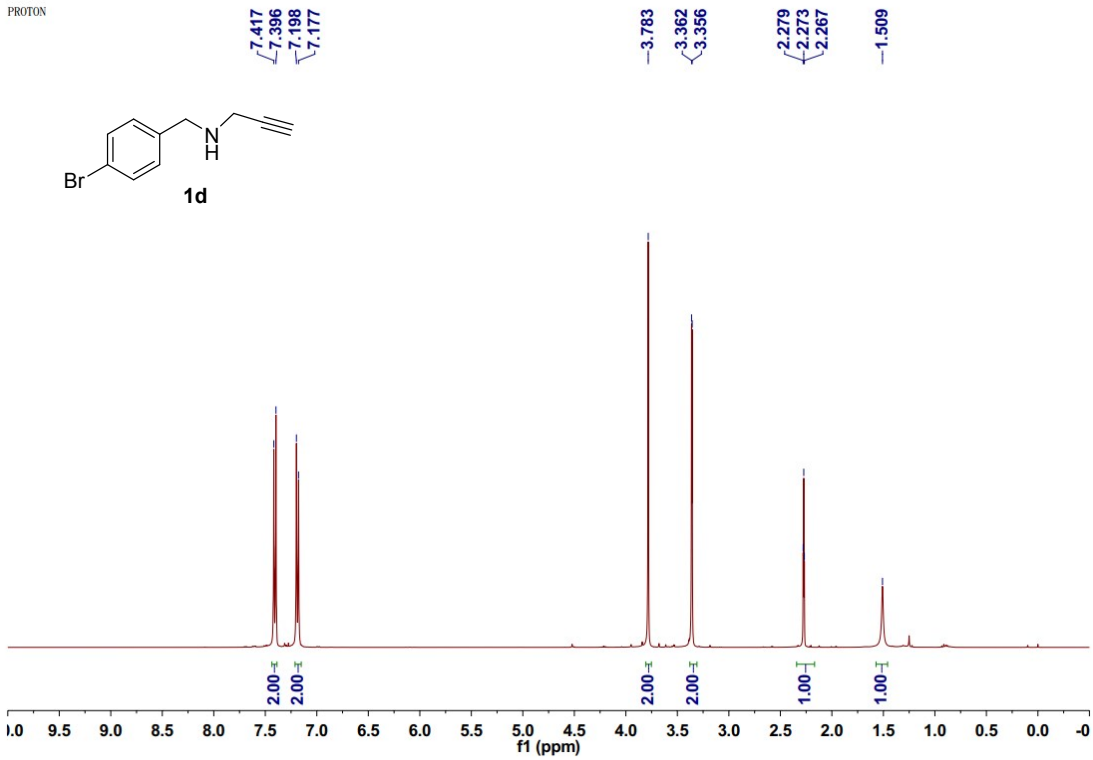
PROTON
7.417
7.396
7.198
7.177
3.783
3.362
3.356
2.279
2.273
2.267
1.509
Br
N
H
1d
2.00
2.00
2.00
2.00
1.00
1.00
f1 (ppm)

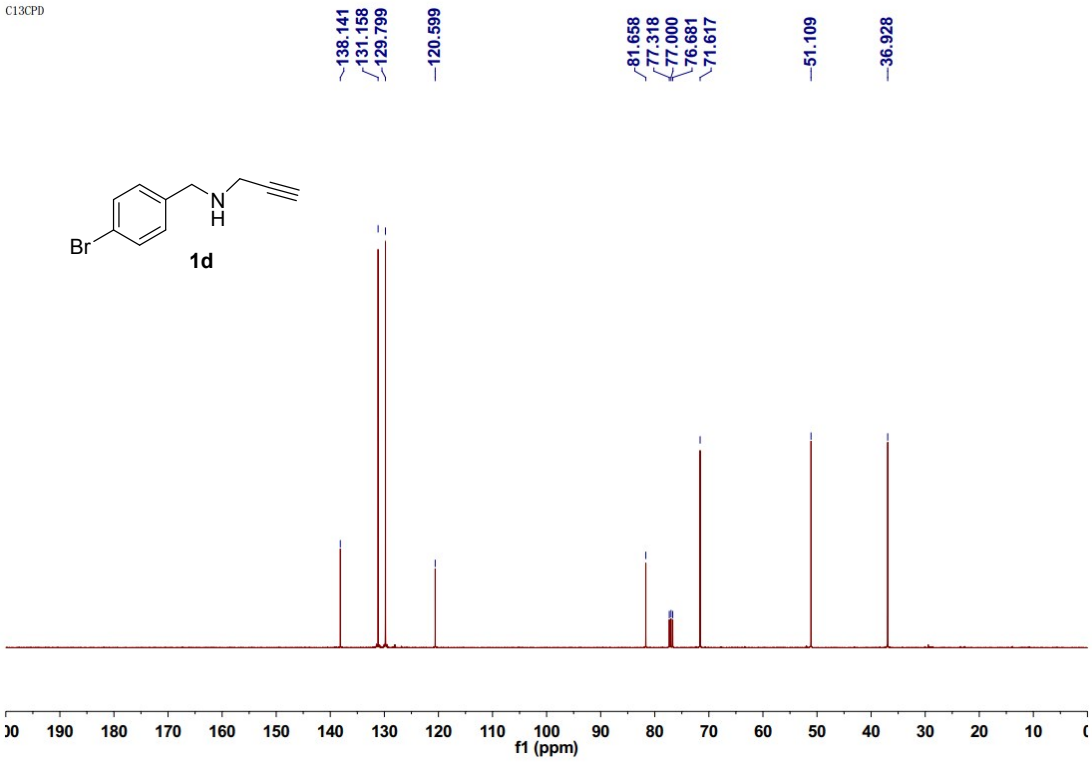
C13CPD
138.141
131.158
129.799
120.599
81.658
77.318
77.000
76.681
71.617
51.109
36.928
Br
N
H
1d
f1 (ppm)

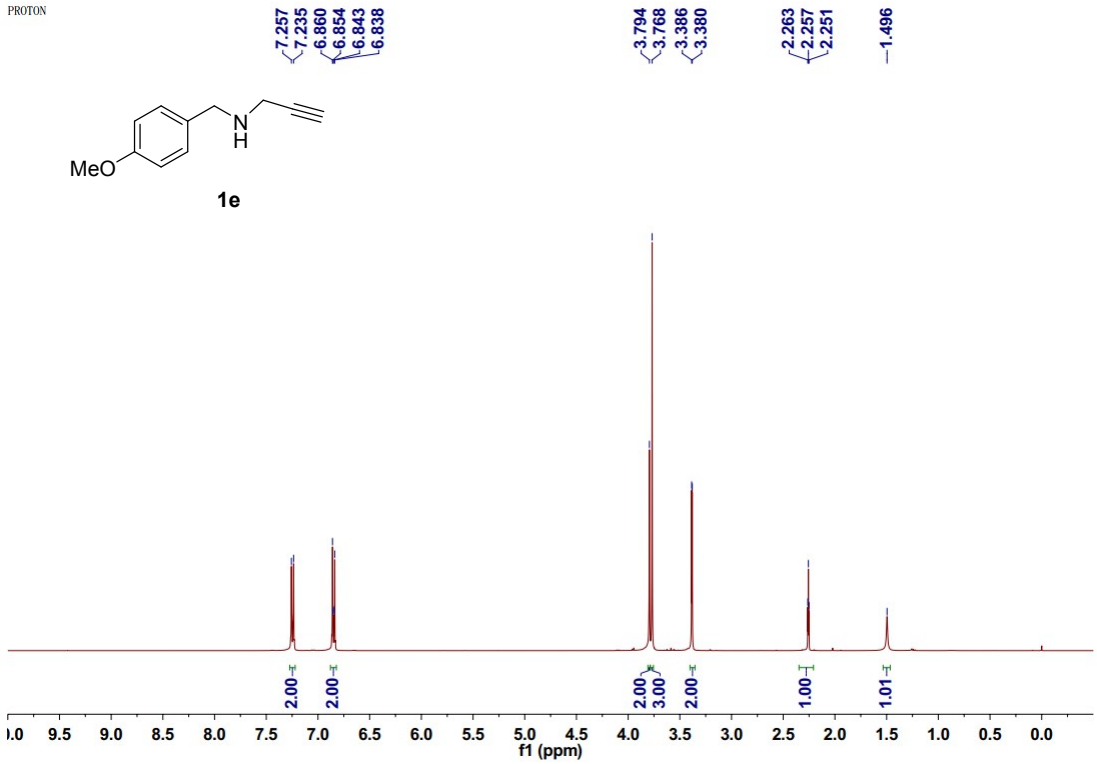
PROTON
7.257
7.235
6.860
6.854
6.843
6.838
3.794
3.768
3.386
3.380
2.263
2.257
2.251
1.496
MeO
N
H
1e
2.00
2.00
2.00
3.00
2.00
1.00
1.01
f1 (ppm)

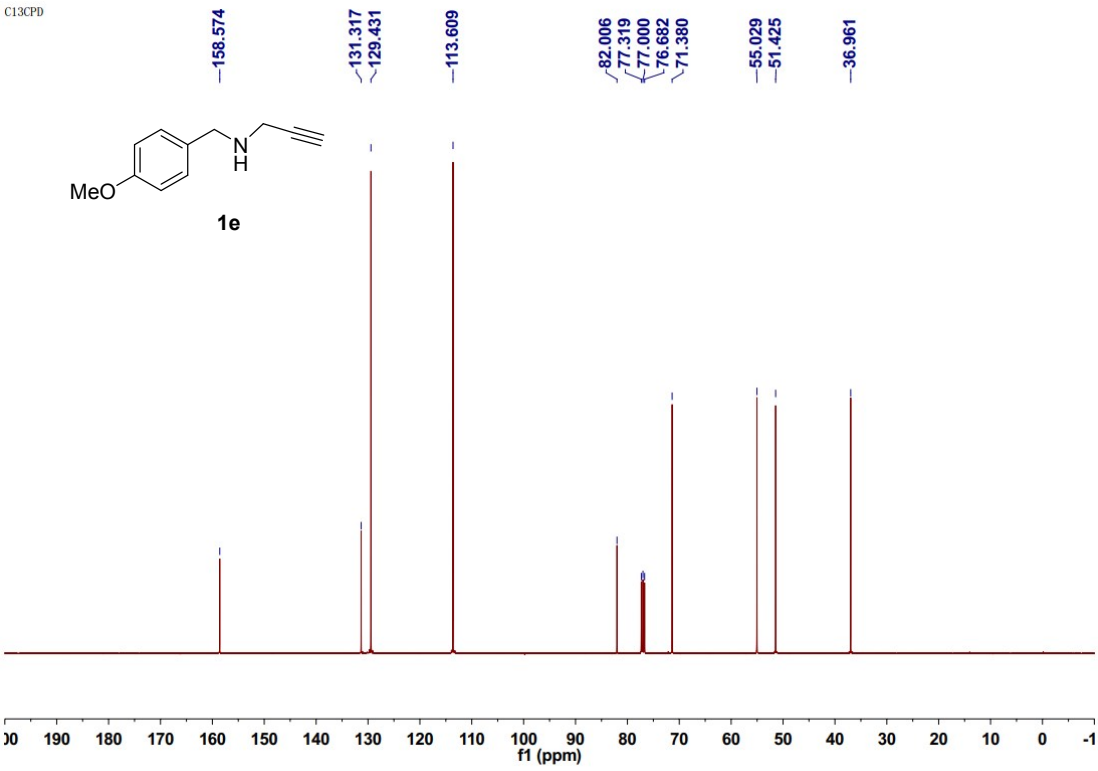
C13CPD
158.574
131.317
129.431
113.609
82.006
77.319
77.000
76.682
71.380
55.029
51.425
36.961
MeO
N
H
1e
f1 (ppm)

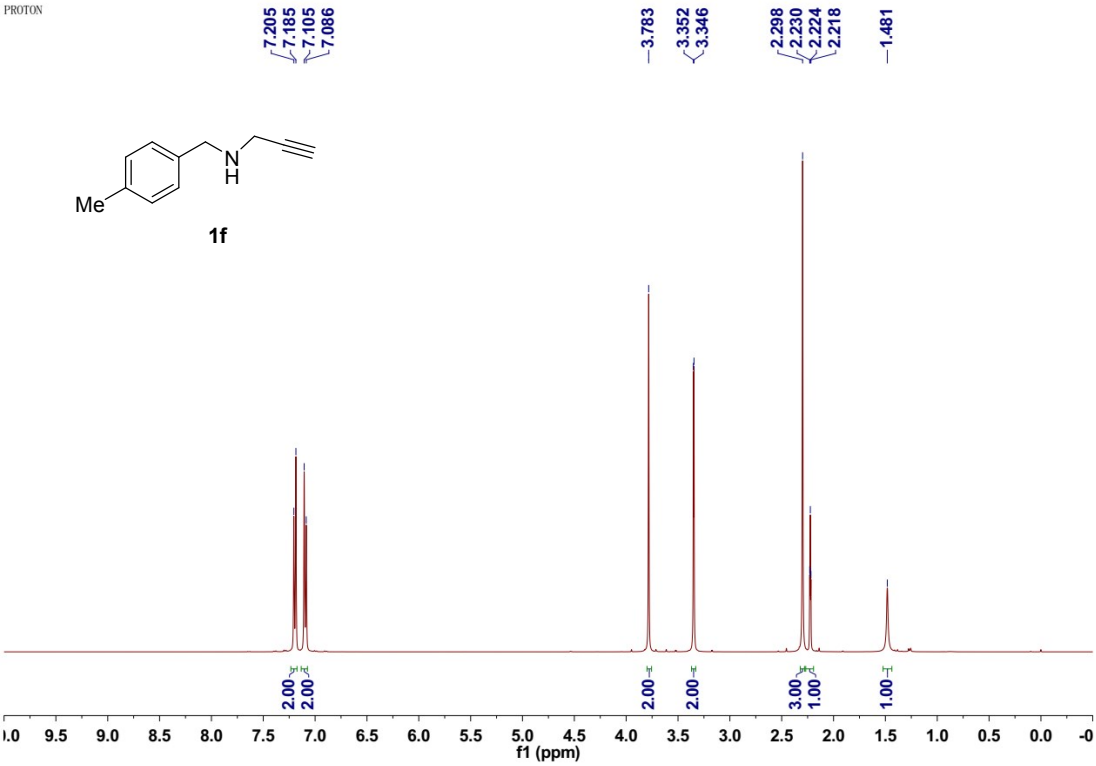
PROTON
7.205
7.185
7.105
7.086
3.783
3.352
3.346
2.298
2.230
2.224
2.218
1.481
Me
N
H
1f
2.00
2.00
2.00
2.00
3.00
1.00
1.00
f1 (ppm)

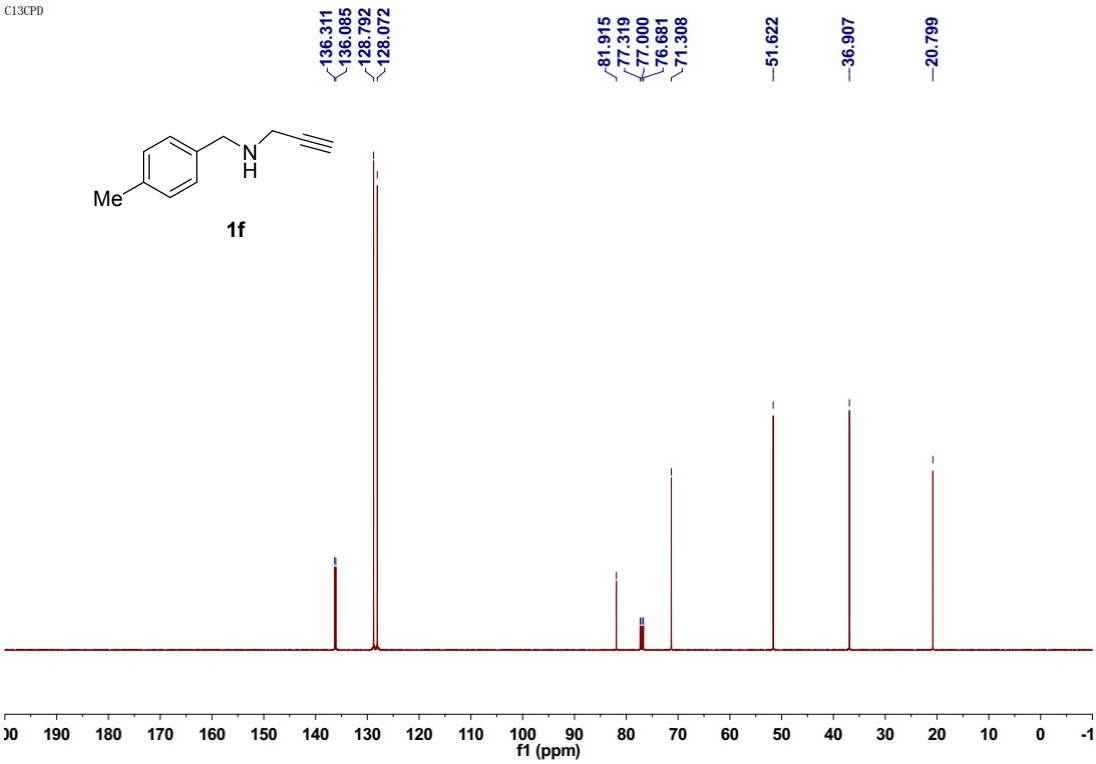
C13CPD
136.311
136.085
128.792
128.072
81.915
77.319
77.000
76.681
71.308
51.622
36.907
20.799
Me
N
H
1f
f1 (ppm)

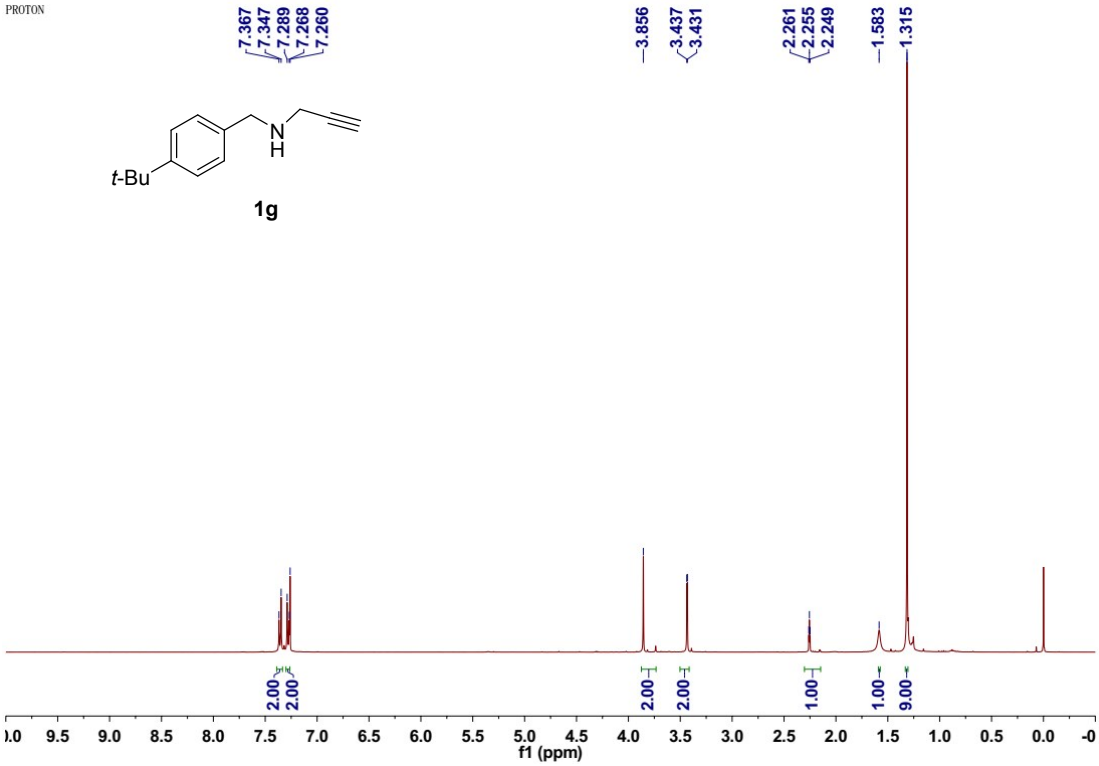
PROTON
7.367
7.347
7.289
7.268
7.260
3.856
3.437
3.431
2.261
2.255
2.249
1.583
1.315
N
H
t-Bu
1g
2.00
2.00
2.00
2.00
1.00
1.00
9.00
f1 (ppm)

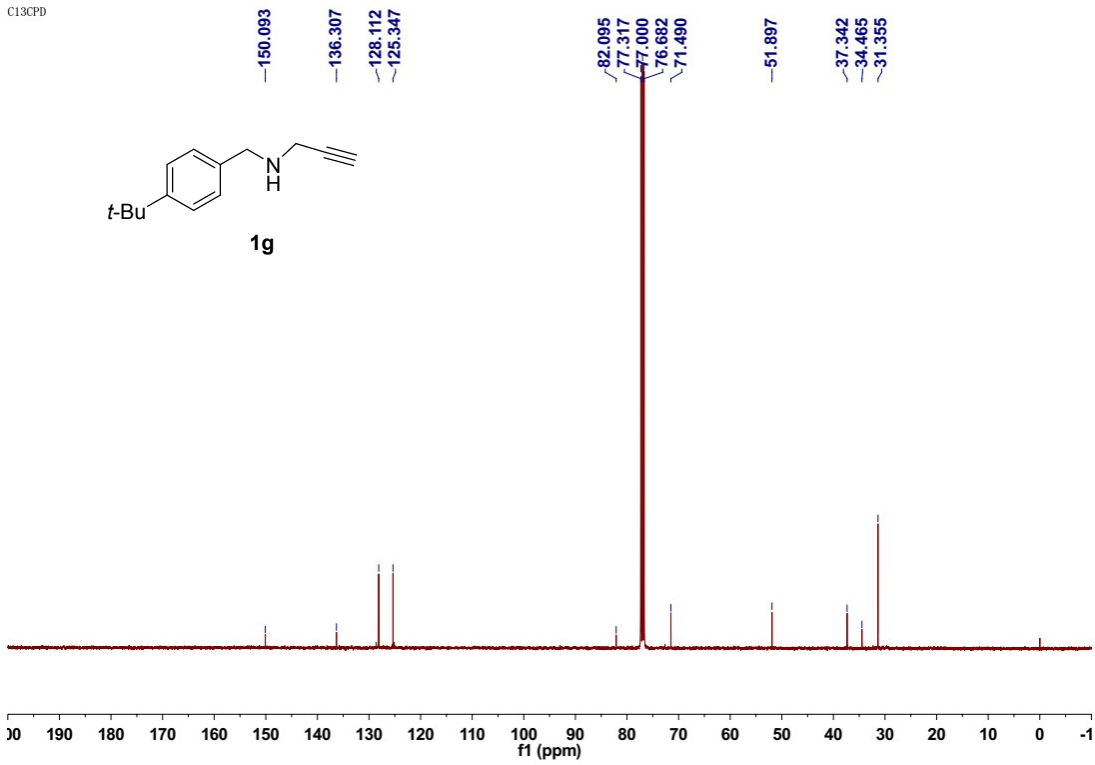
C13CPD
150.093
136.307
128.112
125.347
82.095
77.317
77.000
76.682
71.490
51.897
37.342
34.465
31.355
N
H
t-Bu
1g
f1 (ppm)

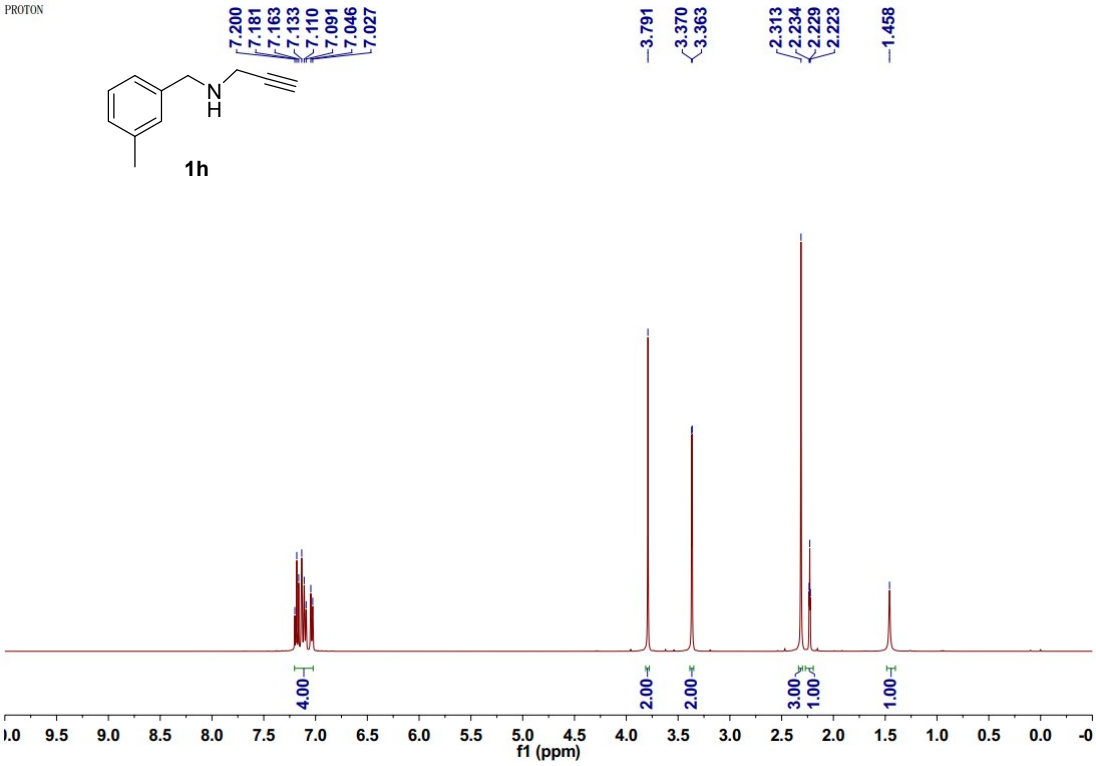
PROTON
7.200
7.181
7.163
7.133
7.110
7.091
7.046
7.027
3.791
3.370
3.363
2.313
2.234
2.229
2.223
1.458
N
H
1h
4.00
2.00
2.00
3.00
1.00
1.00
f1 (ppm)

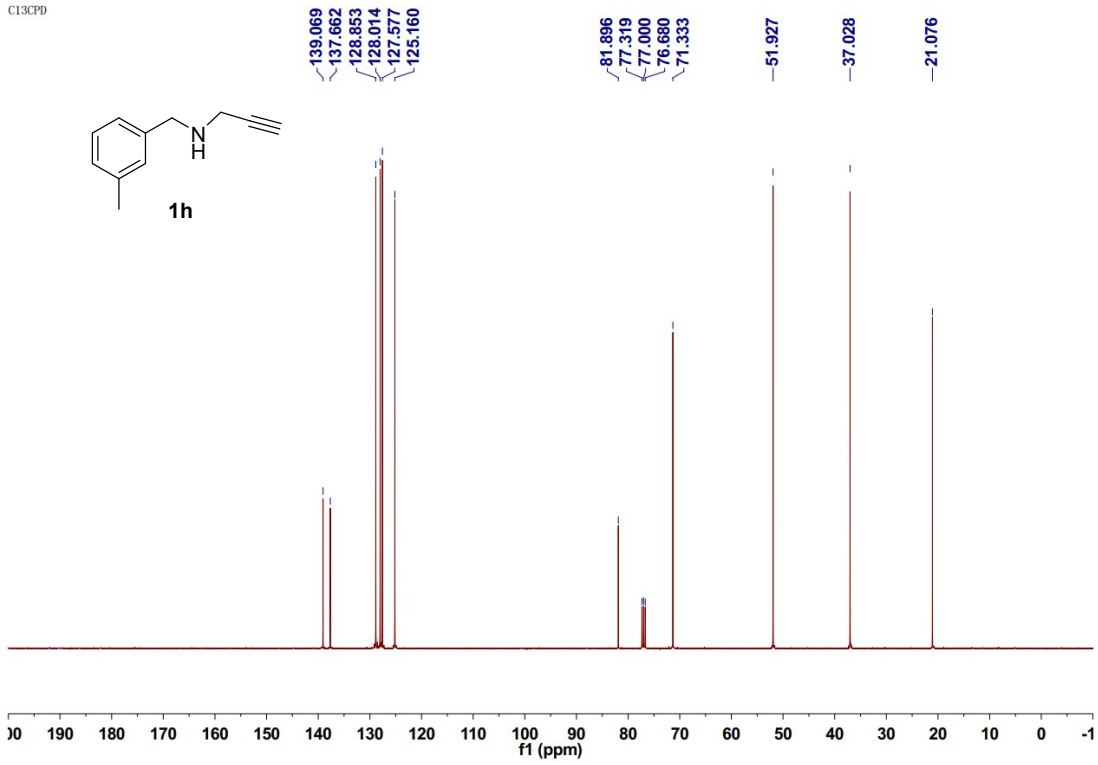
C13CPD
139.069
137.662
128.853
128.014
127.577
125.160
81.896
77.319
77.000
76.680
71.333
51.927
37.028
21.076
N
H
1h
f1 (ppm)

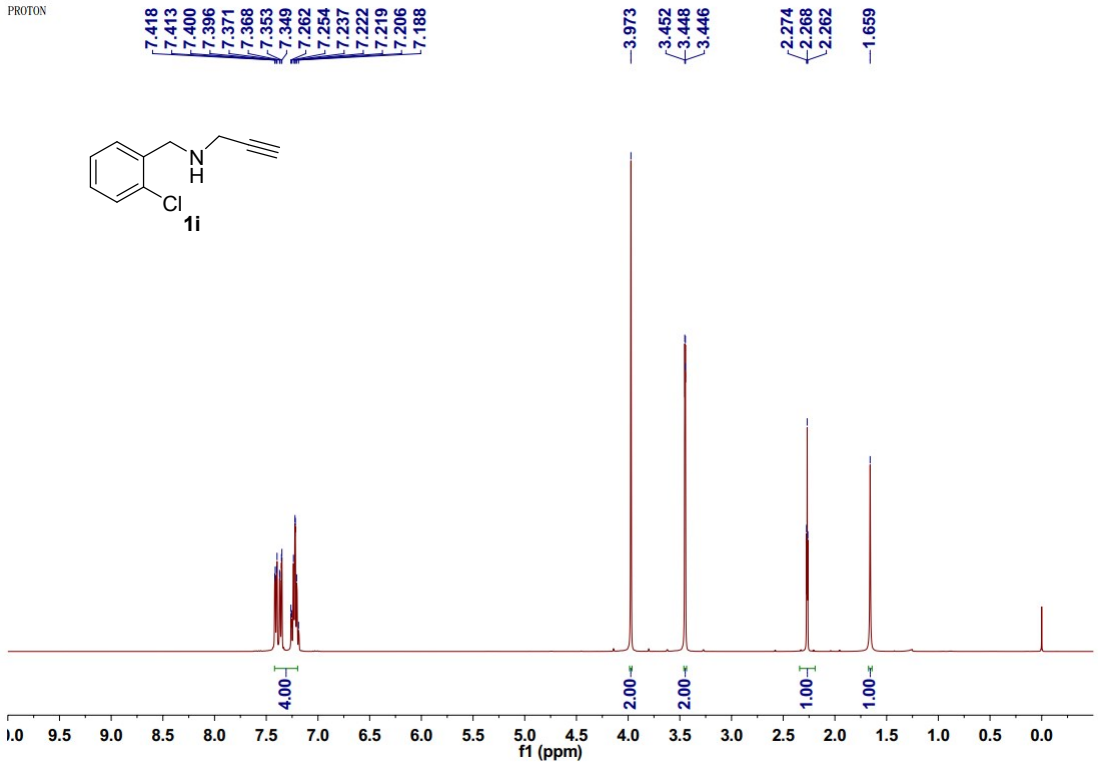
PROTON
7.418
7.413
7.400
7.396
7.371
7.368
7.353
7.349
7.262
7.254
7.237
7.222
7.219
7.206
7.188
3.973
3.452
3.448
3.446
2.274
2.268
2.262
1.659
N
H
Cl
1i
4.00
2.00
2.00
1.00
1.00
f1 (ppm)

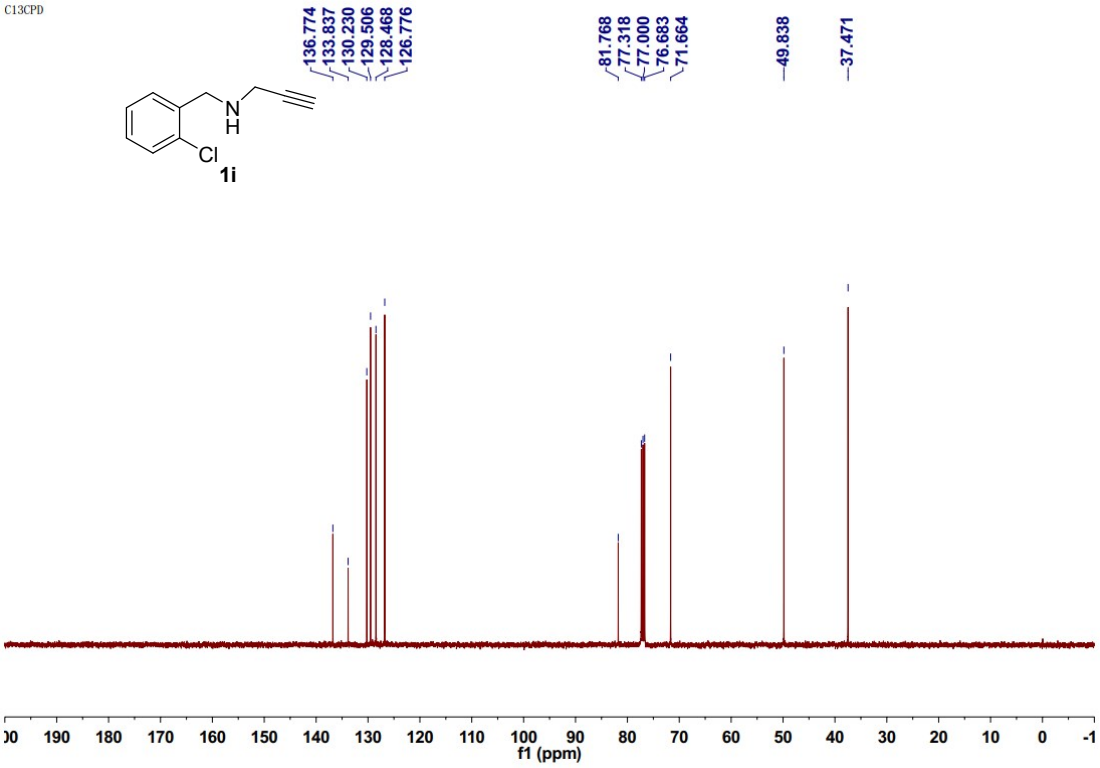
C13CPD
136.774
133.837
130.230
129.506
128.468
126.776
81.768
77.318
77.000
76.683
71.664
49.838
37.471
N
H
Cl
1i
f1 (ppm)

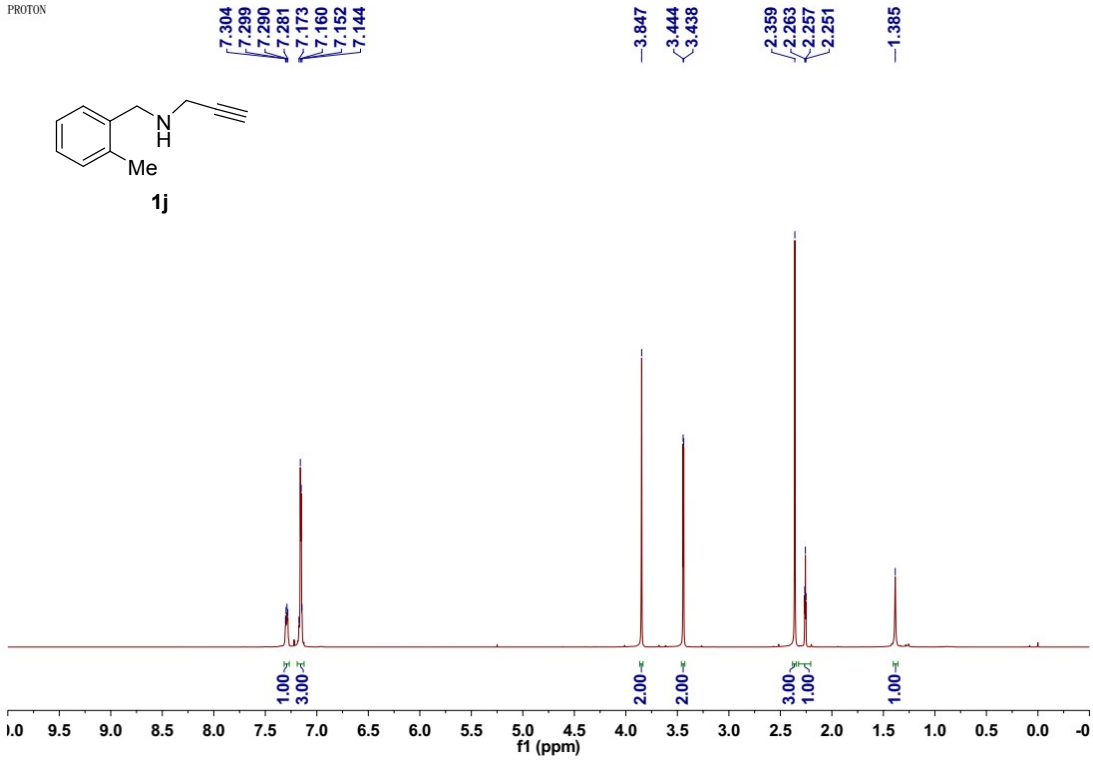
PROTON
7.304
7.299
7.290
7.281
7.173
7.160
7.152
7.144
3.847
3.444
3.438
2.359
2.263
2.257
2.251
1.385
N
H
Me
1j
1.00
3.00
2.00
2.00
3.00
1.00
1.00
f1 (ppm)

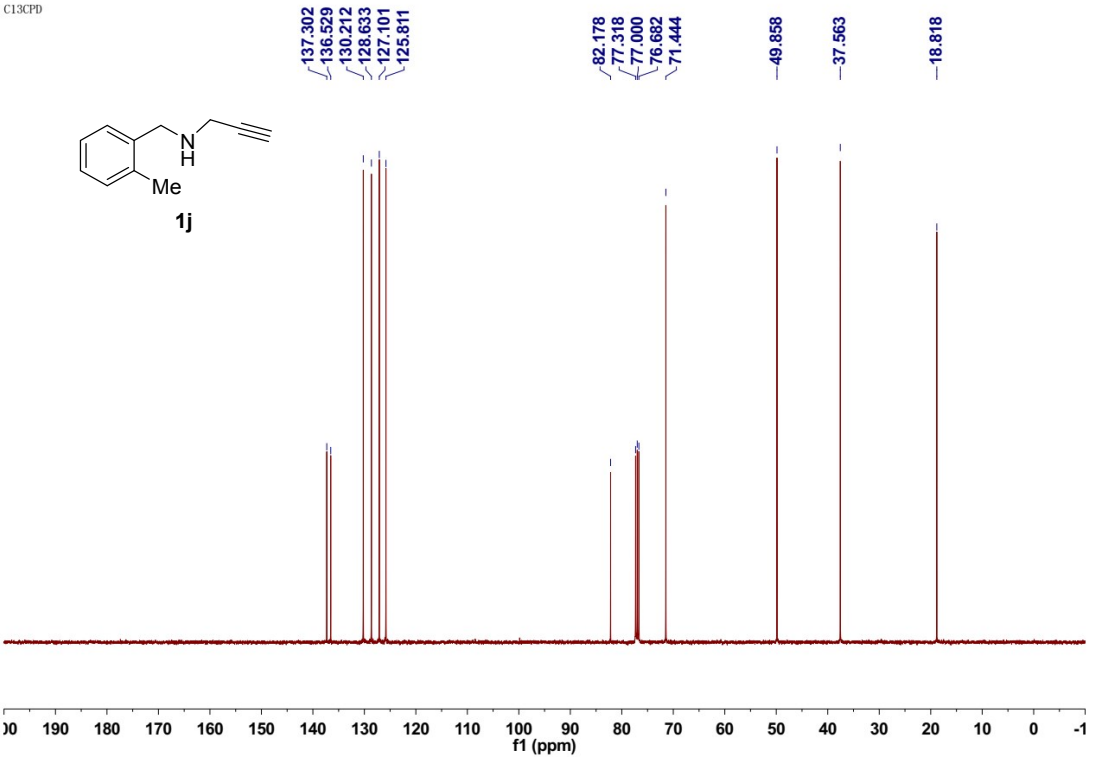
C13CPD
137.302
136.529
130.212
128.633
127.101
125.811
82.178
77.318
77.000
76.682
71.444
49.858
37.563
18.818
N
H
Me
1j
f1 (ppm)

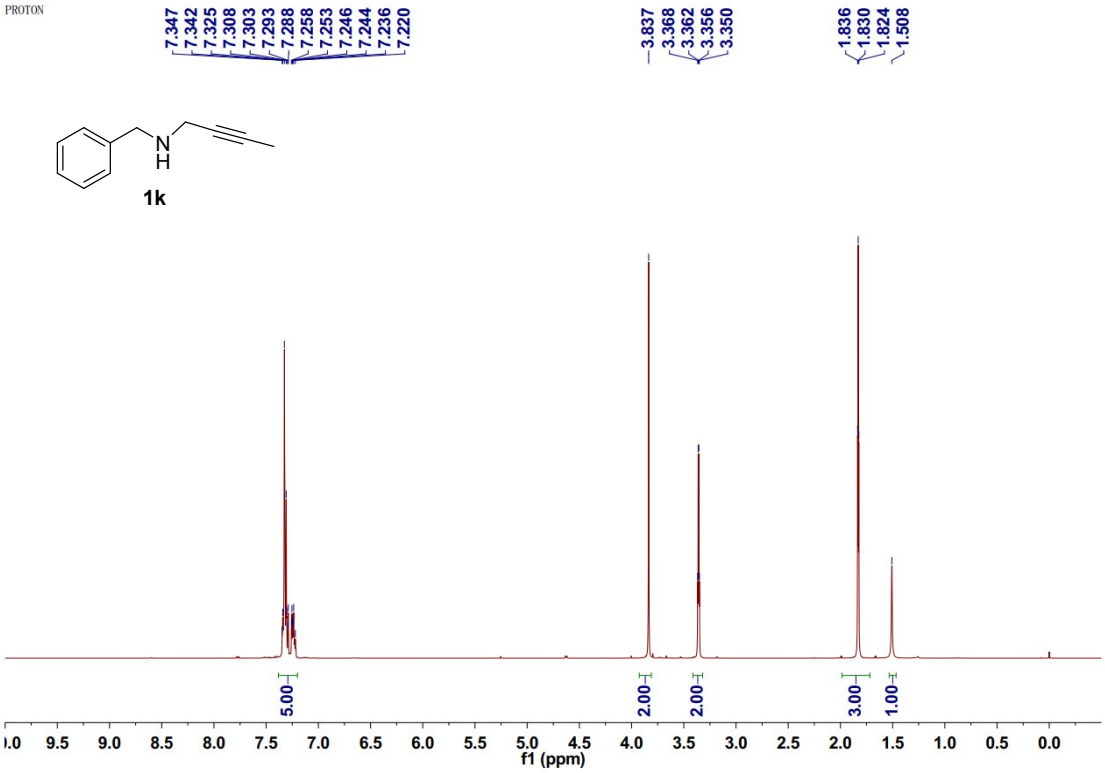
PROTON
7.347
7.342
7.325
7.308
7.303
7.293
7.288
7.258
7.253
7.246
7.244
7.236
7.220
3.837
3.368
3.362
3.356
3.350
1.836
1.830
1.824
1.508
N
H
1k
5.00
2.00
2.00
3.00
1.00
f1 (ppm)

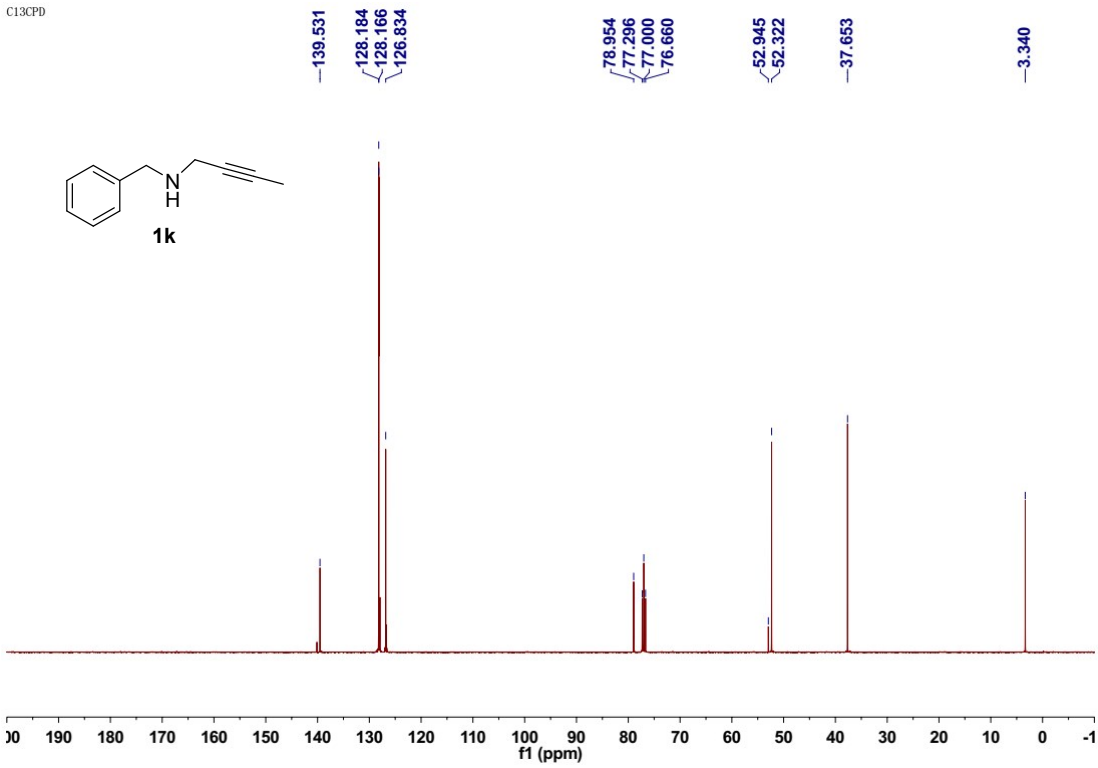
C13CPD
139.531
128.184
128.166
126.834
78.954
77.296
77.000
76.660
52.945
52.322
37.653
3.340
N
H
1k
f1 (ppm)

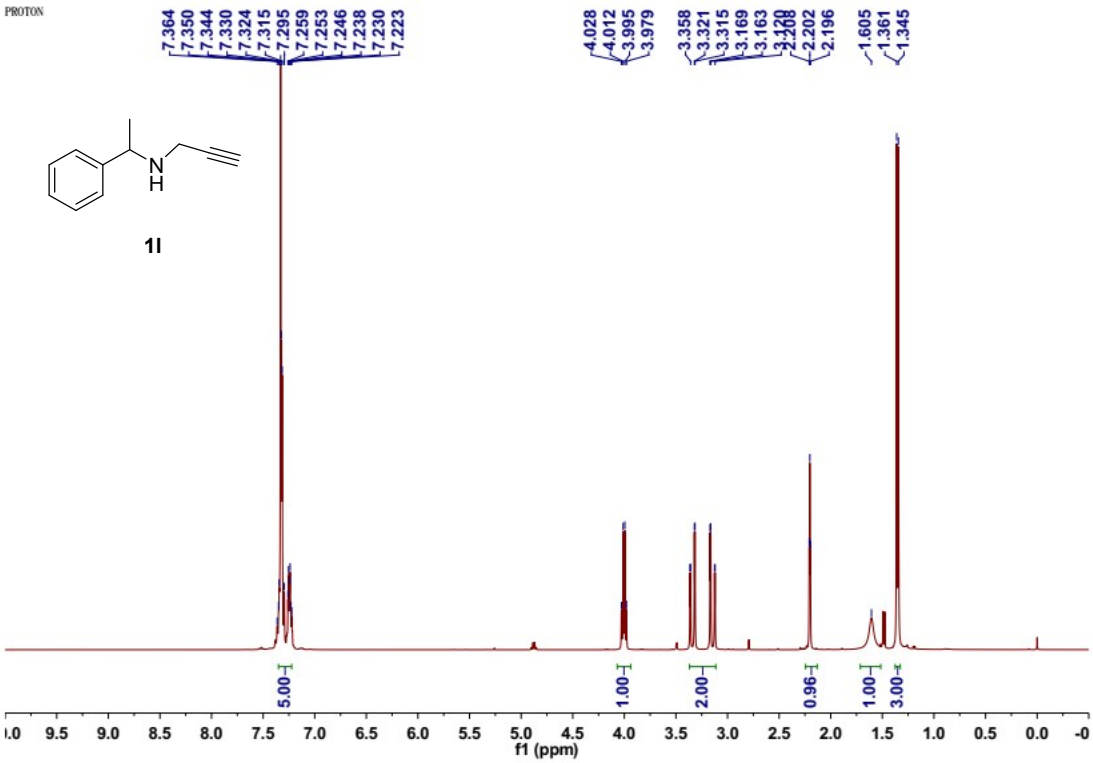
PROTON
7.364
7.350
7.344
7.330
7.324
7.315
7.295
7.259
7.253
7.246
7.238
7.230
7.223
4.028
4.012
3.995
3.979
3.358
3.321
3.315
3.169
3.163
2.202
2.196
1.605
1.361
1.345
N
H
1l
5.00
1.00
2.00
0.96
1.00
3.00
f1 (ppm)

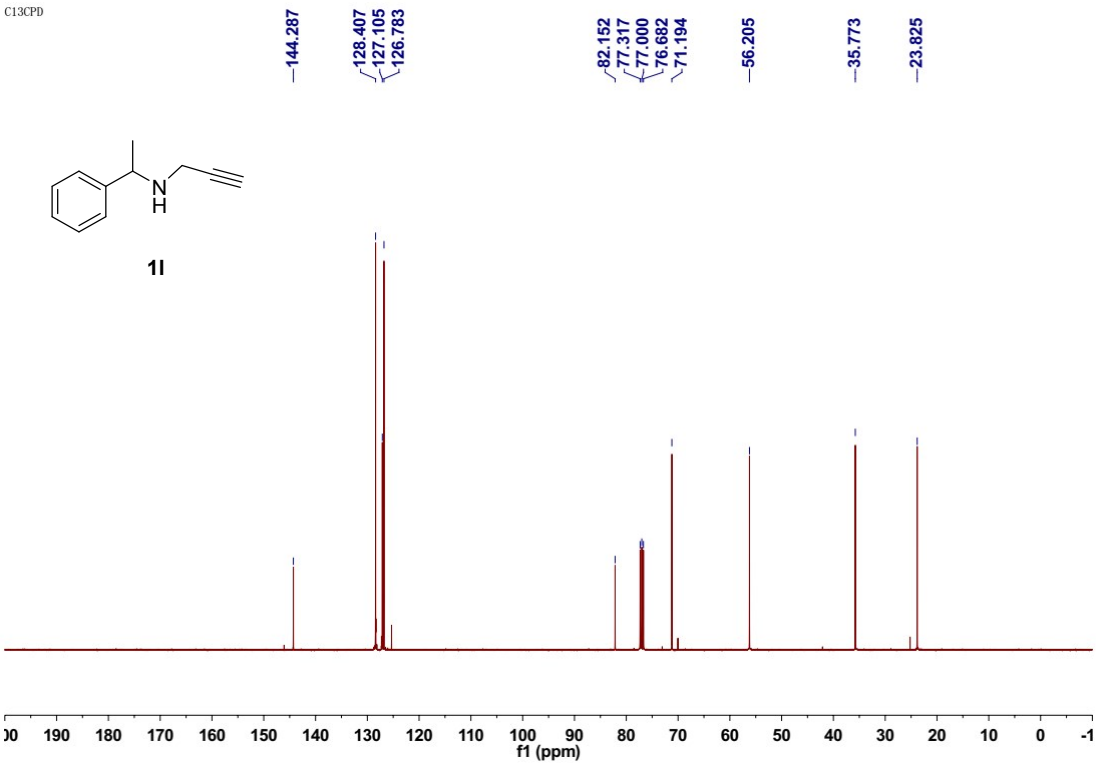
C13CPD
144.287
128.407
127.105
126.783
82.152
77.317
77.000
76.682
71.194
56.205
35.773
23.825
N
H
1l
f1 (ppm)

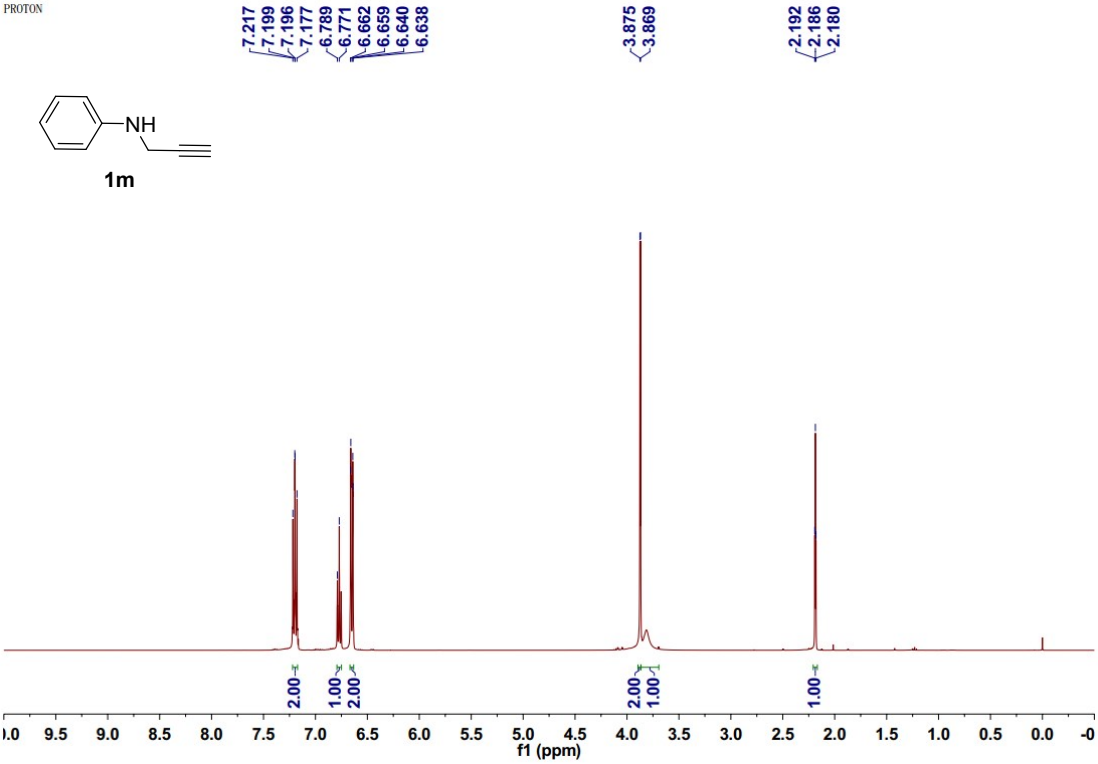
PROTON
7.217
7.199
7.196
7.177
6.789
6.771
6.662
6.659
6.640
6.638
3.875
3.869
2.192
2.186
2.180
NH
1m
2.00
1.00
2.00
2.00
1.00
1.00
f1 (ppm)

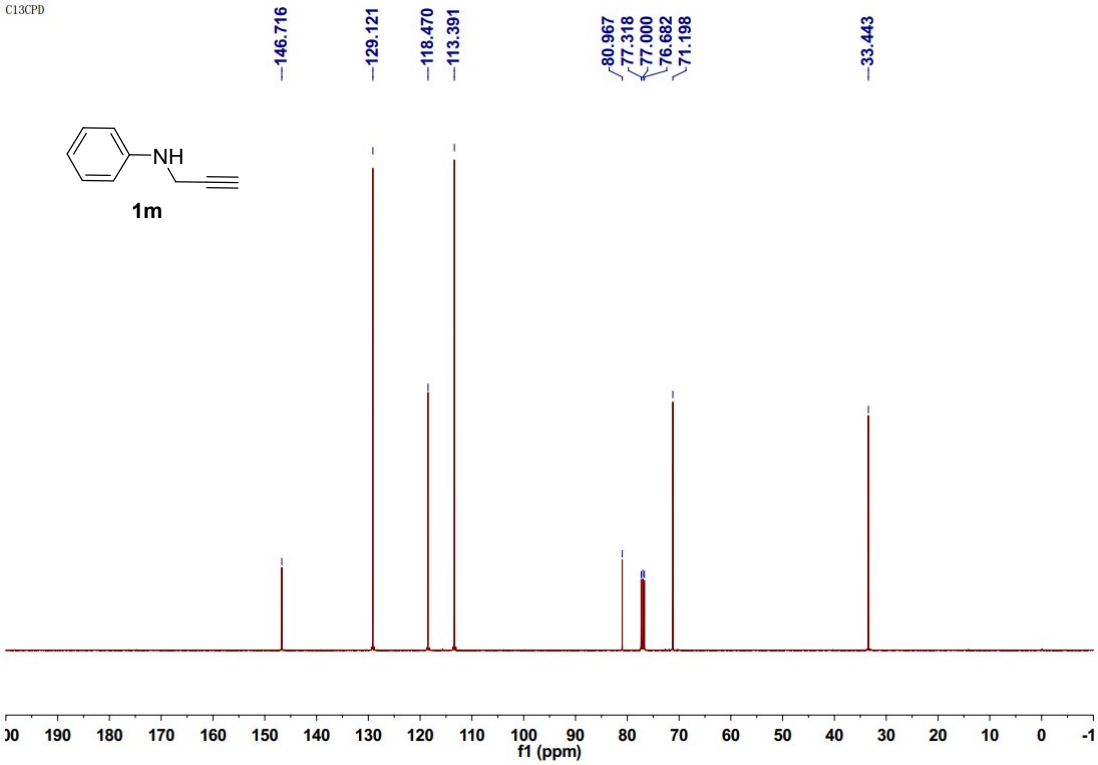
C13CPD
146.716
129.121
118.470
113.391
80.967
77.318
77.000
76.682
71.198
33.443
NH
1m
f1 (ppm)

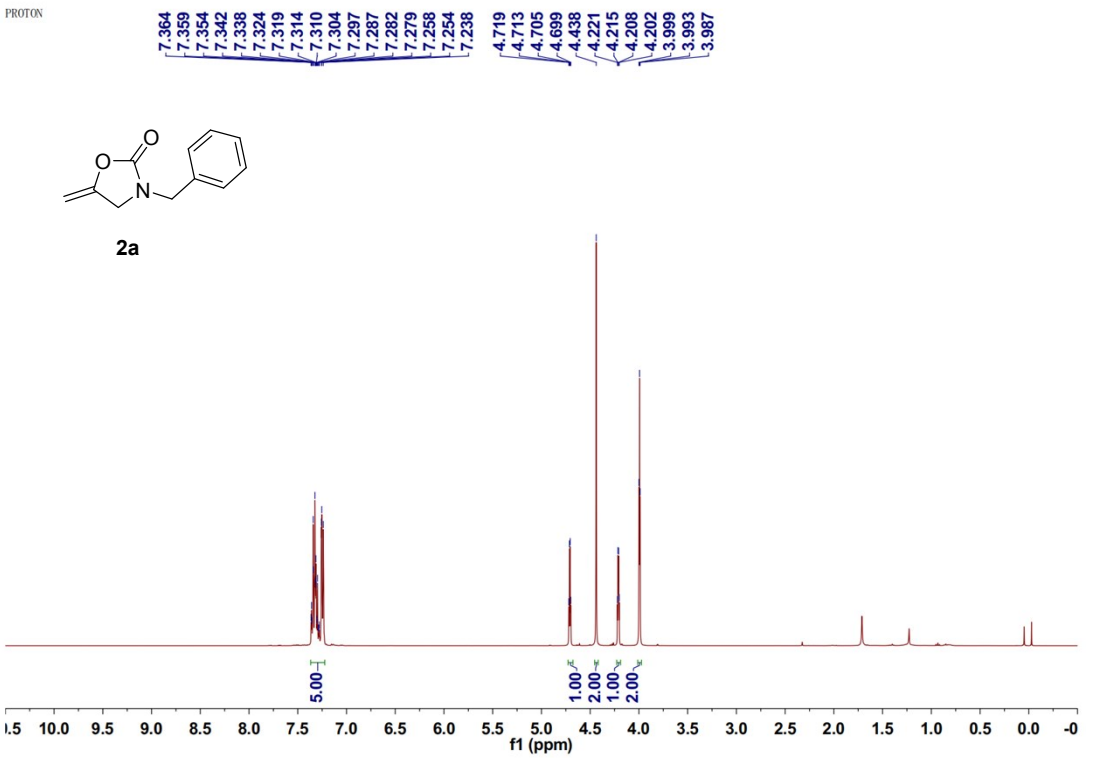
PROTON
7.364
7.359
7.354
7.342
7.338
7.324
7.319
7.314
7.310
7.304
7.297
7.287
7.282
7.279
7.258
7.254
7.238
4.719
4.713
4.705
4.699
4.438
4.221
4.215
4.208
4.202
3.999
3.993
3.987
2a
5.00
1.00
2.00
1.00
2.00
f1 (ppm)

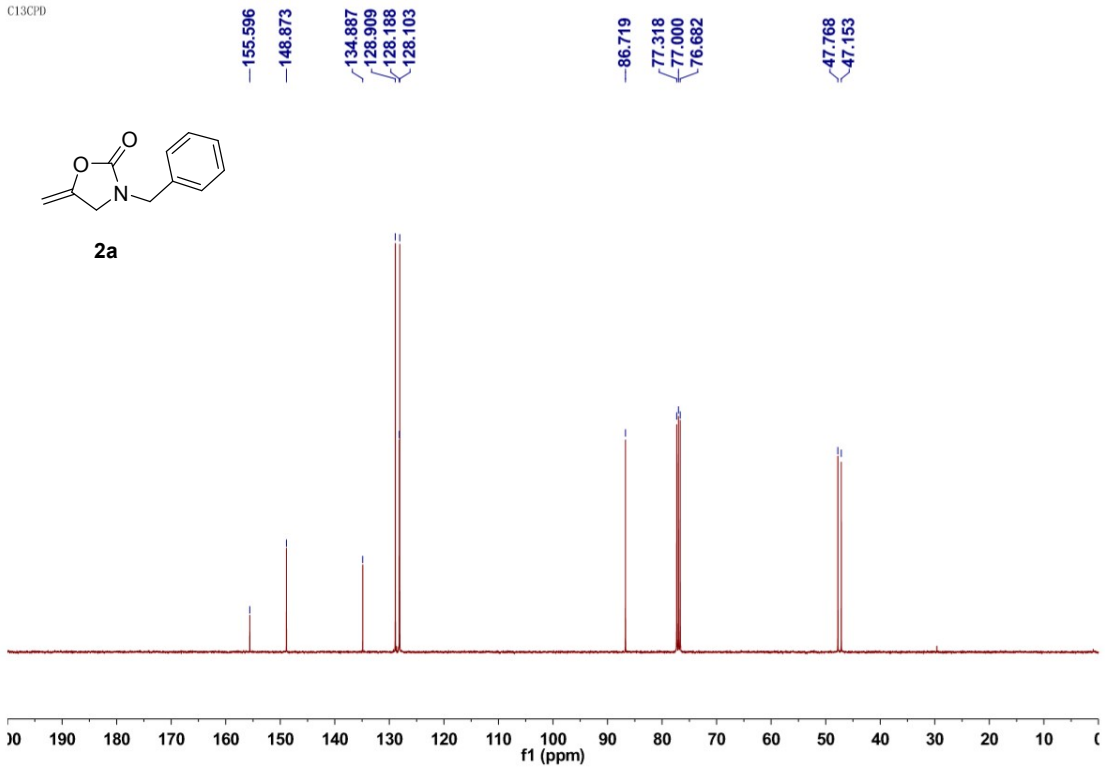
C13CPD
155.596
148.873
134.887
128.909
128.188
128.103
86.719
77.318
77.000
76.682
47.768
47.153
2a
f1 (ppm)

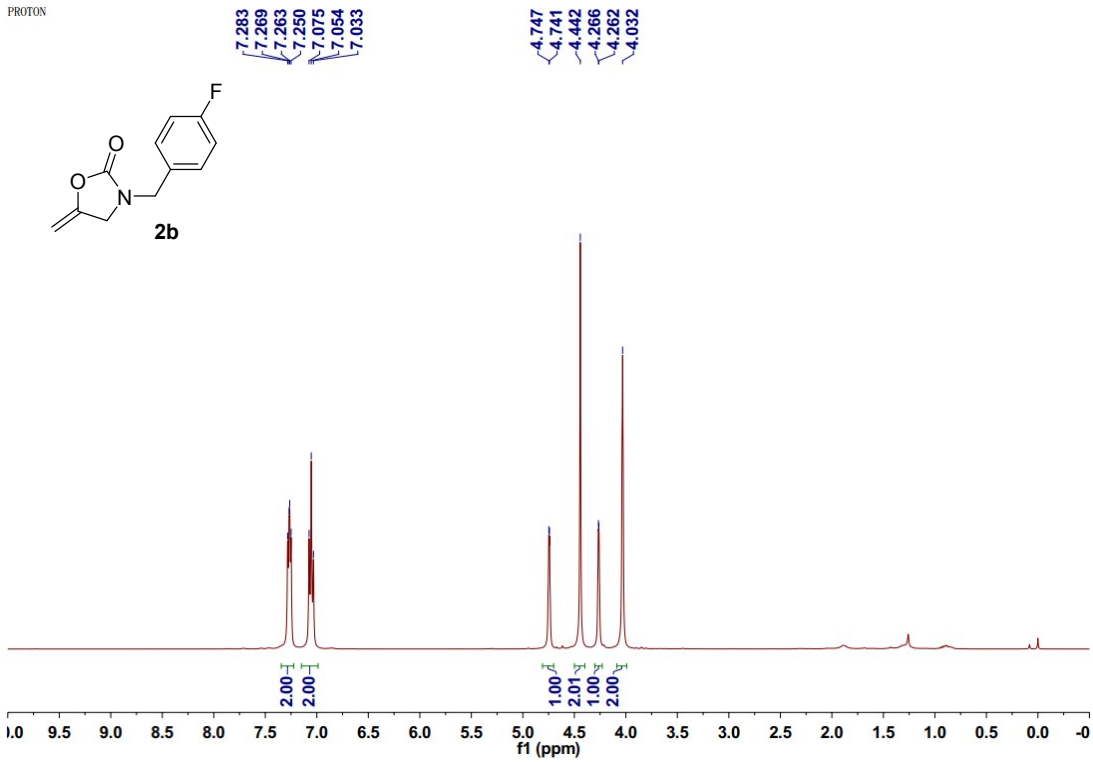
PROTON
7.283
7.269
7.263
7.250
7.075
7.054
7.033
4.747
4.741
4.442
4.266
4.262
4.032
F
O
O
N
2b
2.00
2.00
1.00
2.01
1.00
2.00
f1 (ppm)

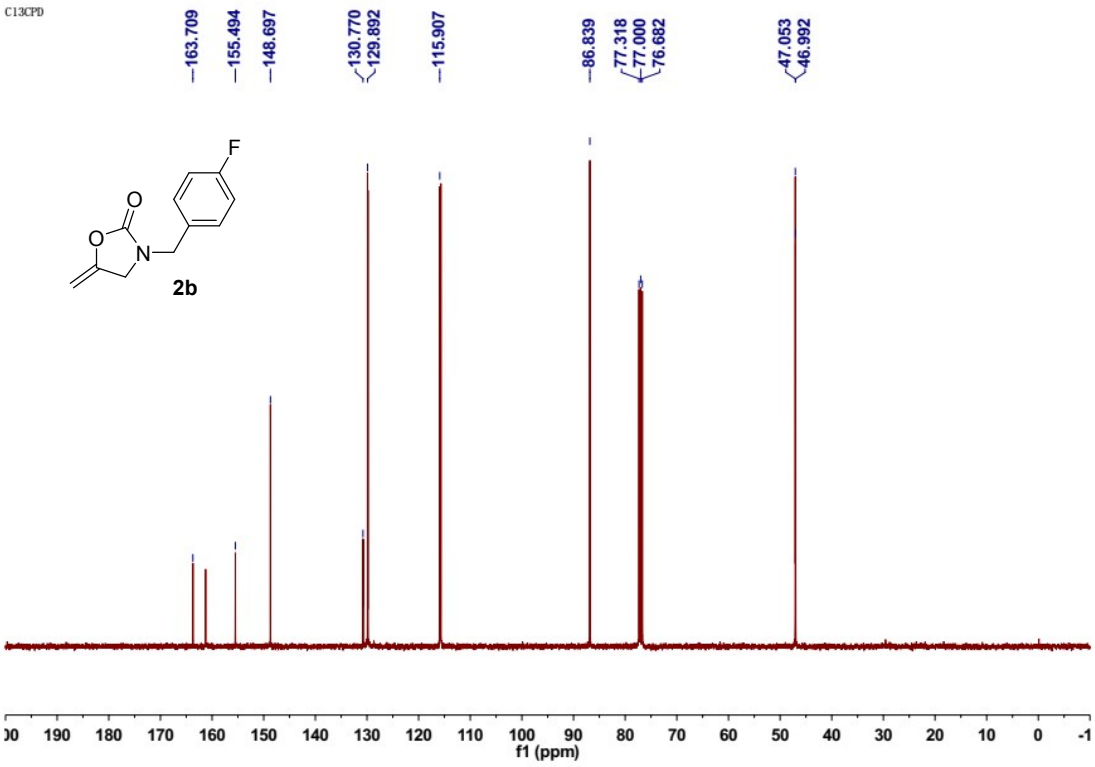
C13CPD
163.709
155.494
148.697
130.770
129.892
115.907
86.839
77.318
77.000
76.682
47.053
46.992
F
O
O
N
2b
f1 (ppm)

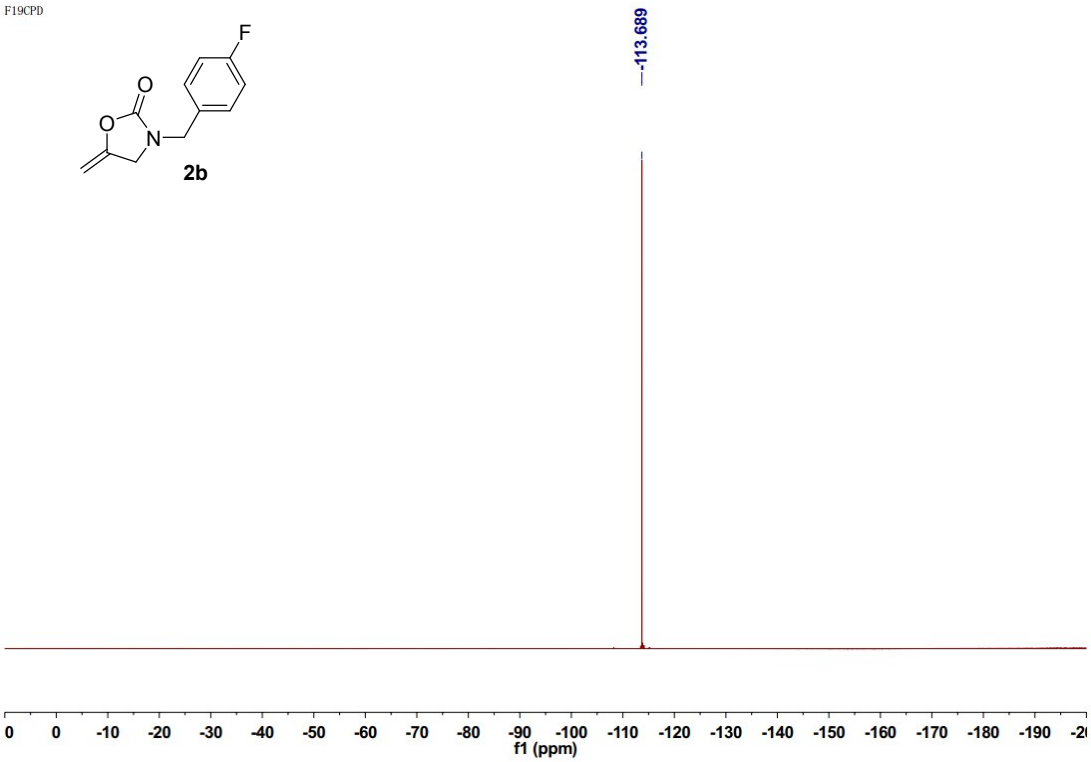
F19CPD
F
O
O
N
2b
-113.689
0
0
-10
-20
-30
-40
-50
-60
-70
-80
-90
-100
-110
-120
-130
-140
-150
-160
-170
-180
-190
f1 (ppm)

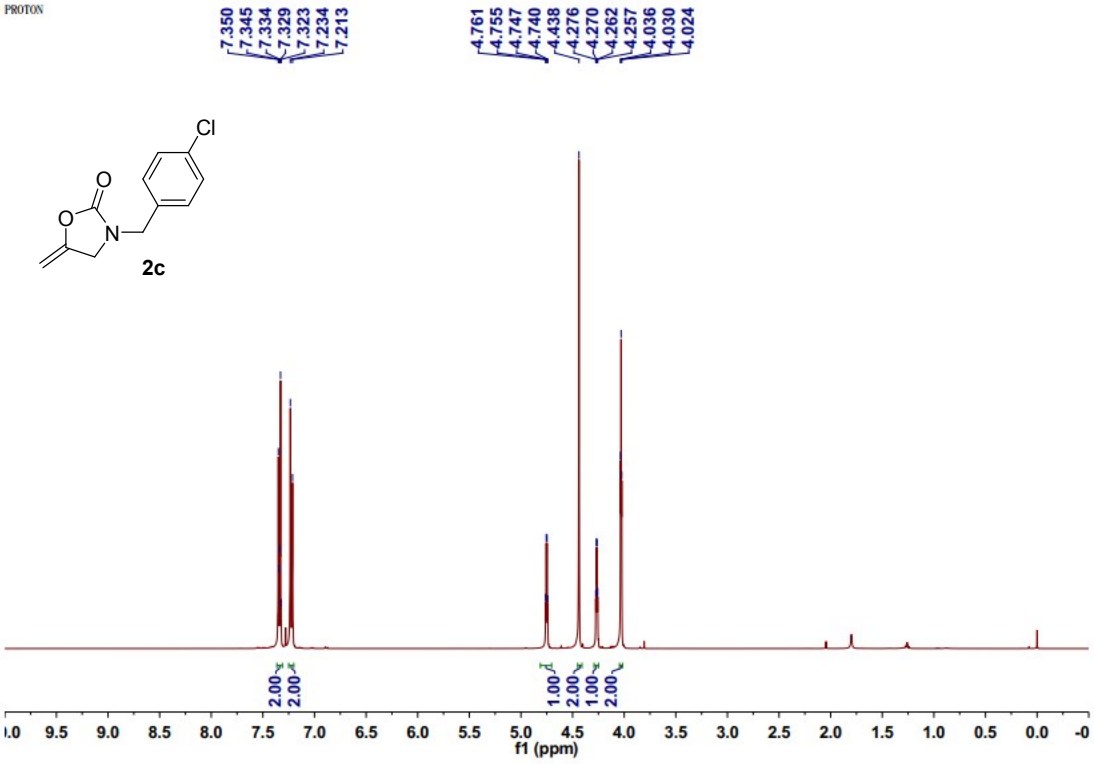
PROTON
7.350
7.345
7.334
7.329
7.323
7.234
7.213
4.761
4.755
4.747
4.740
4.438
4.276
4.270
4.262
4.257
4.036
4.030
4.024
Cl
O
O
N
2c
2.00
2.00
1.00
2.00
1.00
2.00
f1 (ppm)

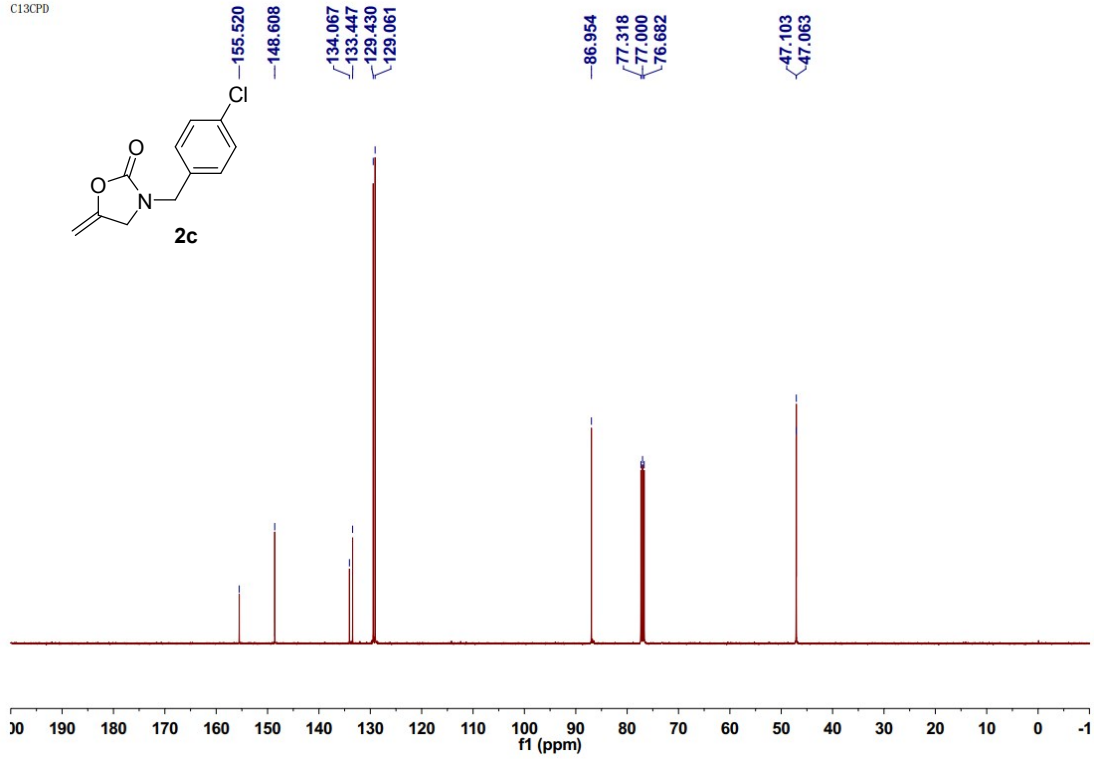
C13CPD
155.520
148.608
134.067
133.447
129.430
129.061
86.954
77.318
77.000
76.682
47.103
47.063
Cl
O
O
N
2c
f1 (ppm)

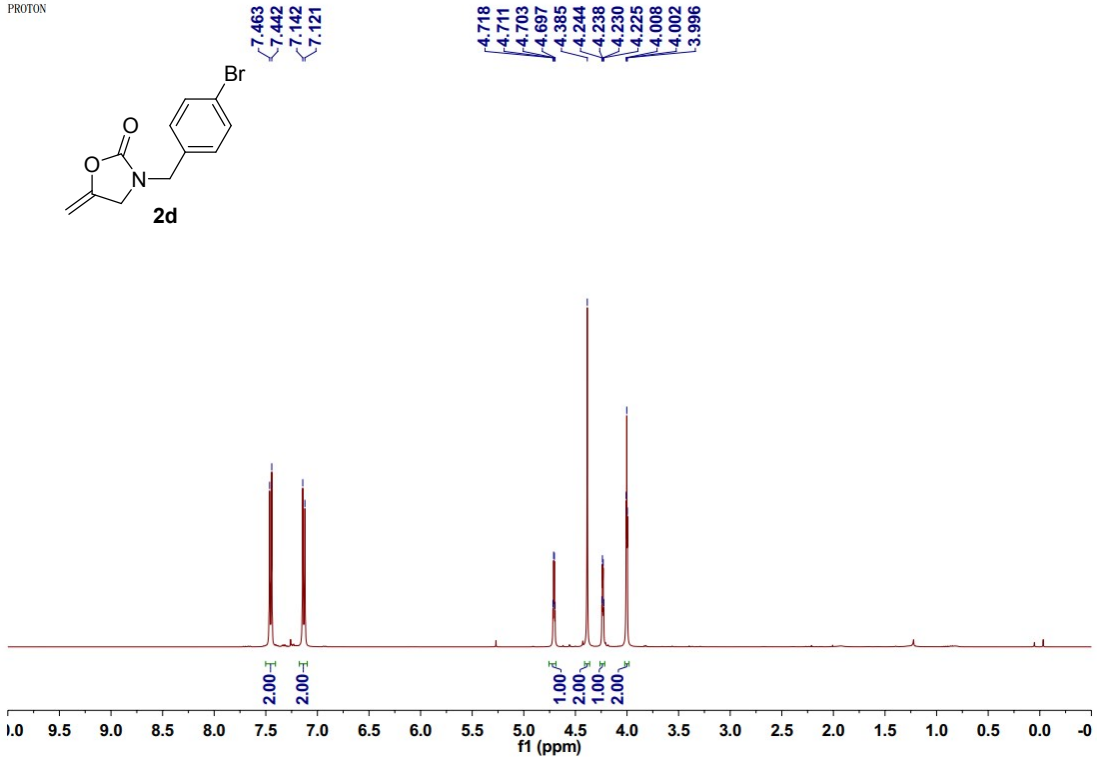
PROTON
7.463
7.442
7.142
7.121
4.718
4.711
4.703
4.697
4.385
4.244
4.238
4.230
4.225
4.008
4.002
3.996
Br
O
O
N
2d
2.00
2.00
1.00
2.00
1.00
2.00
f1 (ppm)

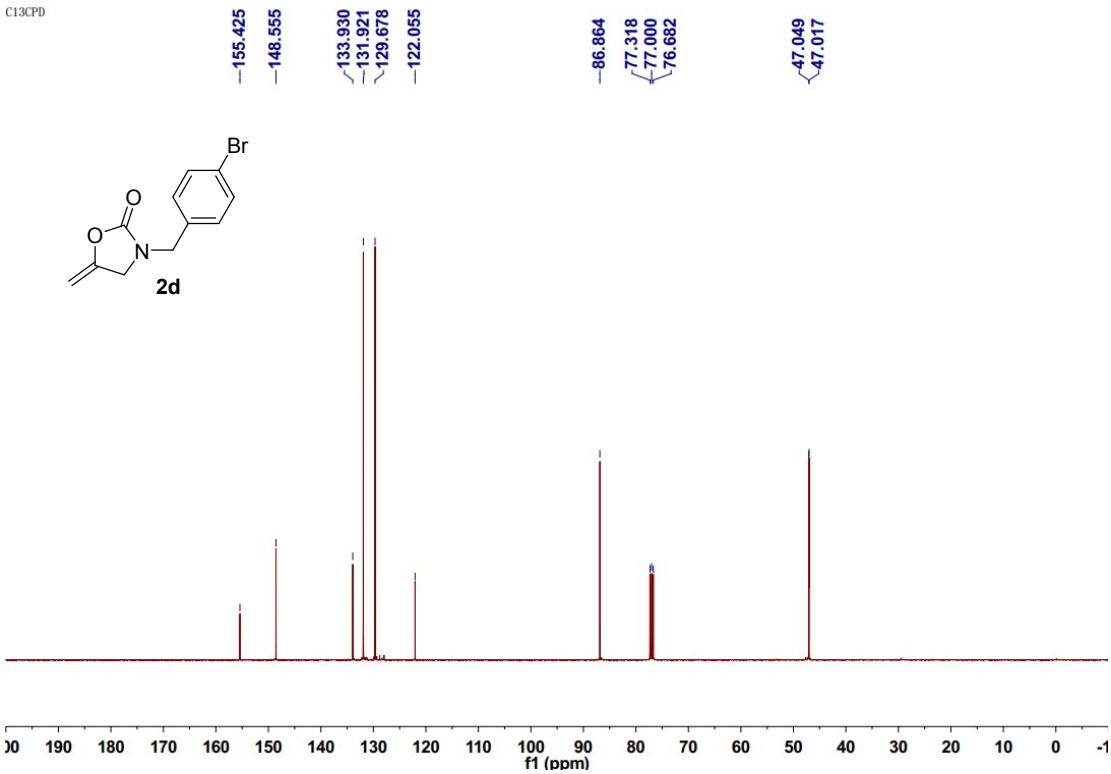
C13CPD
155.425
148.555
133.930
131.921
129.678
122.055
86.864
77.318
77.000
76.682
47.049
47.017
Br
O
O
N
2d
f1 (ppm)

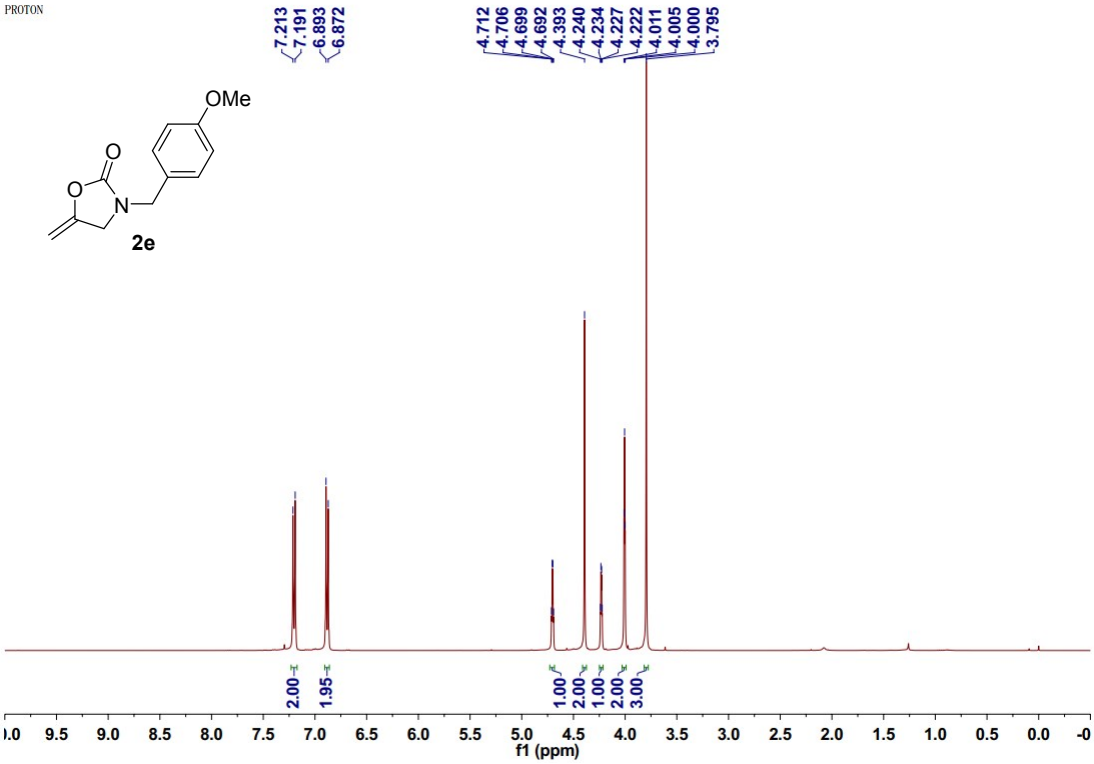
PROTON
7.213
7.191
6.893
6.872
4.712
4.706
4.699
4.692
4.393
4.240
4.234
4.227
4.222
4.011
4.005
4.000
3.795
OMe
O
O
N
2e
2.00
1.95
1.00
2.00
1.00
2.00
3.00
f1 (ppm)

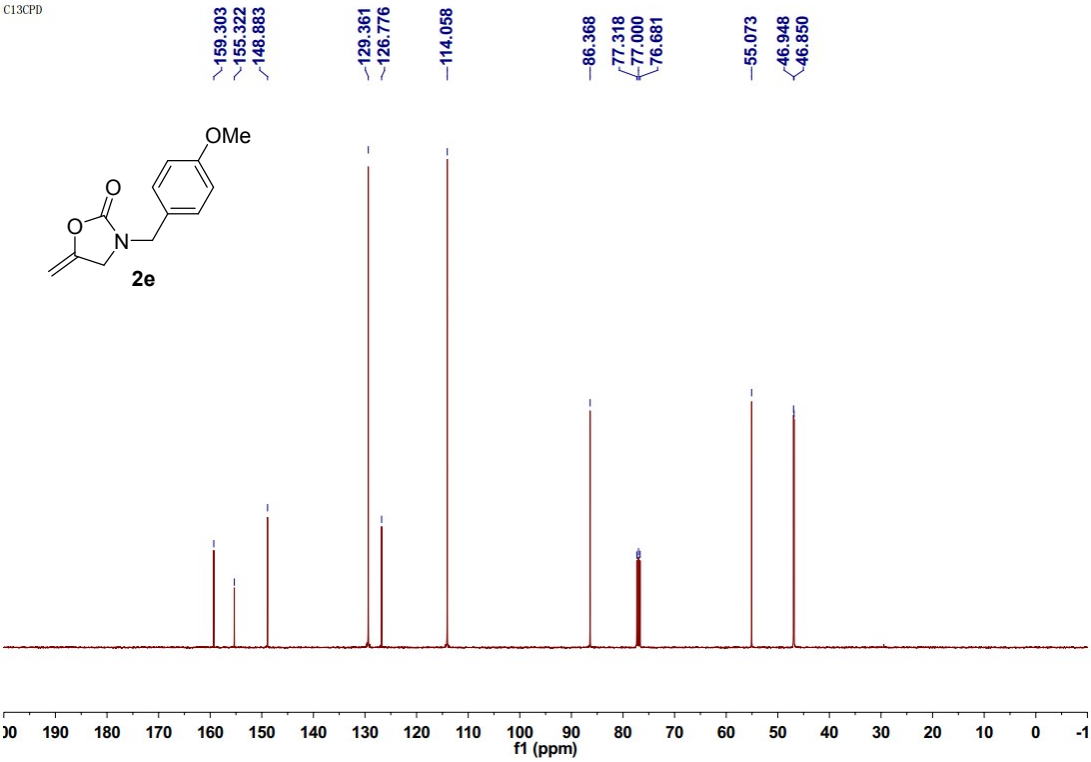
C13CPD
159.303
155.322
148.883
129.361
126.776
114.058
86.368
77.318
77.000
76.681
55.073
46.948
46.850
OMe
O
O
N
2e
f1 (ppm)

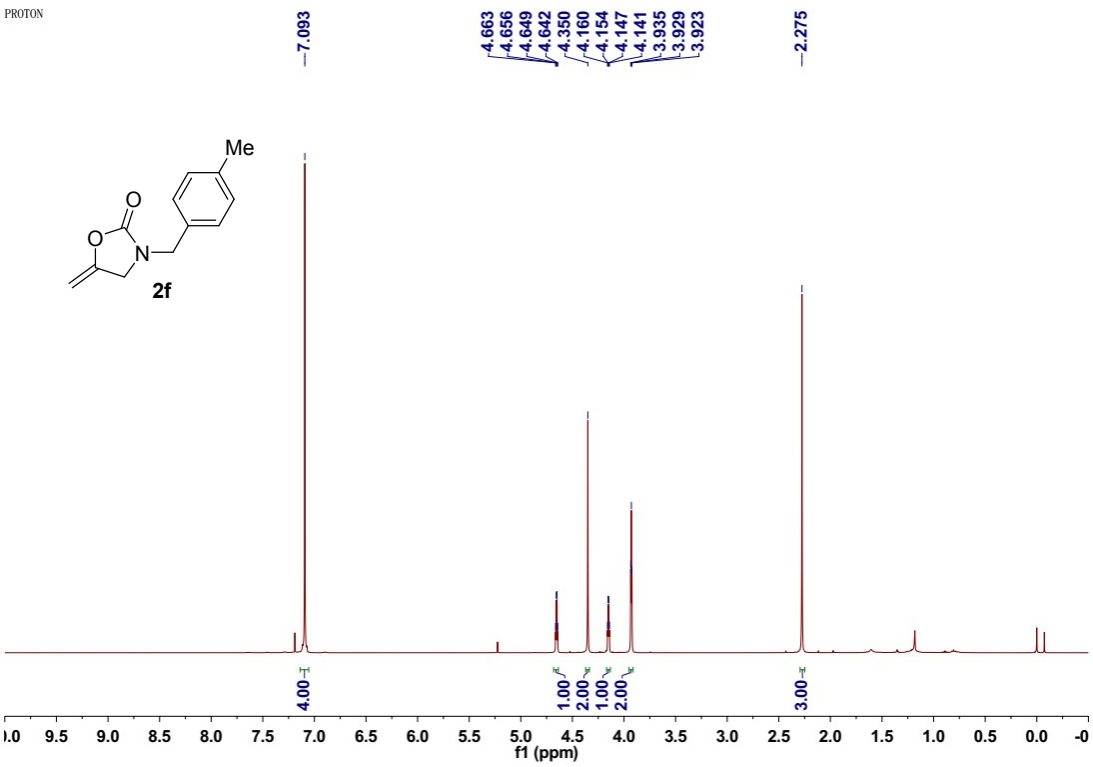
PROTON
7.093
4.663
4.656
4.649
4.642
4.350
4.160
4.154
4.147
4.141
3.935
3.929
3.923
2.275
Me
O
O
N
2f
4.00
1.00
2.00
1.00
2.00
3.00
f1 (ppm)

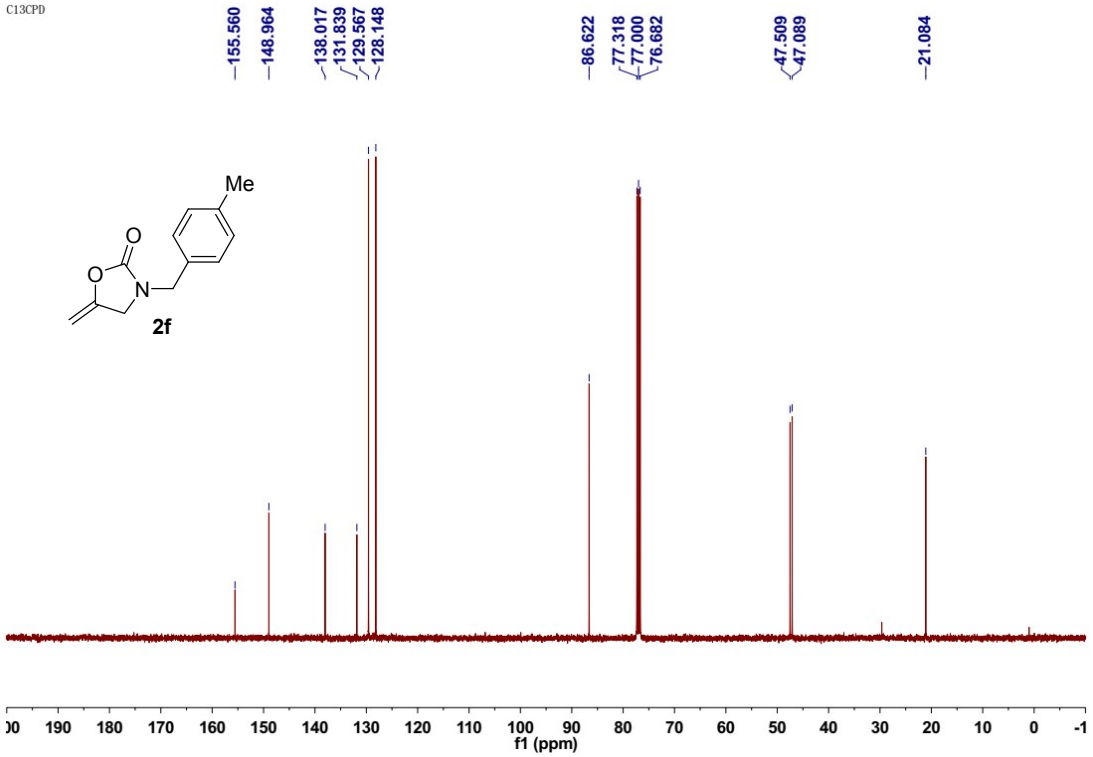
C13CPD
155.560
148.964
138.017
131.839
129.567
128.148
86.622
77.318
77.000
76.682
47.509
47.089
21.084
Me
O
O
N
2f
f1 (ppm)

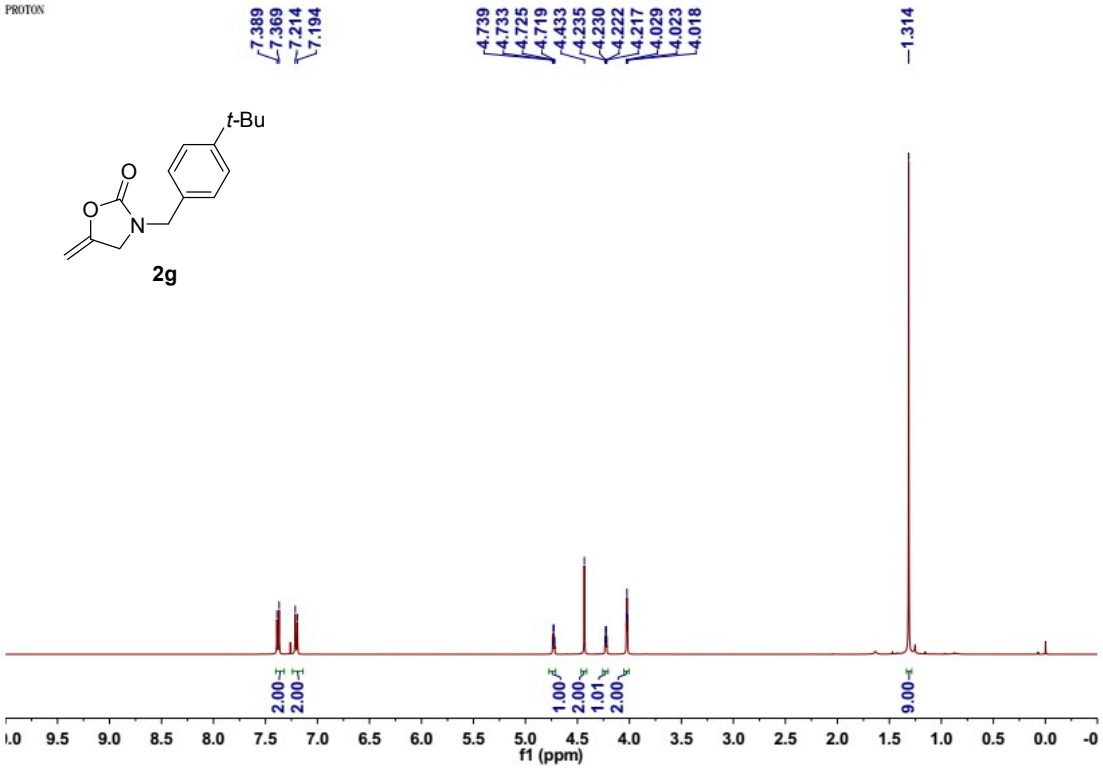
PROTON
7.389
7.369
7.214
7.194
4.739
4.733
4.725
4.719
4.433
4.235
4.230
4.222
4.217
4.029
4.023
4.018
1.314
t-Bu
O
O
N
2g
2.00
2.00
1.00
2.00
1.01
2.00
9.00
f1 (ppm)

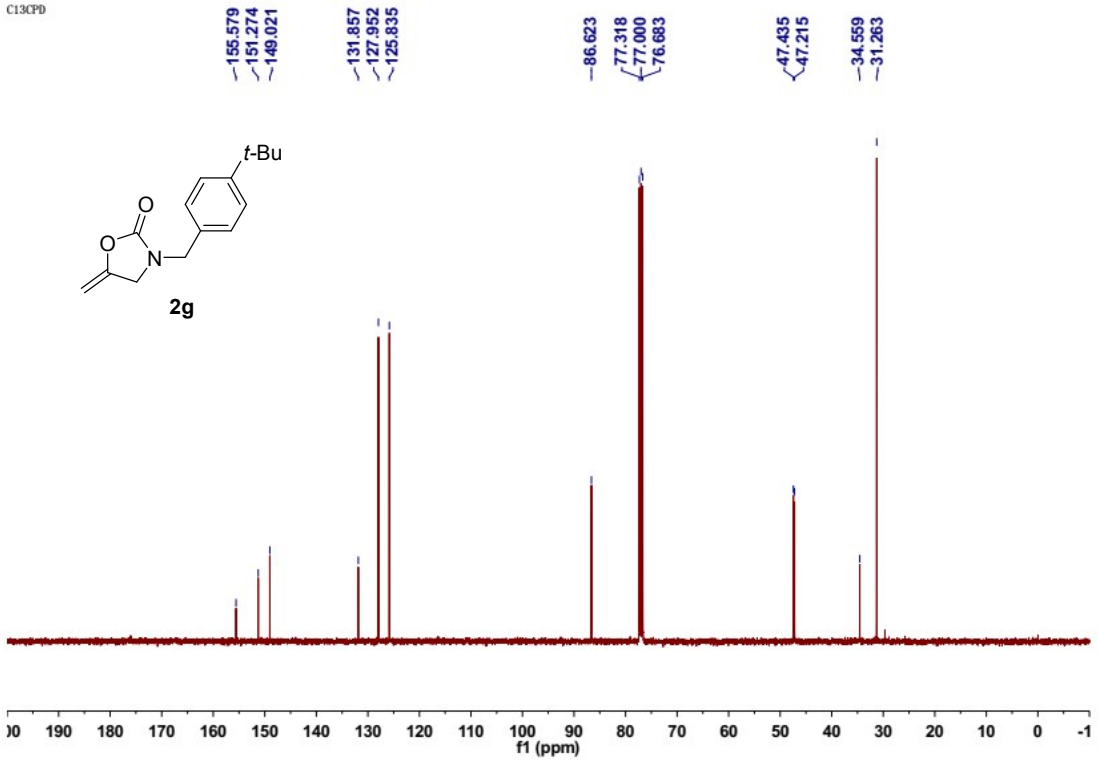
C13CPD
155.579
151.274
149.021
131.857
127.952
125.835
86.623
77.318
77.000
76.683
47.435
47.215
34.559
31.263
t-Bu
O
O
N
2g
f1 (ppm)

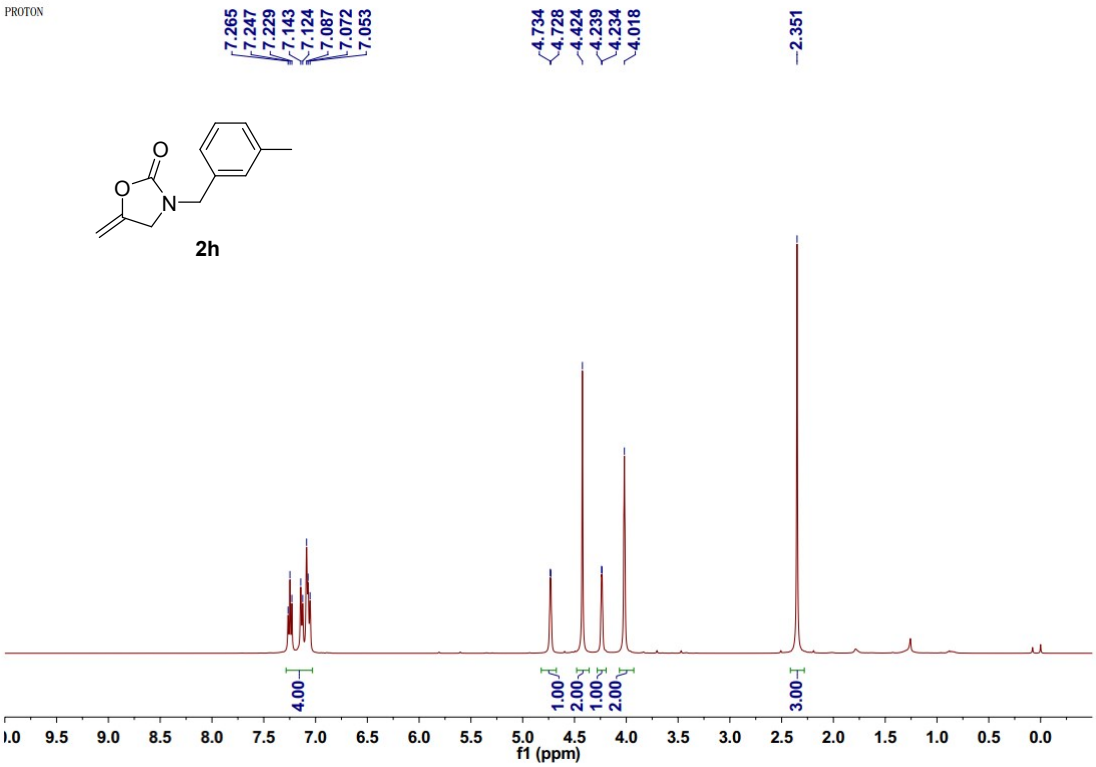
PROTON
7.265
7.247
7.229
7.143
7.124
7.087
7.072
7.053
4.734
4.728
4.424
4.239
4.234
4.018
2.351
2h
4.00
1.00
2.00
1.00
2.00
3.00
f1 (ppm)

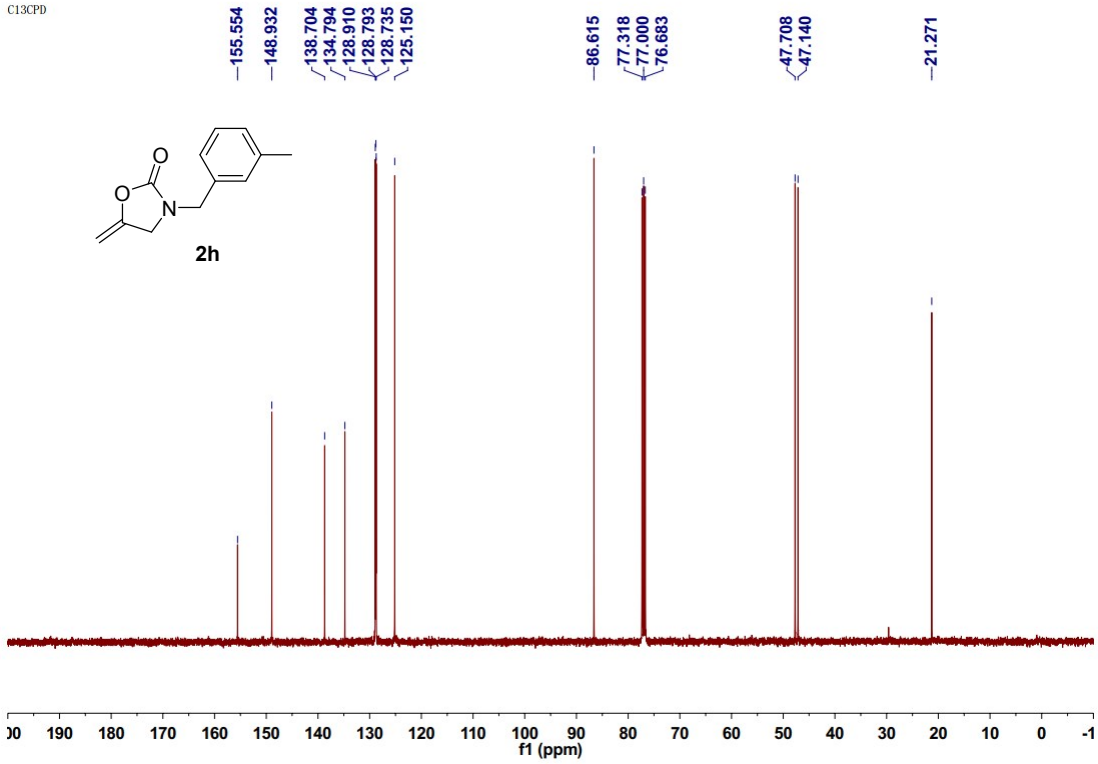
C13CPD
155.554
148.932
138.704
134.794
128.910
128.793
128.735
125.150
86.615
77.318
77.000
76.683
47.708
47.140
21.271
2h
f1 (ppm)

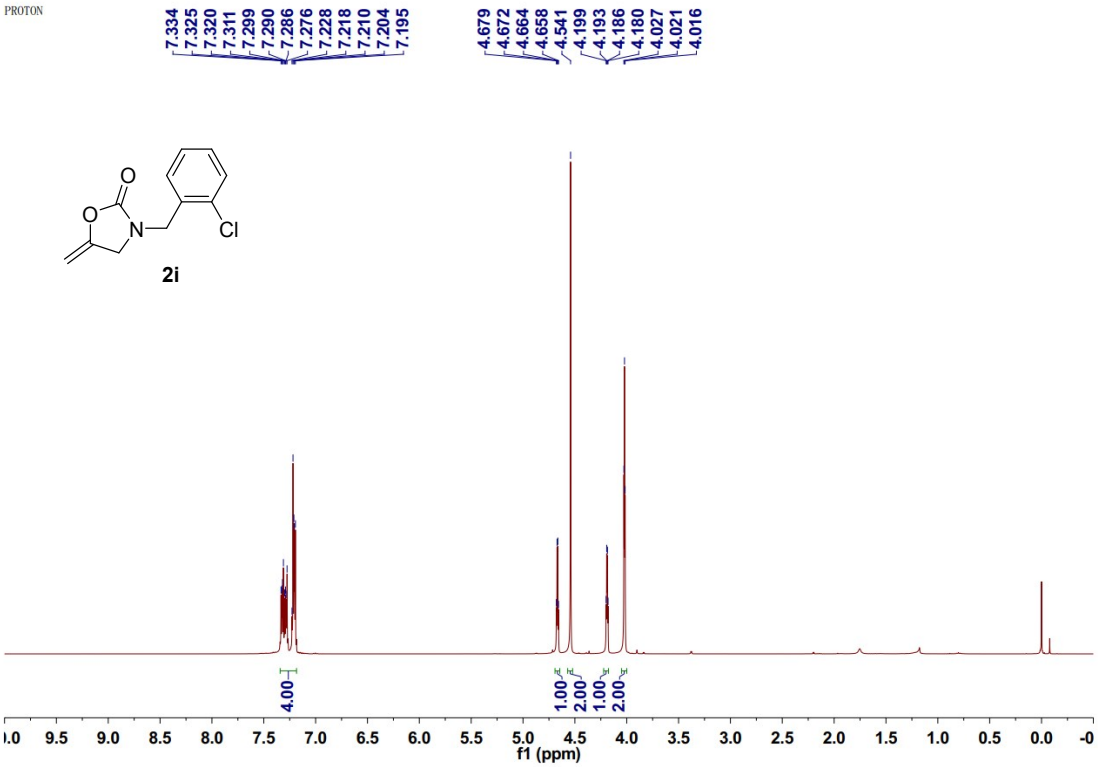
PROTON
7.334
7.325
7.320
7.311
7.299
7.290
7.286
7.276
7.228
7.218
7.210
7.204
7.195
4.679
4.672
4.664
4.658
4.541
4.199
4.193
4.186
4.180
4.027
4.021
4.016
O
O
N
Cl
2i
4.00
1.00
2.00
1.00
2.00
f1 (ppm)

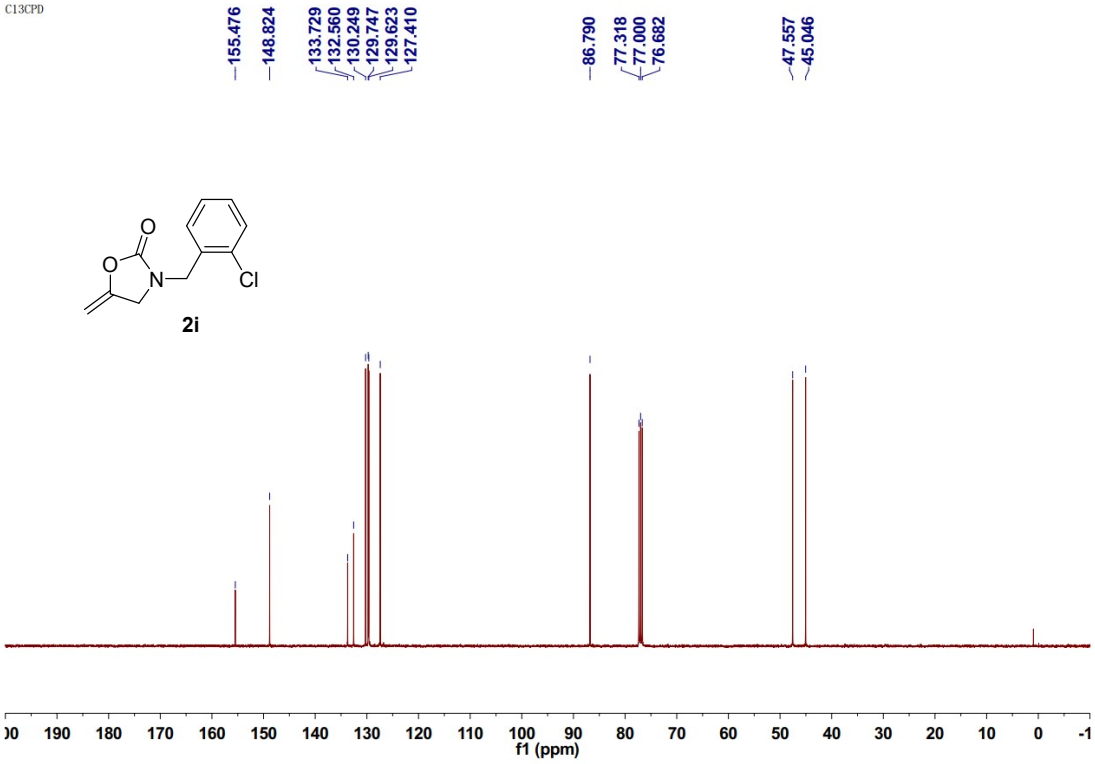
C13CPD
155.476
148.824
133.729
132.560
130.249
129.747
129.623
127.410
86.790
77.318
77.000
76.682
47.557
45.046
O
O
N
Cl
2i
f1 (ppm)

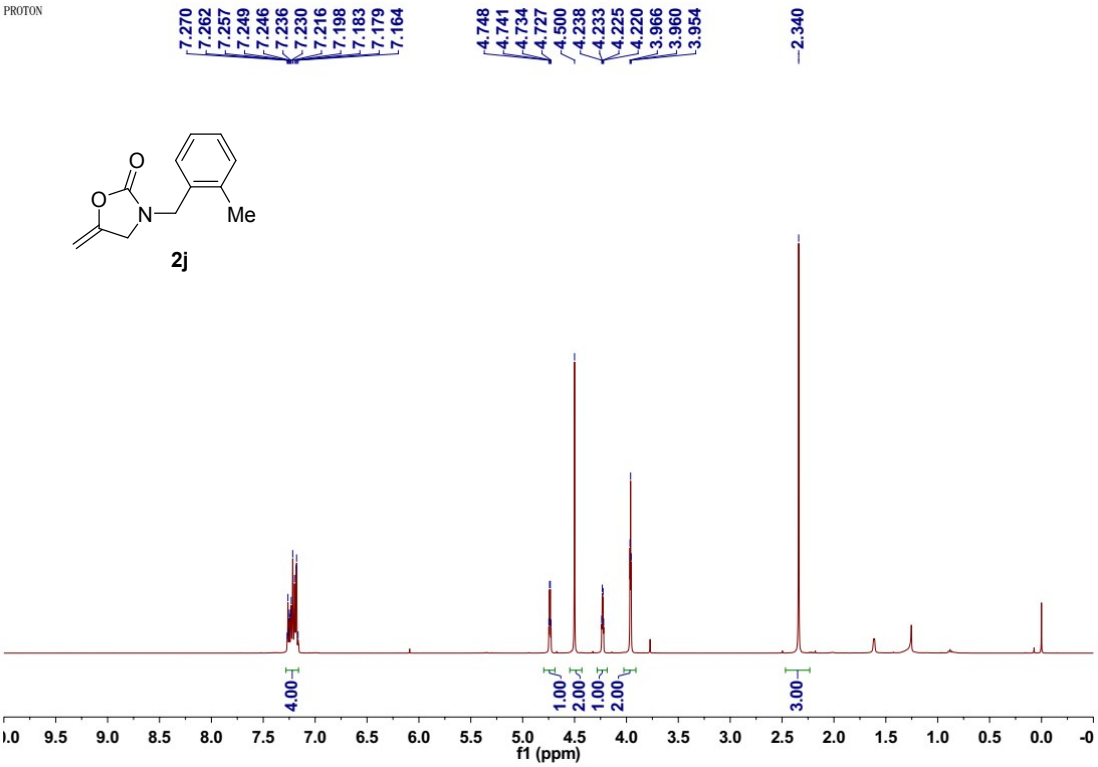
PROTON
7.270
7.262
7.257
7.249
7.246
7.236
7.230
7.216
7.198
7.183
7.179
7.164
4.748
4.741
4.734
4.727
4.500
4.238
4.233
4.225
4.220
3.966
3.960
3.954
2.340
O
O
N
Me
2j
4.00
1.00
2.00
1.00
2.00
3.00
f1 (ppm)

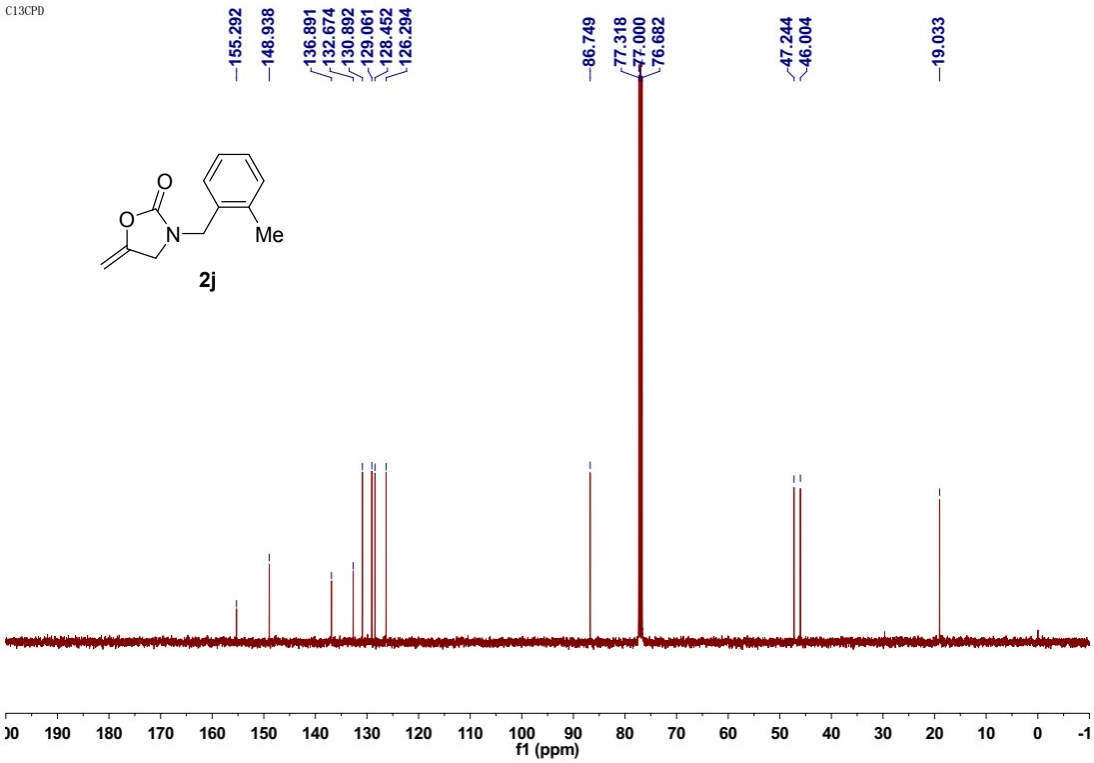
C13CPD
155.292
148.938
136.891
132.674
130.892
129.061
128.452
126.294
86.749
77.318
77.000
76.682
47.244
46.004
19.033
O
O
N
Me
2j
f1 (ppm)

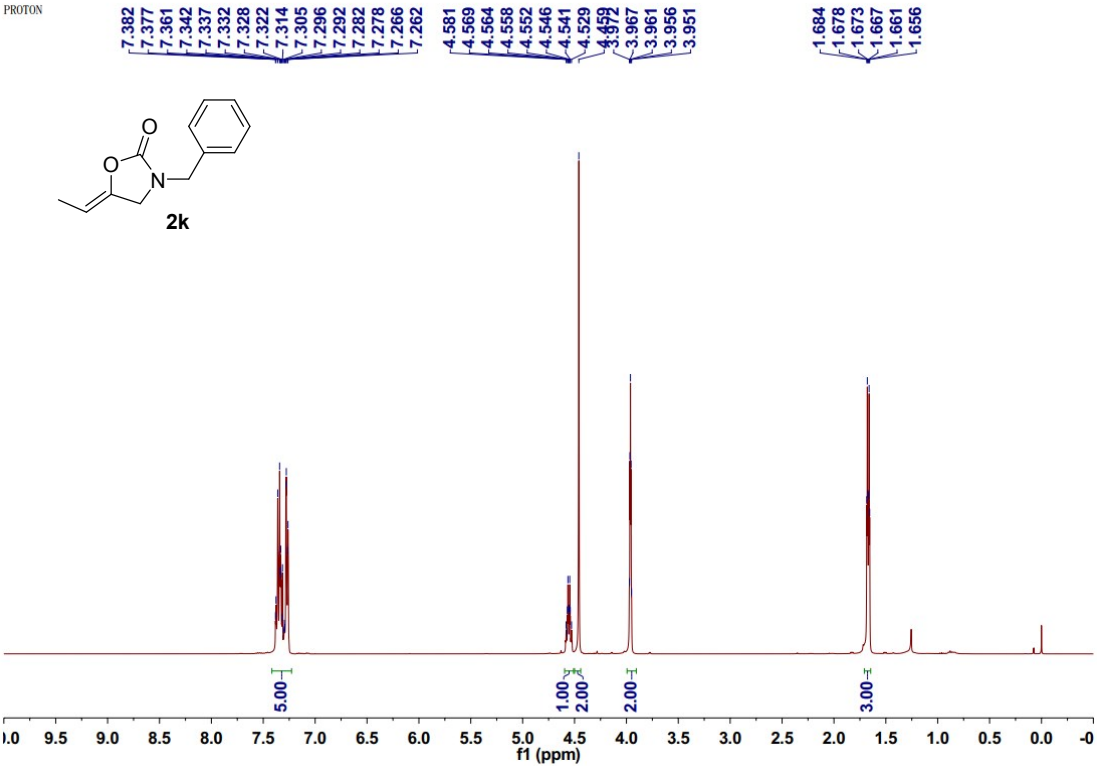
PROTON
7.382
7.377
7.361
7.342
7.337
7.332
7.328
7.322
7.314
7.305
7.296
7.292
7.282
7.278
7.266
7.262
4.581
4.569
4.564
4.558
4.552
4.546
4.541
4.529
4.459
3.972
3.967
3.961
3.956
3.951
1.684
1.678
1.673
1.667
1.661
1.656
O
O
N
2k
5.00
1.00
2.00
2.00
3.00
f1 (ppm)

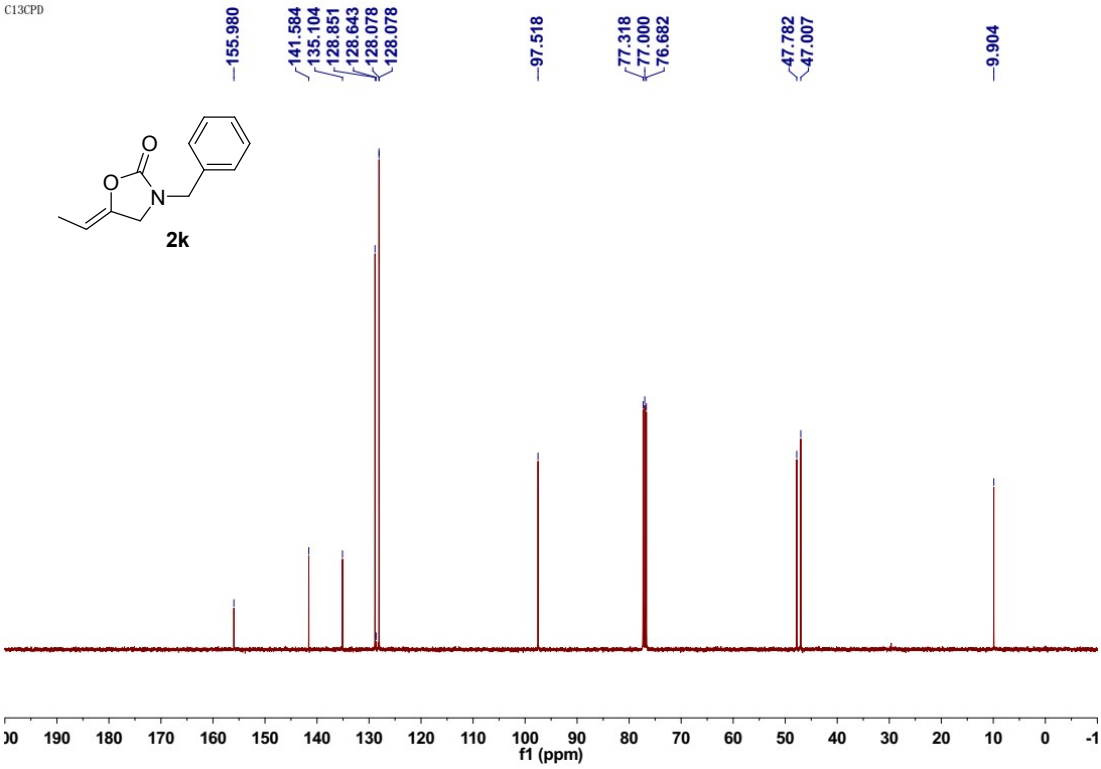
C13CPD
155.980
141.584
135.104
128.851
128.643
128.078
128.078
97.518
77.318
77.000
76.682
47.782
47.007
9.904
O
O
N
2k
f1 (ppm)

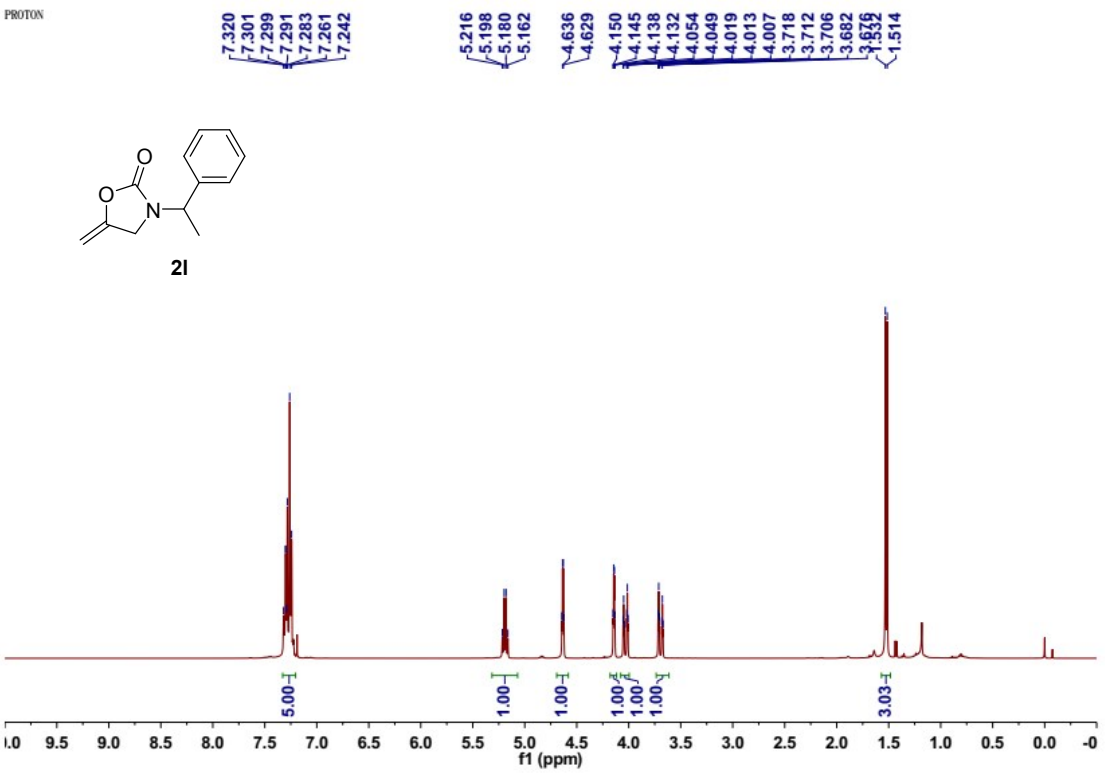

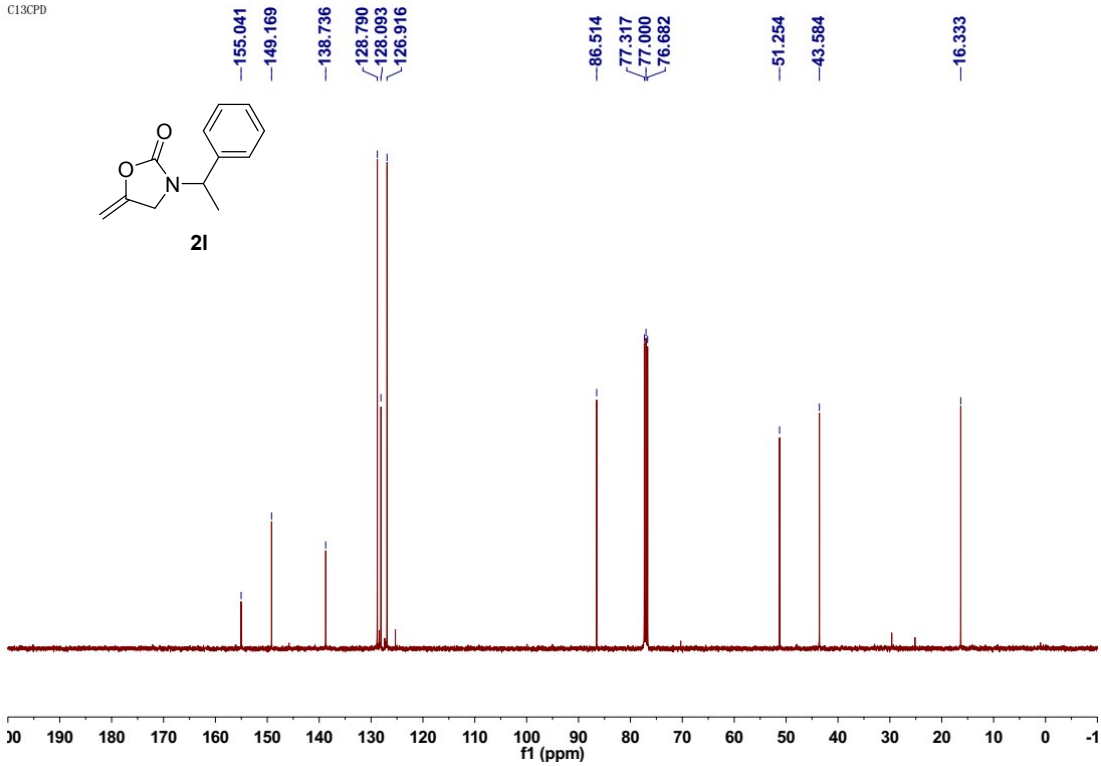

Table S1 The different amounts of Ag/Cu loadings on Pyr-GDY determined by ICP-MS.

Catalysts	Cu loading (%)	Cu loading (μmol/mg)	$AgNO_3$ (μmol)	Ag loading (%)	Ag loading (μmol/mg)
Cu/Pyr-GDY	13.5	2.1	0	0	0
Ag/Pyr-GDY-2.8	9.4	1.5	3.1	2.8	0.3
Ag/Pyr-GDY-3.1	9.9	1.6	6.3	3.1	0.3
Ag/Pyr-GDY-4.4	7.3	1.2	12.5	4.4	0.4
Ag/Pyr-GDY-5.3	8.6	1.4	25.0	5.3	0.5
Ag/Pyr-GDY-12.0	4.2	0.7	50.0	12.0	1.1
Ag/Pyr-GDY-19.5	1.4	0.2	100	19.5	1.8
Ag/Pyr-GDY-24.6	0.8	0.1	200	24.6	2.3
Pyr-GDY	0	0	0	0	0
Ag/Pyr-GDY-0.4 (Cu-Free)	0	0	25.0	0.4	0.3
Ag/Pyr-GDY-6.0 (Cu-Free)	0	0	50.0	6.0	0.6

Table S2. The values of TON and TOF for the reactions.

Entry	**1a** (mmol)	reaction time	conversion	catalyst (% Ag loading)	TON	TOF (h^{-1})
1	0.2	2 h	100%	Ag-Pyr-GDY -12.0	120	59
2	0.2	2 h	100%	Ag-Pyr-GDY-5.3	274	137
3	8	20 h	35%	Ag-Pyr-GDY-5.3	3840	192
4	8	40 h	71%	Ag-Pyr-GDY-5.3	7790	195
5	8	60 h	100%	Ag-Pyr-GDY-5.3	10971	183
6	18	20 h	16%	Ag-Pyr-GDY-5.3	3949	197
7	18	40 h	31%	Ag-Pyr-GDY-5.3	7652	191
8	18	60 h	36%	Ag-Pyr-GDY-5.3	8886	148
9	18	90 h	44%	Ag-Pyr-GDY-5.3	10861	121
10	18	150 h	68%	Ag-Pyr-GDY-5.3	16785	112
11	18	220 h	83%	Ag-Pyr-GDY-5.3	20488	93

Table S3. A comparison of TONs and conversions for Ag-Pyr-GDY-5.3 with those of reported catalysts.

Catalysts	**Homogeneous /Heterogeneous**	**Loading**	**Solvent**	**Temp**	**Pressure**	**Time**	**Yield**	**TON**	**Ref**
$(^nC_7H_{15})_4NBr$	Homogeneous	2.5 mol %	-	60 °C	balloon	20 h	0 %	0	1
$[(^nC_{16}H_{33})\ (CH_3)_3N]_6\ [\alpha\text{-}SiW_{11}O_{39}Cu]$	Homogeneous	2.5 mol %	-	60 °C	balloon	20 h	86 %	34.4	1
$[(^nC_4H_9)_4N]_6\ [\alpha\text{-}SiW_{11}O_{39}Cu]$	Homogeneous	2.5 mol %	-	60 °C	balloon	20 h	95 %	38	1
$[(^nC_7H_{15})_4N]_6\ [\alpha\text{-}SiW_{11}O_{39}Co]$	Homogeneous	2.5 mol %	-	60 °C	balloon	20 h	66 %	26.4	1
$[(^nC_7H_{15})_4N]_6\ [\alpha\text{-}SiW_{11}O_{39}Cu]$	Homogeneous	2.5 mol %	-	60 °C	balloon	20 h	99 %	39.6	1
$[(^nC_7H_{15})_4N]_6\ [\alpha\text{-}SiW_{11}O_{39}Fe]$	Homogeneous	2.5 mol %	-	60 °C	balloon	20 h	18 %	7.2	1
$[(^nC_7H_{15})_4N]_6\ [\alpha\text{-}SiW_{11}O_{39}Fe]$	Homogeneous	2.5 mol %	-	60 °C	balloon	20 h	18 %	7.2	1
$[(^nC_7H_{15})_4N]_6\ [\alpha\text{-}SiW_{11}O_{39}Mn]$	Homogeneous	2.5 mol %	-	60 °C	balloon	20 h	43 %	17.2	1
$[(^nC_7H_{15})_4N]_6\ [\alpha\text{-}SiW_{11}O_{39}Ni]$	Homogeneous	2.5 mol %	-	60 °C	balloon	20 h	16%	6.4	1
$[(^nC_7H_{15})_4N]_6\ [\alpha\text{-}SiW_{11}O_{39}Zn]$	Homogeneous	2.5 mol %	-	60 °C	balloon	20 h	45 %	18	1
$CuCl_2$	Homogeneous	2.5 mol %	-	60 °C	balloon	20 h	67 %	26.8	1
$CuCl_2$ / $(^nC_7H_{15})_4NBr$	Homogeneous	2.5 mol %	-	60 °C	balloon	20 h	68 %	27.2	1
$K_6\ [SiW_{11}O_{39}Cu]$	Homogeneous	2.5 mol %	-	60 °C	balloon	20 h	43 %	17.2	1
$K_8\ [\alpha\text{-}SiW_{11}O_{39}]$	Homogeneous	2.5 mol %	-	60 °C	balloon	20 h	0 %	0	1
[DBUH][MIm]	Homogeneous	200 mol %	-	60 °C	0.1 MPa	6 h	95 %	-	2
t-BuOI	Homogeneous	1.0 equiv.	MeCN	-20 °C	0.1 MPa	24 h	94 %	0.94	3
1G1[PEG]	Homogeneous	1 mol %	MeOH	40 °C	0.1 MPa	48 h	87 %	87	4
AuCl(IPr)	Homogeneous	2 mol %	MeOH	40 °C	0.1 MPa	48 h	76 %	38	4
2G1[PEG]	Homogeneous	1 mol %	H_2O	r.t.	0.1 MPa	48 h	87 %	87	5
Ag_2O / DBU	Heterogeneous	0.5 mol %	DMSO	60 °C	air	16 h	92 %	184	6

$AgNO_3$ / DBU	Homogeneous	0.5 mol %	DMSO	60 °C	air	33 h	94 %	188	6
AgOAc / DBU	Homogeneous	0.5 mol %	DMSO	60 °C	air	18 h	90 %	180	6
AgOAc / DBU	Homogeneous	0.5 mol %	DMSO / H_2O	60 °C	air	24 h	86 %	172	6
$Cu(OAc)_2$ / DBU	Homogeneous	0.5 mol %	DMSO / H_2O	60 °C	air	78 h	78 %	156	6
CuI / DBU	Heterogeneous	0.5 mol %	DMSO/ H_2O	60 °C	air	63 h	63 %	126	6
$PtCl_2$ / DBU	Homogeneous	0.5 mol %	DMSO / H_2O	60 °C	air	240 h	69 %	138	6
AgCl(IPr)	Heterogeneous	2 mol %	MeOH	40 °C	1 atm	15 h	52 %	26	7
AuCl(IPr)	Homogeneous	2 mol %	MeOH	40 °C	1 atm	15 h	91 %	45.5	7
CuCl(IPr)	Homogeneous	2 mol %	MeOH	40 °C	1 atm	15 h	19 %	9.5	7
AgOAc / $(^nC_7H_{15})_4NBr$	Homogeneous	0.1 mol %	DMSO	60 °C	0.1 MPa	48 h	54 %	544	8
AgOAc / iPrNH-GlyNa	Homogeneous	10 mol %	PEG150	40 °C	1 atm	-	91 %	-	9
Au(OH)(IPr)	Homogeneous	2 mol %	THF	40 °C	0.1 MPa	20 h	54 %	27	10
CuBr / DBU	Homogeneous	10 mol %	DMSO	50 °C	0.1MPa	6 h	69 %	6.9	11
CuCl / DBU	Homogeneous	10 mol %	DMSO	50 °C	0.1MPa	6 h	<1 %	< 0.1	11
CuCN / DBU	Homogeneous	10 mol %	DMSO	50 °C	0.1MPa	6 h	76 %	7.6	11
CuI / DBU	Heterogeneous	10 mol %	DMSO	50 °C	0.1MPa	6 h	99 %	9.9	11
CuO / DBU	Heterogeneous	10 mol %	DMSO	50 °C	0.1MPa	6 h	41 %	4.1	11
MTBD	Homogeneous	10 mol %	MeCN	75 °C	5 bar	18 h	100%	10	12

TMG	Homogeneous	10 mol %	DMSO	75 °C	5 bar	18 h	100 %	10	12
AgOAc	Homogeneous	2 mol %	DMSO	25 °C	0.1 MPa	1.5 h	99 %	49.5	13, 14
$Pd(OAc)_2$	Homogeneous	5 mol %	toluene	50 °C	40 kg/cm3	48 h	85 %	17	15
$PdCl_2$ (dppf) / NaO^tBu	Homogeneous	2.5 mol %	DMSO	40 °C	1 atm	22 h	90 %	36	16
PdI_2 / KI	Homogeneous	1 mol %	MeOH	75 °C	40 bar	24 h	27 %	27	17
Pd@BBA-1, Pd@BBA-2	Heterogeneous	1 mol %	DMSO	80 °C	1 bar	0.5 h	98 %	98	18
Triethanolamine	Homogeneous	10 mol %	-	90 °C	0.1 MPa	10 h	99 %	9.9	19
ItBu	Homogeneous	2 mol %	^iPrOH	90 °C	0.6 MPa	24 h	97 %	48.5	20, 21
-	-	-	supercritical CO_2	100 °C	9 MPa	18 h	88 %	-	22
Fe_3O_4/KCC-1/tetrazolylidene/Au	Heterogeneous	1 mg (1 mmol propargylic amine)	H_2O	r.t.	0.5 MPa	18 h	95 %	-	23
HPG@KCC-1/PPh_2/Au	Heterogeneous	2 mg (1 mmol propargylic amine)	H_2O	reflux	1.5 MPa	48 h	92 %	-	24
Basic alumina	Heterogeneous	5 mol %	supercritical CO_2	90 °C	80 bar	21 h	85 %	17	25
Hydrotalcite MG30	Heterogeneous	5 mol %	supercritical CO_2	90 °C	80 bar	21 h	67 %	13.4	25

Hydrotalcite MG70	Heterogeneous	5 mol %	supercritical CO_2	90 °C	80 bar	21 h	58 %	11.6	25
SiO_2-$(CH_2)_3$-NEt_2	Heterogeneous	5 mol %	supercritical CO_2	90 °C	80 bar	21 h	72 %	14.4	25
SiO_2-TBD	Heterogeneous	5 mol %	supercritical CO_2	90 °C	80 bar	21 h	88 %	17.6	25
TNS-Ag8	Heterogeneous	0.1 mol %	MeCN	25 °C	0.1 MPa	180 h	76 %	760	26
TOS-Ag4	Heterogeneous	0.1 mol %	MeCN	25 °C	0.1 MPa	96 h	93 %	930	26
$CoBr_2$/[EEIM][OAc]	Homogeneous	0.05 mol%	-	60 °C	balloon	106 h	87%	1740	27
Ag-MOF-1	Heterogeneous	4 mol%	MeCN	25 °C	0.1 MPa	24 h	95%	23.8	28
AuNP@PAMAM/C	Heterogeneous	1 mol%	H_2O-toluene	40 °C	balloon	10 h	99%	99	29
$[Cu(bpy)_2(1,2,4,5\text{-}BTMS)_{0.5}(H_2O)_{0.5}]_n$	Heterogeneous	10 mol%	DMSO	50 °C	0.1 MPa	6 h	99%	9.9	30
NiBDP-AgS	Heterogeneous	0.5 mol%	DMSO	25 °C	0.1 MPa	4 h	99%	200	31
KCC-1/IL/Ni@Pd NPs	Heterogeneous	0.1 mg catalyst/1 mmol substrate	-	25 °C	1 MPa	3 h	96%	-	32
KCC-1/Salen/Ru(II) NPs	Heterogeneous	1 mg catalyst/1 mmol substrate	-	100 °C	1 MPa	1 h	98%	-	33
$[Au(dpb^F)]SbF_6$	Homogeneous	0.5 mol%	DMSO	25 °C	air	24 h	78%	156	34
Bu_4NF	Homogeneous	1 mol%	t-Bu-OH	110 °C	0.5 MPa	18 h	91%	91	35

$[Zn_{22}(Trz)_8(OH)_{12}(H_2O)_x]_n$	Heterogeneous	0.27 mol% catalyst/substrate	MeCN	70 °C	0.1 MPa	12 h	99%	367	36
Ag27-MOF	Heterogeneous	0.025 mol%	MeCN	25 °C	0.1 MPa	240 h	34%	1333	37
Ag@TpTta	Heterogeneous	0.01429 mol %	-	25 °C	balloon	16 h	96%	67	38
Ag@TpPa-1	Heterogeneous	0.01429 mol %	-	25 °C	balloon	16 h	89%	62	38
Ag/Pyr-GDY-5.3	Heterogeneous	0.0036 mol %	-	25 °C	balloon	60 h	100%	10971	This work
Ag/Pyr-GDY-5.3	Heterogeneous	0.0036 mol %	-	25 °C	balloon	220 h	83%	20488	This work

References

[1] M. Y. Wang, Q. W. Song, R. Ma, J. N. Xie and L. N. He, Efficient conversion of carbon dioxide at atmospheric pressure to 2-oxazolidinones promoted by bifunctional Cu(II)-substituted polyoxometalate-based ionic liquids, *Green Chem.*, 2016, **18**, 282-287.

[2] J. Hu, J. Ma, Q. Zhu, Z. Zhang, C. Wu and B. Han, Transformation of Atmospheric CO_2 Catalyzed by Protic Ionic Liquids: Efficient Synthesis of 2−Oxazolidinones, *Angew. Chem. Int. Ed.,* 2015, **54**, 5399–5403.

[3] Y. Takeda, S. Okumura, S. Tone, I. Sasaki and S. Minakata, Cyclizative Atmospheric CO_2 Fixation by Unsaturated Amines with *t*-BuOI Leading to Cyclic Carbamates, *Org. Lett*., 2012, **14**, 4874–4877.

[4] K. Fujita, K. Inoue, J. Sato, T. Tsuchimoto and H. C Yasuda, arboxylative cyclization of propargylic amines with CO_2 catalyzed by dendritic N-heterocyclic carbene-gold(I) complexes, *Tetrahedron*, 2016, **72**, 1205-1212.

[5] K. Fujita, J. Sato, K. Inoue, T. Tsuchimoto and H. Yasuda, Aqueous media carboxylative cyclization of propargylic amines with CO_2 catalyzed by amphiphilic dendritic *N*-heterocyclic carbene–gold(I) complexes, *Tetrahedron Letters,* 2014, **55**, 3013–3016.

[6] M. Yoshida, T. Mizuguchi and K. Shishido, Synthesis of Oxazolidinones by Efficient Fixation of Atmospheric CO_2 with Propargylic Amines by using a Silver/1,8-Diazabicyclo [5.4.0]undec-7-ene (DBU) Dual‐Catalyst System, *Chemistry*, 2012, **18**, 15578-15581.

[7] S. Hase, Y. Kayaki and T. Ikariya, NHC–Gold(I) Complexes as Effective Catalysts for the Carboxylative Cyclization of Propargylamines with Carbon Dioxide, *Organometallics*, 2013, **32**, 5285-5288.

[8] Q. W. Song and L. N. He, Robust Silver (I) Catalyst for the Carboxylative Cyclization of Propargylic Alcohols with Carbon Dioxide under Ambient Conditions, *Adv. Synth. Catal.,* 2016, **358**, 1251-1258.

[9] A. H. Liu, R. Ma, C. Song, Z. Z. Yang, A. Yu, Y. Cai, L. N. He, Y. N. Zhao, B. Yu and Q. W. Song, Equimolar CO_2 Capture by N-Substituted Amino Acid Salts and Subsequent Conversion, *Angew. Chem. Int. Ed.*, 2012, **51**, 11306-11310.

[10] K. Yamashita, S. Hase, Y. Kayaki and T. Ikariya, Highly Selective Carboxylative Cyclization of Allenylmethylamines with Carbon Dioxide Using N-Heterocyclic Carbene-Silver(I) Catalysts, *Org. Lett.*, 2015, **17**, 2334-2337.

[11] Y. Zhao, J. Qiu, L. Tian, Z. Li, M. Fan and J. Wang, New Copper(I)/DBU Catalyst System for the Carboxylative Cyclization of Propargylic Amines with Atmospheric CO_2: An Experimental and Theoretical Study, *ACS Sustainable Chem. Eng.*, 2016, **4**, 5553-5560.

[12] R. Nicholls, S. Kaufhold and B. N. Nguyen, Observation of guanidine–carbon dioxide complexation in solution and its role in the reaction of carbon dioxide and propargylamines, *Catal. Sci. Technol.*, 2014, **4**, 3458–3462.

[13] S. Kikuchi, S. Yoshida, Y. Sugawara, W. Yamada, H.-M. Cheng, K. Fukui, K. Sekine, I. Iwakura, T. Ikeno and T. Yamada, Silver-Catalyzed Carbon Dioxide Incorporation and Rearrangement on Propargylic Derivatives, *Bull. Chem. Soc. Jpn.*, 2011, **84**, 698-717.

[14] S. Yoshida, K. Fukui, S. Kikuchi and T. Yamada, Silver-catalyzed Preparation of Oxazolidinones from Carbon Dioxide and Propargylic Amines, *Chem. Lett.*, 2009, **38**, 786-787.

[15] M. Shi and Y. M. Shen, Transition-Metal-Catalyzed Reactions of Propargylamine with Carbon Dioxide and Carbon Disulfide, *J. Org. Chem.,* 2002, **67**, 16–21.

[16] P. García-Domínguez, L. Fehr, G. Rusconi and C. Nevado, Palladium-catalyzed incorporation of atmospheric CO_2: efficient synthesis of functionalized oxazolidinones, *Chem. Sci.*, 2016, **7**, 3914-3918.

[17] A. Bacchi, G. P. Chiusoli, M. Costa, B. Gabriele, C. Righi and G. Salerno, Palladium-catalysed sequential carboxylation–alkoxycarbonylation of acetylenic amines, *Chem. Commun.*, 1997, 1209-1210.

[18] S. Ghosha, S. Riyajuddinb, S. Sarkara, K. Ghoshb and S. M. Islam, Pd NPs Decorated on POPs as Recyclable Catalysts for the Synthesis of 2-Oxazolidinones from Propargylic Amines via Atmospheric Cyclizative CO_2 Incorporation, *ChemNanoMat.*, 2020, **6**, 160-172. Ghosha, S. Riyajuddinb , S. Sarkara , K. Ghoshb, S. M. Islam, *ChemNanoMat.,* **2020**, *6*, 160-172.

[19] B. Yu, D. Kim, S. Kim and S. H. Hong, Cyanuric Acid‐Based Organocatalyst for Utilization of Carbon Dioxide at Atmospheric Pressure, *ChemSusChem,* 2017, **10**, 1080–1084.

[20] K. Fujita, J. Sato, A.Fujii, S.-y.Onozawa and H. Yasuda, A Carboxylative Cyclization of Propargylic Amines with Carbon Dioxide Catalyzed by the N‐Heterocyclic Carbene 1,3‐Di‐*tert*‐butylimidazol‐2‐ylidene (ItBu), *Asian J. Org. Chem.,* 2016, **5**, 828–833.

[21] K. Fujita,. A. Fujii, J. Sato, S. Onozawa and H. Yasuda, Synthesis of 2-oxazolidinone by N-heterocyclic carbene-catalyzed carboxylative cyclization of propargylic amine with CO_2, *Tetrahedron Letters,* 2016, **57**, 1282–1284.

[22] A. Bacchi, G. P. Chiusoli, M. Costa, B. Gabriele, C. Righi and G. Salerno, Palladium-catalysed sequential carboxylation–alkoxycarbonylation of acetylenic amines, *Chem. Commun.*, 1997, 1209-1210.

[23] S. M. Sadeghzadeh, Gold (III) phosphorus complex immobilized on fibrous nano-silica as a catalyst for the cyclization of propargylic amines with CO_2, *J. Mol. Catal. A: Chem.*, 2016, **423**, 216-223.

[24] S. M. Sadeghzadeh, A green approach for the synthesis of 2-oxazolidinones using gold(I) complex immobilized on KCC-1 as nanocatalyst at room temperature, *Appl. Organometal. Chem.*, 2016, **30**, 835-842.

[25] R. Maggi and C. Bertolotti, Synthesis of oxazolidinones in supercritical CO_2 under heterogeneous catalysis, *Tetrahedron Letters,* 2007, **48**, 2131–2134.

[26] Z. Chang, X. Jing, C. He, X. Liu and C. Duan, Silver Clusters as Robust Nodes and π–Activation Sites for the Construction of Heterogeneous Catalysts for the Cycloaddition of Propargylamines, *ACS Catal.*, 2018, **8**, 1384-1391.

[27] Z.-H. Zhou, K.-H. Chen and L.-N. He, Efficient and Recyclable Cobalt(II)/Ionic Liquid Catalytic System for CO_2 Conversion to Prepare 2‐Oxazolinones at Atmospheric Pressure, *Chin. J. Chem.*, 2019, **37**, 1223-1228.

[28] X. Wang, Z. Chang, X. Jing, C. He and C. Duan, Double-Helical Ag–S Rod-Based Porous Coordination Polymers with Double Activation: σ-Active and π-Active Functions, *ACS Omega.*, 2019, **4**, 10828-10833.

[29] H. Matsuo, A. Fujii, J.-C. Choi, T. Fujitani and K. Fujita, Carboxylative Cyclization of Propargylic Amines with Carbon DioxideCatalyzed by Poly(amidoamine)-Dendrimer-Encapsulated Gold Nanoparticles, *Synlett*, 2019, **30**, 1914-1918.

[30] G. Zhang, H. Yang and H. Fei, Unusual Missing Linkers in an Organosulfonate-Based Primitive–Cubic (pcu)-Type Metal–Organic Framework for CO_2 Capture and Conversion under Ambient Conditions, *ACS Catal.*, 2018, **8**, 2519-2525.

[31] H. Yang, X. Zhang, G. Zhang and H. Fei, An alkaline-resistant Ag(i)-anchored pyrazolate-based metal-organic framework for chemical fixation of CO_2, *Chem. Commun.*, 2018, **54**, 4469-4472.

[32] S. M. Sadeghzadeh, R. Zhiani and S. Emrani, Ni@Pd nanoparticles supported on ionic liquid‐functionalized KCC-1 as robust and recyclable nanocatalysts for cycloaddition of propargylic amines and CO_2, *Appl. Organometal. Chem.*, 2018, **32**, e39411.

[33] S. M. Saadati and S. M. Sadeghzadeh, KCC-1 Supported Ruthenium-Salen-Bridged Ionic Networks as a Reusable Catalyst for the Cycloaddition of Propargylic Amines and CO_2, *Catal. Lett.,* 2018, **148**, 1692–1702.

[34] F. Inagaki, K. Maeda, K. Nakazawa and C. Mukai, Construction of the Oxazolidinone Framework from Propargylamine and CO_2 in Air at Ambient Temperature: Catalytic Effect of a Gold Complex Featuring an L_2/Z‐Type Ligand, *Eur. J. Org. Chem.*, 2018, 2972-2976.

[35] A. Fujii, H. Matsuo, J.-C. Choi, T. Fujitani and K.-i. Fujita, Efficient synthesis of 2-oxazolidinones and quinazoline-2,4(1*H*,3*H*)-diones from CO_2 catalyzed by tetrabutylammonium fluoride, *Tetrahedron,* 2018, **74***,* 2914–2920.

[36] C.-S. Cao, S.-M. Xia, Z.-J. Song, H. Xu, Y. Shi, L.-N. He, P. Cheng and B. Zhao, Highly Efficient Conversion of Propargylic Amines and CO_2 Catalyzed by Noble‐Metal‐Free [Zn_{116}] Nanocages, *Angew. Chem. Int. Ed*., 2020, **59**, 8586-8593.

[37] M. Zhao, S. Huang, Q. Fu, W. Li, R. Guo, Q. Yao, F. Wang, P. Cui, C.-H. Tung and D. Sun, Ambient Chemical Fixation of CO_2 Using a Robust Ag_{27} Cluster‐Based Two‐Dimensional Metal–Organic Framework, *Angew. Chem. Int. Ed.*, 2020, **59**, 20031-20036.

[38] S. Ghosh, T. S. Khan, A. Ghosh, A. H. Chowdhury, M. A. Haider, A. Khan and S. M. Islam, Utility of Silver Nanoparticles Embedded Covalent Organic Frameworks as Recyclable Catalysts for the Sustainable Synthesis of Cyclic Carbamates and 2-Oxazolidinones via Atmospheric Cyclizative CO_2 Capture, *ACS Sustainable Chem. Eng*., 2020, **8**, 5495-551.